

**TECHNISCHE UNIVERSITÄT MÜNCHEN**

**Molekulare Ernährungsmedizin**

**Analysis of  
uncoupling protein 1 and CideA function  
in two mammalian cell lines**

Verena Hirschberg

Vollständiger Abdruck der von der Fakultät Wissenschaftszentrum Weihenstephan für Ernährung,  
Landnutzung und Umwelt der Technischen Universität München zur Erlangung des akademischen  
Grades eines

Doktors der Naturwissenschaften

genehmigten Dissertation.

Vorsitzender:

Univ.-Prof. Dr. D. Haller

Prüfer der Dissertation:

1. Univ.-Prof. Dr. M. Klingenspor

2. Univ.-Prof. Dr. H. Daniel

Die Dissertation wurde am 01.02.2012 bei der Technischen Universität München eingereicht und  
durch die Fakultät Wissenschaftszentrum Weihenstephan für Ernährung, Landnutzung und Umwelt  
am 09.05.2012 angenommen.

<b>Abbreviations.....</b>	<b>IV</b>
<b>Figures.....</b>	<b>VI</b>
<b>Tables.....</b>	<b>VIII</b>
<b>1 Introduction.....</b>	<b>1</b>
<b>1.1 Uncoupled respiration and its physiological significance.....</b>	<b>1</b>
<b>1.2 Molecular aspects of UCP1 function.....</b>	<b>3</b>
<b>1.3 Beneficial effects of increased uncoupling and human BAT.....</b>	<b>5</b>
<b>1.4 Test systems for UCP1 function.....</b>	<b>6</b>
<b>1.5 Cidea.....</b>	<b>8</b>
<b>2 Material and Methods.....</b>	<b>10</b>
<b>2.1 Molecular biology.....</b>	<b>10</b>
2.1.1 RNA isolation, cDNA synthesis, qRT PCR.....	10
2.1.2 Protein extraction and quantification.....	11
2.1.3 Immunological detection of proteins.....	13
<b>2.2 Liposome analysis.....</b>	<b>16</b>
2.2.1 Purification and reconstitution of mouse UCP1.....	17
2.2.2 Heterologous expression and purification of Cidea in <i>E.coli</i> .....	18
2.2.3 Analysis of UCP1 function in liposomes.....	20
<b>2.3 Cell culture.....</b>	<b>21</b>
2.3.1 Cultivation of HEK293 and HEK293 UCP1 cells.....	21
2.3.2 Transient or stable calcium-phosphate-mediated transfection.....	22
2.3.3 Cultivation of immortalised brown preadipocytes.....	23
2.3.4 Analysis of lipid storage and lipolysis.....	26
<b>2.4 Isolation of mitochondria.....</b>	<b>28</b>
2.4.1 Isolation of HEK293 mitochondria.....	28
2.4.2 Isolation of mitochondria from cultured brown adipocytes.....	29
2.4.3 Isolation of mitochondria from brown adipose tissue.....	29
<b>2.5 Measurements of mitochondrial and cellular bioenergetics.....</b>	<b>30</b>
2.5.1 Determination of proton leak kinetics of isolated mitochondria.....	30
2.5.2 Analysis of oxygen consumption of trypsinised cells.....	37
2.5.3 Analysis of oxygen consumption of adherently growing cells.....	37
<b>2.6 Statistical analysis.....</b>	<b>39</b>

<b>3</b>	<b>Results .....</b>	<b>41</b>
<b>3.1</b>	<b>UCP1 activity in liposomes, HEK293 cells, immortalised brown adipocytes and isolated BAT mitochondria .....</b>	<b>41</b>
3.1.1	UCP1 activity in liposomes .....	41
3.1.2	UCP1 activity in HEK293 cells .....	43
3.1.3	UCP1 activity in immortalised brown adipocytes (BFC) .....	54
3.1.4	UCP1 activity in mitochondria isolated from mouse BAT .....	61
3.1.5	Comparison of UCP1-dependent proton leak and catalytic activity in different test systems .....	63
<b>3.2</b>	<b>Interaction of CideA and UCP1 in different test systems.....</b>	<b>67</b>
3.2.1	Generation of an antibody for CideA detection.....	67
3.2.2	CideA expression in mouse tissues.....	69
3.2.3	Interaction of CideA and UCP1 reconstituted into liposomes .....	69
3.2.4	Interaction of CideA and UCP1 in HEK293 cells .....	72
3.2.5	Overexpression of CideA in immortalised brown adipocytes.....	75
<b>4</b>	<b>Discussion .....</b>	<b>80</b>
<b>4.1</b>	<b>Suitability of HEK293 cells and BFC as test systems for UCP function .....</b>	<b>80</b>
4.1.1	Expression of UCP1 in HEK293 UCP1 and BFC .....	80
4.1.2	Regulation of UCP1 activity in HEK293 UCP1 and BFC mitochondria .....	84
4.1.3	UCP1 in HEK293 UCP1 and BFC: No uncoupling artefact or contribution to basal leak .....	85
4.1.4	Basal activity of UCP1 in the cellular context.....	86
4.1.5	Secondary effects of UCP1 expression in HEK293 and BFC .....	88
4.1.6	Catalytic activity of UCP1 in the different test systems .....	90
4.1.7	Potential of the HEK293 cells and BFC for UCP research .....	92
<b>4.2</b>	<b>Interaction of UCP1 and CideA in different test systems.....</b>	<b>94</b>
4.2.1	CideA, a mitochondrial protein? .....	94
4.2.2	No effect of CideA expression on UCP1 activity in the test systems .....	94
4.2.3	CideA as a regulator of lipid metabolism? .....	96
4.2.4	Interaction of CideA and UCP1 via fatty acid levels .....	97
<b>5</b>	<b>Summary and Conclusion .....</b>	<b>99</b>
<b>6</b>	<b>References.....</b>	<b>101</b>
<b>7</b>	<b>Appendix.....</b>	<b>110</b>
<b>7.1</b>	<b>Material .....</b>	<b>110</b>
<b>7.2</b>	<b>qRT PCR.....</b>	<b>112</b>
<b>7.3</b>	<b>Vectors.....</b>	<b>113</b>
<b>7.4</b>	<b>Seahorse protocol.....</b>	<b>113</b>

<b>8</b>	<b><i>Kurzfassung (Abstract)</i></b> .....	<b>114</b>
<b>9</b>	<b><i>Erklärung</i></b> .....	<b>115</b>
<b>10</b>	<b><i>Curriculum Vitae</i></b> .....	<b>116</b>
<b>11</b>	<b><i>Danksagung</i></b> .....	<b>119</b>

## Abbreviations

AA	Amino acid
ACC	Acetyl-CoA-carboxylase
ADP	Adenosine diphosphate
ANT	Adenine nucleotide translocase
BAT	Brown adipose tissue
BFC	Brown fat cell line
CAT	Carboxyatractylate
CCCP	Carbonyl cyanide 3-chlorophenylhydrazone
CideA	Cell death inducing DFFa like effector A
DMEM	Dulbecco's modified eagle medium
FAF	Fatty acid free
FBS	Fetal bovine serum
FCCP	Carbonyl cyanide 4-(trifluoromethoxy)phenylhydrazone
FFA	Free fatty acids
GDP	Guanidine diphosphate
HCP	Highest common potential
HEK293	Human embryonic kidney cells
HNE	4-Hydroxy-2-nonenal
IBMX	3-Isobutyl-1-methylxanthine
IPTG	Isopropyl- $\beta$ -D-thiogalactopyranosid
PAGE	Polyacrylamide gel electrophoresis
PBS	Phosphate- buffered saline
PVC	Polyvinylchloride

RCR	Respiratory control ratio
RT	Room temperature (22-24°C)
SDS	Sodiumdodecylsulfate
TBS	Tris-buffered saline
TPMP	Methyltriphenylphosphonium
T3	Triiodo-L-Thyronin
UCP	Uncoupling protein
WT	Wildtype

## Figures

Figure 1 Coupled and uncoupled respiration. ....	2
Figure 2 Models for activation of UCP1 catalysed proton flux by fatty acids. ....	4
Figure 3 Schematic illustration of CideA primary structure. ....	8
Figure 4 Principle of liposome assay for UCP1 function. ....	21
Figure 5 Clark-electrode. ....	31
Figure 6 Setup for proton leak measurements. ....	34
Figure 7 Principle of Seahorse XF96 analysis. ....	38
Figure 8 Analysis of UCP1 activity in liposomes. ....	42
Figure 9 Regulation of UCP1 activity in liposomes. ....	42
Figure 10 Subcellular localisation of UCP1 in HEK293 UCP1 cells. ....	44
Figure 11 Quantification of UCP1 standard solution and generation of a standard curve for UCP1 immunological signals. ....	45
Figure 12 Abundance of UCP1 protein in HEK293 UCP1 mitochondria and BAT mitochondria from RT-acclimated mice. ....	45
Figure 13 Proton leak kinetics of mitochondria isolated from HEK293 (A) and HEK293 UCP1 cells (B). ....	46
Figure 14 Comparison of mitochondrial leak respiration for HEK293 and HEK293 UCP1. ....	47
Figure 15 Basal proton leak of mitochondria isolated from HEK293 and HEK293 UCP1 cells. ....	48
Figure 16 Respiration ( $J_o$ ) of mitochondria isolated from HEK293 and HEK293 UCP1 cells. ....	49
Figure 17 Schematic illustration of Xpress-tagged UCP1 (tagUCP1) and immunological detection of tagUCP1 in mitochondria isolated from stably transfected HEK293 cells. ....	50
Figure 18 Proton leak kinetics of mitochondria isolated from HEK293 tagUCP1 cells. ....	51
Figure 19 Comparison of HEK293 UCP1 and HEK293 tagUCP1 mitochondrial leak respiration. ....	51
Figure 20 Respiration of trypsinised HEK293 and HEK293 UCP1 cells. ....	52
Figure 21 Oxygen consumption rate (OCR) of adherently growing HEK293 and HEK293 UCP1 cells in different respiratory states. ....	53
Figure 22 Fat accumulation in BFC during differentiation. ....	54
Figure 23 Stimulation of UCP1 expression in differentiated BFC. ....	55
Figure 24 Immunological detection of UCP1 and CideA in protein extracts from differentiated immortalised brown adipocytes. ....	56
Figure 25 Expression of UCP1 and CideA transcripts in differentiated and stimulated BFC. ....	57
Figure 26 RNA expression level of mitochondrial carriers and markers for mitochondrial proliferation in differentiated BFC after agonist treatments. ....	57
Figure 27 Proton leak kinetics of mitochondria isolated from differentiated and stimulated BFC. ....	58
Figure 28 Comparison of leak respiration of BFC mitochondria in different measurement conditions. ....	59

Figure 29 Respiration states and respiratory control ratio of isolated BFC mitochondria. ....	59
Figure 30 Oxygen consumption rate (OCR) of adherently growing BFC. ....	60
Figure 31 Proton leak kinetics of BAT mitochondria isolated from mice acclimated to RT or 30°C. ....	61
Figure 32 Comparison of leak respiration of BAT mitochondria isolated from mice acclimated to RT or thermoneutrality. ....	62
Figure 33 UCP1 expression in BAT mitochondria from mice acclimated to RT or 30°C. ....	63
Figure 34 UCP1-dependent proton leak in HEK293 UCP1 mitochondria. ....	64
Figure 35 UCP1-dependent proton leak in differentiated BFC cells. ....	65
Figure 36 UCP1-dependent proton leak in BAT mitochondria from mice kept at RT or at 30°C. ....	65
Figure 37 Catalytic activity of UCP1 in different test systems, expressing UCP1 at different expression levels. ....	66
Figure 38 CideA primary structure and epitopes chosen for the generation of a CideA antibody. ....	67
Figure 39 Development of immunoreactivity with CideA protein in the serum of a rabbit immunised with the CideA peptide Cter. ....	68
Figure 40 Specificity of CideA- immunoreactive signal. ....	68
Figure 41 Detection of CideA in different mouse tissues. ....	69
Figure 42 Expression of full length CideA and the N- and C-terminal half of CideA in <i>E. coli</i> . ....	69
Figure 43 Purification and refolding of full length CideA on a nickel-column. ....	71
Figure 44 Effect of Full length CideA and the N-terminal half of CideA on lauric acid-induced liposome polarisation. ....	72
Figure 45 Maximum respiratory capacity of trypsinised HEK293 and HEK293 UCP1 cells transfected with empty pcDNA3 vector or pcDNA3 CideA. ....	73
Figure 46 Respiration of trypsinised HEK293 and HEK293 UCP1 cells transfected with empty pcDNA3 vector and pcDNA3 CideA. ....	73
Figure 47 Immunological detection of CideA in HEK293 and HEK293 UCP1 cells, transiently transfected with pcDNA3 or pcDNA3 CideA for analysis of cellular respiration. ....	74
Figure 48 Oxygen consumption rate (OCR) of adherently growing HEK293 and HEK293 UCP1 cells, overexpressing GFP or CideA. ....	75
Figure 49 CideA expression during differentiation of BFC after viral transduction as preadipocytes. ....	75
Figure 50 Lipid accumulation in BFC expressing GFP or CideA. ....	76
Figure 51 Analysis of lipid droplet number and size after stimulation treatment in BFC expressing GFP or CideA. ....	77
Figure 52 Glycerol release during 48 h stimulation of thermogenic phenotype in BFC and upon subsequent acute 2 h stimulation with different isoproterenol concentrations. ....	78
Figure 53 Comparison of cell number in wells used for glycerol release assays and transfected with different viruses for expression of GFP or CideA. ....	79
Figure 54 Simplified illustration of the UCP1 promoter. ....	83
Figure 55 Hypothesis on the indirect interaction of CideA and UCP1. ....	98



**Tables**

Table 1 Antibodies for immunological detection of proteins. ....	15
Table 2 UCP1 expression in different experimental systems, species and at different acclimation temperatures. ....	82
Table 3 Comparison of the two mammalian cell lines used for UCP1 analysis.....	93

## 1 Introduction

The obesity epidemic and its secondary complications like diabetes and vascular diseases signify a constantly growing risk and burden to western societies. Therefore it is of major importance to develop efficient strategies to counteract this problem. Current strategies have proven to be inadequate so far, not being able to circumvent the body's mechanisms to defend its body weight. As therapies aiming at a consequent change of lifestyle seem to have low success on the long term, the pharmacological increase of energy expenditure provides an attractive opportunity to reduce lipid stores. A possible target for such a strategy is brown adipose tissue (BAT), which is an energy dissipating organ that has recently been shown to be present in adult humans (Cypess et al., 2009; van Marken Lichtenbelt et al., 2009; Virtanen et al., 2009). As BAT activation could release excess energy as heat and alongside improve lipid and glucose homeostasis (Whittle 2011), research focuses on the one hand on approaches aiming to increase the amount of brown adipose tissue in the body or on the other hand on finding direct activators of uncoupling.

### 1.1 Uncoupled respiration and its physiological significance

The efficiency of mitochondrial energy fixation contributes significantly to the overall energy balance of an organism. Analyses of rat muscle and hepatocytes established the estimation that inefficiency of oxidative phosphorylation is responsible for 20-30 % of basal metabolic rate (Brand et al., 1994; Rolfe and Brand, 1996). A further pharmacological reduction of the efficiency might be a strategy to treat obesity and prevent its secondary complications, referred to as the metabolic syndrome (Whittle et al., 2011).

The molecular process underlying the inefficiency of oxidative phosphorylation is a proton leak across the mitochondrial inner membrane. Protons, which have been pumped to the intermembrane space by the complexes of the respiratory chain, can get back into the mitochondrial matrix by a pathway different from ATP-synthase. This can be detected as oxygen consumption in the absence of ATP-synthesis which would not occur if the coupling of respiration and ATP synthesis via the proton cycling across the mitochondrial inner membrane were perfect. Activity of the respiratory chain in the absence of ATP synthesis reflects the compensation of these proton fluxes, needed to maintain proton motive force across the membrane (**Figure 1**).

All mitochondria have a basal proton leak and the molecular basis of this leak is not yet fully understood although a contribution of the ANT (adenine nucleotide translocase) was demonstrated in *Drosophila* (Brand et al., 2005). In addition to basal proton leak some mitochondria possess an inducible proton leak. Inducible proton leak is mediated by proteins in the mitochondrial inner

membrane which can be activated to mediate a net proton flux into the mitochondrial matrix. A group with major importance among these proteins are the uncoupling proteins (UCPs).

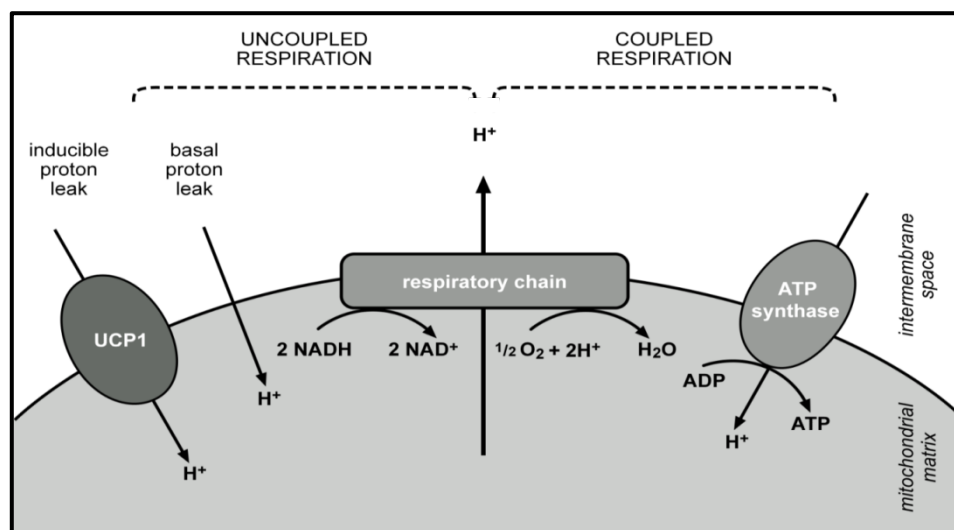


**Figure 1** Coupled and uncoupled respiration.

At the mitochondrial inner membrane energy from nutrient combustion is chemically fixed by phosphorylation of ADP to ATP. This reaction is catalysed by ATP synthase and driven by a proton gradient across the membrane. The gradient is built up by the complexes of the respiratory chain which receive electrons from reduction equivalents and pass them along a redox gradient on to oxygen, which is reduced to water. The energy released during this exergonic process is used to pump protons into the intermembrane space, creating the driving force for ATP synthesis. Oxygen consumption which serves to fuel this process is called coupled respiration. Oxygen consumption which is needed to maintain the driving force for ATP synthesis against alternative processes that reduce the proton gradient is called uncoupled respiration. The proton gradient across the membrane can be reduced by processes summed up as basal leak, which is present in all cells, and against inducible proton leak, which is dependent on catalytic proteins and their activation or inhibition. Inducible leak is not present in every cell. Major constituents of inducible leak are uncoupling proteins, like uncoupling protein 1, which is expressed in BAT mitochondria.

UCP1 was discovered first and is the best characterised uncoupling protein. It is expressed almost exclusively in brown adipose tissue, a specialised fat tissue. UCP2 and UCP3, which have been discovered due to sequence similarity to UCP1 are expressed in beta-cells and immune cells, or in skeletal muscle, heart and BAT. Expression levels are far below that of UCP1, which can constitute up to 8 % of mitochondrial protein mass (Lin and Klingenberg, 1980). The physiological role of UCP2 and UCP3 is less well understood, as knockout animals do not have a clear phenotype. There is evidence that UCP2 is involved in the regulation of insulin secretion, and UCP3 might be involved in fatty acid handling. Both are discussed to protect the cell from excess production of reactive oxygen species (ROS) (Brand and Esteves, 2005). The physiological role of UCP1 as an important component of the energy-dissipating reactions in BAT is generally accepted.

Small mammals, hibernators and rodents can defend their body temperature in a cold environment for long periods of time without the need to shiver, as they are able to produce heat in BAT. BAT can be distinguished from white adipose tissue (WAT) due to the presence of multilocular lipid vesicles, high mitochondrial content and strong vascularisation. When the tissue is activated by cold it can efficiently hydrolyse fat and produce heat. UCP1 is necessary for this fast cold-induced metabolic

switch, demonstrated by the cold-sensitive phenotype of UCP1-knockout mice, which are acutely exposed to the cold (Enerback et al., 1997; Golozoubova et al., 2001; Meyer et al., 2010). A constant activation of UCP1 would be of major significance for the overall energy balance due to its high expression level and energy dissipating function.

## 1.2 Molecular aspects of UCP1 function

In the attempts of understanding the extraordinary metabolism of brown adipocytes, it was found that the removal of free fatty acids as well as the addition of purine nucleotides was able to restore respiratory control, which means the coupling of oxygen consumption with ATP production (Rafael et al., 1969; Nicholls and Rial, 1999). Photoaffinity labelling experiments identified a 33 kDa protein as the nucleotide binding site and studies on purified UCP1 demonstrated that it was responsible for the nucleotide sensitive proton conductance of brown adipose tissue mitochondria (Heaton et al., 1978; Lin and Klingenberg, 1982). When finally the UCP1 cDNA sequence was identified, the protein was accessible for the expression in heterologous systems and for mutation studies (Aquila et al., 1985; Bouillaud et al., 1986).

UCP1 belongs to the family of mitochondrial anion carrier proteins, which comprises the UCPs the ANT, phosphate carrier and different transporters which are needed to supply the substrates for citric acid cycle and beta-oxidation (citrate, oxoglutarate, carnitine, etc.). UCP1 catalyses a net proton flux, which can be activated by free fatty acids and inhibited by purine di- and tri-nucleotides. In detail analysis of UCP1 activation by different fatty acids revealed that fatty acids with a chain length of 10 or more carbon atoms are very efficient activators and further that the higher the degree of unsaturation was, the stronger was the activation. Fatty acid activation is also dependent on pH and increases with lower pH, most likely as this increases the chance of having an unesterified carboxylgroup at the end of the fatty acid chain, a requirement for efficient activation of UCP1 by fatty acids (Rial et al., 1983).

The exact mechanism of UCP1-catalysed proton flux is still debated. This can partly be explained by the fact that the three-dimensional structure of UCP1 could not be resolved so far, which would allow to predict transport pathways and interacting surfaces for activators and inhibitors. One model for fatty acid activated proton transport suggests that fatty acids are necessary cofactors which are inserted into the proton transport channel and provide the interaction surface, allowing protons to cross the phospholipid membrane (**Figure 2A**) (Klingenberg and Huang, 1999). Another model proposes that fatty acids are cofactors, which are necessary to overcome inhibition by purine nucleotides and allow proton translocation by UCP1 (**Figure 2B**) (Shabalina et al., 2004; Winkler and Klingenberg, 1994). A third hypothesis postulates that fatty acid anions are the substrate of transport for UCP1 and that their export from the mitochondrial matrix followed or preceded by a flip-flop of

the protonated fatty acid from the intermembrane space into the mitochondrial matrix leads to the net proton flux catalysed by UCP1 (**Figure 2C**) (Garlid et al., 1998; Jezek et al., 1994; Skulachev, 1991).

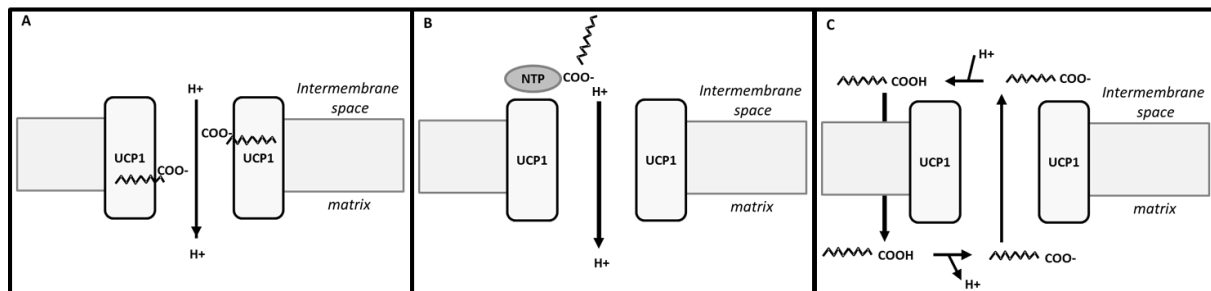


**Figure 2 Models for activation of UCP1 catalysed proton flux by fatty acids.**

In A, fatty acids are cofactors which bind to UCP1 and provide the hydrophilic surface in the transport channel, interacting with the transported protons. In B, fatty acids are needed to overcome the inhibition of UCP1 mediated proton transport by purine nucleotides (NTP). In C, fatty acids anions are the transported substrate of UCP1 and proton flux is established as the protonated fatty acid crosses the membrane via a flip-flop mechanism and releases a proton in the mitochondrial matrix (adapted from (Krauss et al., 2005)).

Characterisation of nucleotide inhibition on the one hand identified the affinity of different nucleotides to UCP1 and established its dependence on pH (Nicholls, 1976). These first studies already suggested that fatty acids and nucleotides act on different sites of the protein, which is in accordance with the model of competitive kinetics of the two regulators, established by Shabalina and colleagues (Shabalina et al., 2004). On the other hand mutational studies have led to the identification of a nucleotide binding site in the UCP1 sequence. It seems that a region in the C-terminal part of the protein as well as individual amino acid residues distributed in the primary sequence provide charges for the interaction (Winkler et al., 1997; Modriansky et al., 1997; Echtay et al., 1998). According to the three-dimensional model these residues position in close proximity to each other.

Since its identification and the more detailed description of the regulation by fatty acids and purine nucleotides, few new regulators of UCP1 function have been identified. Activation by HNE (4-hydroxy-2-nonenal) and superoxide has been demonstrated for all three uncoupling proteins and regulation by these molecules supports the idea that uncoupling proteins also help to prevent the production of reactive oxygen species (ROS) by a feedback mechanism (Echtay et al., 2002; Echtay et al., 2003). ROS are more likely produced at high membrane potential and if they would activate uncoupling their excess accumulation could be prevented by a feedback loop (Skulachev, 1996). An additional small molecule, genipin, has been published as inhibitor of UCP2 function (Zhang et al., 2006) and a protein, CideA (cell death-inducing DFFA-like effector A), has been published as direct inhibitor of UCP1 (Zhou et al., 2003).

### 1.3 Beneficial effects of increased uncoupling and human BAT

UCP2 and UCP3 were always known to be present in adult humans, but they were never really regarded as targets for pharmacological obesity therapy, as their low expression level precluded a significant contribution to metabolic rate. Furthermore, the UCP2- and the UCP3- as well as the UCP2/ UCP3 double-knockout mouse did not have increased susceptibility to obesity (Arsenijevic et al., 2000; Gong et al., 2000; Vidal-Puig et al., 2000). On the other hand, several mouse models with ectopic expression or overexpression of uncoupling proteins, for example in fat tissue or skeletal muscle, were protected from obesity (Kopecky et al., 1995; Clapham et al., 2000). Beneficial effects of uncoupling on survival rate have also been shown for mice, as Speakman and colleagues measured metabolic rate of a cohort of mice and assigned them to groups of high and low metabolic rate. Animals with high metabolic rate had a higher degree of uncoupling in skeletal muscle mitochondria but showed increased survival rates (Speakman et al., 2004). Pharmacological strategies which globally increase peripheral uncoupling have been applied to treat human obesity in the 1930s, by application of the mitochondrial uncoupler DNP (2,4-dinitrophenol). It was no longer applied after 1938 as it had only a narrow therapeutical window and deleterious side effects, including death, upon wrong dosage (Harper et al., 2008). A much more feasible approach would be the use of uncouplers with a broad therapeutic range or with only one specific target tissue. This could reduce general disturbances of bioenergetics in the body, like ATP-production, metabolite transport or ROS metabolism, which can be expected as side effects of treatment with global uncouplers.

In 2009 several publications have established that also adult humans possess functional BAT and not only newborns at the thermoregulatory challenging phase of birth (Cypess et al., 2009; van Marken Lichtenbelt et al., 2009; Virtanen et al., 2009). Since then there are increasing efforts to manipulate BAT proliferation and differentiation and find molecules which can activate BAT-mediated uncoupling. This should exert some of the beneficial effects of uncoupling which have been described above and would represent a targeted uncoupling in a specific tissue, which has evolved to fulfil specifically this purpose. Besides their effect on energy balance activators of BAT function could also improve glucose homeostasis and lipid metabolism, given the large disposal of these nutrients in BAT (Bartelt et al., 2011; Meyer et al., 2010).

Alongside all of these attempts to increase BAT mass and find activators of the tissue there is still the need to understand the mechanistic function, which is underlying all these beneficial effects. Direct pharmacological activation of UCP1 is probably a much more feasible approach to manipulate energy balance than to interfere with complex central regulation and recruitment processes. Answering mechanistic and regulatory questions will depend on the availability of suitable test systems, which are sufficiently accessible to manipulations, show little inter-experimental variability but are still close to the physiological background of uncoupling proteins, in case of UCP1 the mammalian brown adipocyte.

## 1.4 Test systems for UCP1 function

Questions on uncoupling protein function have been addressed in test systems ranging in their complexity between phospholipid bilayer membranes and knockout animals. Before the identification of the UCP1 sequence research relied on BAT mitochondria and protein which had been isolated from the native source. The availability of the cDNA sequence allowed using heterologous expression in model organisms. The different experimental models mainly differ in their susceptibility to manipulation and their similarity to the native background. Depending on the experimental question, a more *in vitro* or *in vivo* model should be applied.

Studies in proteoliposomes could show that no other proteins are needed to mediate the fatty acid mediated and nucleotide sensitive proton transport and they were used to determine the influence of membrane composition on UCP1 activity (Brookes et al., 1997; Heaton et al., 1978; Lin and Klingenberg, 1982). Heterologous expression in *E. coli* and yeast has been performed to produce native or mutant protein for analyses in membrane systems. Such studies have been conducted to characterise the purine nucleotide binding site for example (Echtay et al., 1998; Winkler et al., 1997). Yeast has also been used as a direct source for mitochondria containing UCP1, for example establishing the role of Coenzyme Q for UCP1 function (Esteves et al., 2004). A disadvantage of the yeast system is however, that UCP1 expression above a critical level can cause an uncoupling artefact, a proton flux which cannot be regulated (Stuart et al., 2001b). Nevertheless yeast has been used for a proteomic study, comparing the mitoproteome of control cells and yeast with heterologous overexpression of UCP1, an attempt to characterise the physiological consequences of uncoupling in the cell (Douette et al., 2006). Different attempts have been made to create mammalian cell culture models, either heterologous expression models or brown adipocyte lines, allowing the analysis of UCP1 function in a system which is close to the native background but still easy to manipulate. UCP1 in CHO cells seemed to be regulated in an initial study but showed UCP1 expression of 10 % of what is found in warm acclimated mice (Casteilla et al., 1990; Mozo et al., 2006b). Low expression level of UCP1 in a test system on the one hand complicates functional analyses and on the other hand does not reflect the native environment of UCP1, as its energy dissipating function depends on the high expression level. UCP1 expression in immortalised adipocyte cell lines, another test system, was also mostly too low to be detectable on the protein level. Studies on UCP1 RNA expression have largely increased the knowledge about the regulation of the expression of UCP1 (Klein et al., 2002; Klaus et al., 1994). These cell lines were applied to understand changes occurring during the differentiation of the brown adipocyte, which contribute to maintain thermogenic function.

The most important model for the determination of the physiological role of UCP1 is the UCP1 knockout (KO) mouse. It was established in 1997 and these animals are not able to defend their body temperature upon acute cold exposure (Enerback et al., 1997). The expected effect of an increased

body weight was not observed in these animals and was disputed later as it seemed to be absent due to the acclimation temperature of the animals. The fact that knockout animals are even leaner than wildtypes (WT) when kept at moderate cold (Liu et al., 2003), suggested that alternative heat production in knockout animals demanded more energy and masked the obesogenic effect when they were kept at room temperature (RT). A higher susceptibility of UCP1-knockouts towards obesity was present at thermoneutral housing temperature of mice (30°C) (Feldmann et al., 2009). Studies trying to elucidate the alternative mechanism of heat production in knockout mice suggest either white fat or skeletal muscle to be the source of the heat (Monemdjou et al., 1999; Ukropec et al., 2006; Meyer et al., 2010). Whatever mechanism that is, it seems to be inferior to UCP1 mediated thermogenesis and leads to reduced survival of knockout animals in the cold, maybe also due to an increased ROS production (Golozoubova et al., 2001; Oelkrug et al., 2010). The knockout mouse is very useful to dissect UCP1 mediated effects from other reactions taking place in mitochondria. They have for example been applied to answer the question of a contribution of UCP1 to basal proton leak. Parker and colleagues found increased basal leak in brown adipose tissue mitochondria of WT compared to KO mice, which was not confirmed by Shabalina *et al.* in a later study (Parker et al., 2009; Shabalina et al., 2010).

Transgenic mouse models with overexpression or ectopic expression have been especially useful to evaluate the possible beneficial effect of increased uncoupling on whole body energy homeostasis, which is a crucial question regarding the therapeutic potential of UCP1 mediated uncoupling (Kopecky et al., 1995; Clapham et al., 2000).

A disadvantage of transgenic mouse models is illustrated by the finding, that the thermo-sensitive phenotype of the knockout mouse is dependent on its genetic background (Hofmann et al., 2001). Individual life history and compensatory reactions of animals can lead to misleading results. This disadvantage can be overcome by using knockout models which can be induced at adult age, but this has not been done for UCP1 yet.

Increasing the amount of active BAT and identification of drugs that allow its activation are the two major tasks to make it a possible target for the treatment of obesity. Cell culture systems seem to be the most promising approach for drug screenings, although proteoliposomes have also been suggested for such high-throughput screenings (Mozo et al., 2006a). Considering the non-native function of UCP1 in this and other existing expression systems and the low expression levels in adipocyte models it would be of great advantage to have a new mammalian cell line for this purpose. This is why we generated the HEK293 UCP1 cell line, which was characterised in detail in this thesis and compared with a brown adipocyte cell line. Both cell lines were applied to reproduce and understand the interaction of UCP1 and CideA, which besides purine nucleotides is the only known inhibitory factor of UCP1 and the only known interacting protein for UCP1.



## 1.5 CideA

CideA is a 25 kDa globular protein which was identified due to homology to the DNA fragmentation factor. It belongs to the CIDE protein family, whose members all share a homology domain in the N-terminal half of the protein which is supposed to mediate interaction with other proteins and thereby regulate protein activity (Inohara et al., 1998a). Possible protein functions of CideA are regulation of apoptosis, regulation of lipolysis and regulation of UCP1 activity and different functions could be assigned to different subdomains of the protein (**Figure 3**) (Inohara et al., 1998a; Zhou et al., 2003).



**Figure 3** Schematic illustration of CideA primary structure.

The N-terminus (Cidea\*) is unique for CideA within the CIDE family. The CideN and CideC domain are also found in the other members of the CIDE family. CideN is similar to a domain of DNA fragmentation factor  $\alpha$  and seems to be important for interaction with other proteins and regulation of protein activity. The C-terminal domain seems to be involved in the apoptotic function (Inohara et al., 1998a).

The function of CideA was further characterised by the analysis of a knockout mouse model. These mice were resistant to diet-induced obesity, had higher metabolic rate, higher lipolysis and higher core body temperature when exposed to the cold. Due to altered lipid metabolism adipose storage in WAT and BAT was diminished (Zhou et al., 2003). In contrast to that another study found no correlation of CideA expression with the obesity status of mice, but a negative regulation of lipolysis in BAT was found (Nordstrom et al., 2005). An upregulation of CideA in response to high-fat diet feeding could be detected in liver (Baur et al., 2006) and its transcriptional regulation by PPAR $\alpha$  and PPAR $\gamma$ , the major regulators of lipid metabolism, was described (Viswakarma et al., 2007). A regulation of CideA level in response to insulin was shown in human adipocytes (Ito et al., 2011; Ito et al., 2010).

Human CideA is expressed in white adipose tissue and is involved in the regulation of lipid metabolism. Expression levels correlate inversely with body fat status and basal lipolysis and they are altered by reduction of caloric intake (Gummesson et al., 2007). Furthermore a polymorphism in exon 4 could be correlated with BMI (Dahlman et al., 2005).

A recent publication explains the metabolic phenotype of the CideA knockout animals by a downregulation of AMP-activated protein kinase (AMPK) in BAT (Qi et al., 2008). CideA mediates degradation of this kinase which leads to lower rates of lipolysis. The authors also show that CideA and UCP1 are upregulated in BAT of mice fed a high-fat diet. In the same year another group

assigned to CideA a function as lipid droplet protein, which is negatively associated with insulin sensitivity in humans (Puri et al., 2008). CideA expression was correlated with increased lipid droplet size in several cell models, including COS1 cells, human white adipocytes and rodent brown adipocytes.

Besides the interaction with AMPK there is evidence for an interaction of CideA with UCP1, identified during the characterisation of CideA knockout animals. CideA was co-localised with UCP1 in mitochondria and the two proteins could be co-immunoprecipitated. Furthermore co-expression of CideA in yeast with a constitutionally active version of UCP1 inhibited lowering of membrane potential which was observed upon UCP1 expression alone (Zhou et al., 2003). All these data suggest an interaction of CideA and UCP1. The question remains, however, whether the two proteins bind each other *in vivo* in the cellular environment. Although there are conflicting results on its exact function, the suggested importance for the regulation of energy metabolism on the level of lipid storage or energy expenditure in BAT makes CideA an interesting candidate for further studies.

The availability of two mammalian cell culture test systems for UCP1 function created the opportunity to investigate the interaction of CideA and UCP1 in the cellular environment in this thesis. The application of human embryonic kidney cells (HEK293) with stable expression of UCP1 and a cell line of immortalised brown preadipocytes, which can be differentiated into mature brown adipocytes, in this context was also part of their characterisation as test systems for UCP1 function, proving their suitability. Considering the regrown interest in BAT and plans to target it for the treatment of obesity, it is of major importance to answer remaining questions on the mechanistic and physiological function of UCP1 to exclude negative side effects. Such research will largely depend on mammalian model systems, given the disadvantages of liposome or yeast systems mentioned above. Furthermore cell culture systems might be the method of choice for high-throughput screenings, aiming to discover new regulators of UCP function, which would be needed to target human BAT for the treatment of obesity and its secondary complications.

## 2 Material and Methods

### 2.1 Molecular biology

In order to determine heterologous UCP1 and CideA expression and to monitor the expression of further genes, basic methods for the analysis of nucleic acids and proteins were applied.

#### 2.1.1 RNA isolation, cDNA synthesis, qRT PCR

It is known from the literature that stimulation of brown adipocytes with isoproterenol, retinoic acid and rosiglitazone probably activates major signalling cascades and results not only in the upregulation of UCP1, but also in increased expression of various other transcripts, which might contribute to basal or fatty acid-inducible proton leak. The expression level of those was determined with qRT PCR.

The principle of qRT PCR is that the initial amount of a transcript is determined by the timepoint when DNA amount in the PCR reaction reaches a certain threshold. DNA amount is measured during the PCR using the dye SYBR green, which is fluorescent when it binds double-stranded DNA. The efficiency of the PCR reaction for a certain gene is accounted for with a separate standard curve for every pair of primers, which is generated via a serial dilution of a mixture of all templates. In order to correct for differences in cDNA concentration the abundance of transcript for 2 housekeeping genes was determined and expression levels of genes of interest were always related to them.

RNA isolation was performed with a commercial kit, according to the manufacturer's instructions (SV Total RNA Isolation System, PROMEGA). RNA was quantified photometrically (Nanodrop ND 1000, Peqlab) and 500 ng were subjected to denaturing gel electrophoresis, in order to assess the quality and integrity of the samples. The gel was cast as indicated below and samples were denaturated by mixing them with 10 µl DN-buffer and 1 µl of 0.5 mg/ml ethidium-bromide. Samples were incubated at 68°C for 15 min, kept on ice for further 5 min before they were mixed with loading buffer and put on the gel. The gel was run in MOPs buffer and if after the separation distinct bands of 18S rRNA and 28S rRNA were visible the samples were used for cDNA synthesis. cDNA was generated using the Quantitect Reverse Transcription Kit (QIAGEN), according to the manufacturer's instructions, adding 500 ng RNA per 10 µl reaction volume.

For the PCR reaction a commercial PCR mix (Immomix, Bioline), primers, water and SYBR green were mixed and put into the wells of a PCR plate (Eppendorf). The cDNA template was added separately to the single wells in a 1: 10 dilution. Reactions for cDNA samples were performed in triplicate, standard

reactions were performed in duplicate. After pipetting the plate was shortly centrifuged, sealed with a foil and then analysed using a Realplex<sup>4</sup> S mastercycler (Eppendorf).

#### *MOPS buffer*

(20 mM MOPS, 5 mM sodium acetate, 1 mM disodium EDTA, pH 7)

#### *Denaturing RNA gel*

(1 % (w/v) agarose, 5 % (v/v) formaldehyde, MOPS buffer)

#### *DN-buffer*

(60 % (v/v) formamide, 20 % (v/v) formaldehyde, MOPS buffer)

#### *Loading buffer*

(50 % (v/v) glycerol, 0.25 % (w/v) bromphenol-blue, 0.25 % (w/v) xylene blue, 1mM EDTA)

#### *PCR-reaction mix for 1 well*

12.5 µl Immomix (Bioline)

0.5 µl SYBR Green 50x

0.1 µl primer forward (100 pmol/µl)

0.1 µl primer reverse (100 pmol/µl)

10.8 µl water

1 µl template

### 2.1.2 Protein extraction and quantification

Protein samples for assay normalisation and/or subsequent western blot analysis were either obtained by isolation of mitochondria according to the protocols in paragraph 2.4.1 to 2.4.3 or by RIPA-protein extraction from cultured cells or tissues. Depending on buffer composition, sample volume or the needed accuracy of the result protein samples were quantified using one of the following methods. Mitochondria isolated for functional measurements were determined by biuret method, protein samples for immunological analyses mostly with the BCA method while the standard of purified UCP1 was quantified with the Lowry method. All rely on the principle of copper-protein chelation and the subsequent photometrical detection of reduced copper.

### 2.1.2.1 RIPA protein extraction

Total protein extracts of cells were generated by removing the medium of cultured cells, washing them with PBS and freezing them at -80°C. For isolation RIPA buffer was added to the frozen cells which were collected with a rubber-policeman and transferred to an eppendorf tube. Cell lysis was achieved by incubating the cells shaking at 4 °C for 15 min. Solubilised proteins were separated from insoluble membranes and cell debris by 15 min centrifugation at 14,000 g at 4°C. Supernatants were transferred to a new tube and used for assay normalisation or immunological analyses.

#### *RIPA-buffer*

(50mM Tris-Cl, 1 % NP-40, 0.25 % sodium-deoxycholate, 150mM NaCl, 1 mM EDTA, 1/1,000 protease inhibitor cocktail (Sigma # P8340))

### 2.1.2.2 Biuret protein determination

For protein quantification with the Biuret method the absorbance at 540 nm was determined and protein concentration was calculated by comparison to the absorbance of BSA concentrations from 0 to 10 mg/ml in the respective test buffer. Standard solutions were mixed with sodium-deoxycholate and biuret reagent and incubated at RT for 30min. Absorption at 540 nm was plotted against protein concentration and the slope of the resulting curve was the calculation factor for subsequent sample analyses.

Protein concentration of samples was determined by mixing 10 µl of sample with 170 µl of buffer and 20 µl of sodium-deoxycholate in a 1 ml plastic cuvette. 180µl buffer and 20µl sodium-deoxycholate were used as reference. 800 µl of biuret reagent was added to each of them and samples were incubated for 30 min at RT. Subsequently their absorption at 540 nm was determined and protein concentration was calculated by using the standard factor.

#### *Biuret reagent*

(0.15 % (w/v) coppersulfate, 0.6 % (w/v) sodium-potassium-tartrate, 3 % (w/v) sodium-hydroxid, 0.1 % potassium iodide in water)

#### *5 % sodium-deoxycholate*

### 2.1.2.3 *BCA protein determination*

Protein samples for western blot analyses were quantified with the BCA (bicinchoninic acid) method, using a commercial kit from the company ThermoScientific (BCA Protein Assay Kit, ThermoScientific Pierce). Analysis was performed in 96well format according to the manufacturer's instructions, protein samples were diluted between 1:5 and 1:10 to be within the detection range of the assay.

### 2.1.2.4 *Lowry protein determination*

The standard solution of recombinant UCP1 was quantified with the Lowry method, due to better buffer compatibility and higher accuracy compared with other methods for protein determination. A commercial kit from the company ThermoScientific (Modified Lowry Protein Assay Kit, ThermoScientific Pierce) was applied and used in 96well format according to the manufacturer's instructions.

## 2.1.3 Immunological detection of proteins

Immunological detection of the subcellular localization of UCP1 in HEK293 UCP1 cells was performed in fixed cells. But in general protein abundance in a mixed protein sample was tested by separation of protein samples with SDS-PAGE, subsequent transfer of proteins onto a nitrocellulose membrane, followed by immunological detection using specific primary antibodies and secondary antibodies conjugated either with horseradish peroxidase or fluorescent dyes.

### 2.1.3.1 *Immunocytochemistry*

UCP1 was detected in fixed and permeabilised HEK293 UCP1 cells to assess its subcellular localisation. HEK293 UCP1 cells were grown on Poly-D-Lysin coated coverslips, which were kept in the wells of a 12well plate. Incubation and washing steps were also performed in the wells. Subconfluent grown cells were washed with PBS and then fixed by the addition of ice-cold methanol (-20°C). Methanol was removed after 30 min and cells were permeabilised with PBS/0.1 % (v/v) TritonX100 for 10 min. Afterwards unspecific binding sites were blocked by an 1 h incubation with PBS/5 % normal goat serum and then the coverslips were incubated with the primary antibody (Otto3, 1:1000) for 1h at RT. Cells were washed three times for 5 min with PBS before they were incubated with the secondary antibody (goat anti rabbit Alexa<sub>488</sub>, 1:250) for 1 h. Afterwards cells were washed again three times with PBS before the coverslips were mounted on microscope slides.

Mitochondrial staining was performed using mitotracker Deep Red (Invitrogen). Cells were kept in growth medium containing 100nM mitotracker for 15 min afterwards they were fixed, washed and mounted on microscope slides as described above.

#### 2.1.3.2 SDS-PAGE

Gel electrophoresis was performed in the Mini Protean II system (Bio-Rad). Stacking gel and separation gel were cast in the vertical system and submerged in running buffer. Defined amounts of protein were mixed with loading buffer, heated to 95 °C for 5 min and loaded on the gel. Samples were separated at 150 V until the 10 kDa band of the pre-stained marker reached the bottom of the gel.

##### *Separation gel (2 gels, 12.5 % acrylamide)*

(3.33 ml acrylamide-solution (ROTH), 1.25 ml 8x-separation gel buffer (3 M Tris pH 8.8), 5.27 ml H<sub>2</sub>O, 100 µl SDS (10 % (w/v)), 50 µl 10 % (w/v) ammoniumperoxylsulfate (AMPS) (ROTH), 5 µl TEMED (ROTH))

##### *Stacking gel (2 gels, 3 % acrylamide)*

(0.5 ml acrylamide-solution (ROTH), 1.25 ml 4x-separation gel buffer (0.5 M Tris pH 6.8), 3.16 ml H<sub>2</sub>O, 50 µl SDS (10 % (w/v)), 30 µl 10 % (w/v) ammoniumperoxylsulfate (ROTH), 10 µl TEMED (ROTH))

##### *Running buffer*

(25 mM Tris pH 8.3, 192 mM glycine, 1 % (w/v) SDS)

##### *Loading buffer*

(0.0625 M Tris-HCl (pH 6.8), 2 % (w/v) SDS, 0.1 M DTT, 10 % glycerol, 0.1 % bromphenolblue)

##### *PageRuler prestained (Fermentas SM0671)*

#### 2.1.3.3 Protein transfer

Separated proteins were transferred to a nitrocellulose membrane by semi-dry transfer using Transblot SD (Bio-Rad). Gel and membrane were stacked between 4 layers of whatman paper, all components being submerged in transfer buffer before assembly. Proteins were transferred for 1 h at 1mA/cm<sup>2</sup>.

*Transfer buffer*

(48 mM Tris, 1.3 mM SDS, pH 9.2 adjusted with glycine, 20 % (v/v) methanol)

*2.1.3.4 Immunological detection*

Proteins of interest were detected by specific primary antibodies, which were either detected with HRP-conjugated secondary antibodies and visualised with the ECL-reaction on films or using fluorescence labeled secondary antibodies (**Table 1**).

**Table 1** Antibodies for immunological detection of proteins.

Target protein	Primary antibody	Secondary antibody	Figure
UCP1	Otto 3 (rabbit) (1:50,000)	Goat anti rabbit HRP (1: 10,000)	Figure 10C, Figure 17B
UCP1	Otto 3 (rabbit) (1: 50,000)	Goat anti rabbit IRdye <sub>800</sub> (1: 25,000)	Figure 11B, Figure 12A, Figure 23, Figure 24, Figure 33A
UCP1	Otto 3 (rabbit) (1: 1,000)	Goat anti rabbit Alexa <sub>488</sub> (1: 250)	Figure 10B
CideA	Cter#3 (rabbit) (1: 10,000)	Goat anti rabbit HRP (1: 10,000)	Figure 39, Figure 40
CideA	Cter#3 (rabbit) (1: 10,000)	Goat anti rabbit IRdye <sub>800</sub> (1: 25,000)	Figure 24, Figure 47, Figure 49

Membranes were blocked with a TBS-buffer containing 3 % (w/v) BSA before they were incubated with antibodies. Antibodies were diluted in TBS/0.1 % Tween and kept on the membrane over night at 4°C or 1 h at RT. Washing steps between first and second antibody and between second antibody and detection were performed with TBS/0.1 % Tween. The washing procedure started with one brief wash, one 15 min incubation followed by three 5 min washes using fresh buffer for each step. HRP-conjugated antibodies were detected with a chemoluminescence reaction, using a commercial kit (Amersham ECL Western Blotting System, GE Healthcare). Light emission reporting presence of secondary antibody was documented on X-ray films. Antibodies labelled with IR-dye fluorophores were detected via the Odyssey scanner (Licor).



### 2.1.3.5 Coomassie staining of SDS- gels

In order to analyse protein fractions after induction of bacterial cultures and to determine the purity of recombinant UCP1 standard SDS gels were run and subsequently stained in coomassie dye. Gels were kept in the staining solution for 1 h at RT and subsequently incubated for several washing steps in washing solution. This was repeated until protein bands were visible. The band intensity could be quantified by scanning the coomassie fluorescence at 680 nm in the Odyssey scanner (Licor).

#### *Coomassie solution*

(0.2 % (w/v) coomassie blue R-250, 30 % (v/v) EtOH, 10 % (v/v) acetic acid, 60 % (v/v) H<sub>2</sub>O)

#### *Destaining solution*

(30 % (v/v) methanol, 10 % (v/v) acetic acid, 60 % (v/v) H<sub>2</sub>O)

### 2.1.3.6 Determination of standard purity

Recombinant standard purity was determined by separating different amounts of standard on an SDS PAGE and subsequent coomassie-staining of the gel. The intensity of staining was determined for the UCP1 protein band and the entire lane by applying the Licor software. The ratio of band signal to lane signal was averaged for different standard amounts and reported the purity of the standard, which was used to correct the result of the protein quantification with the Lowry-method.

## 2.2 Liposome analysis

UCP1 was reconstituted into liposomes and its function was assessed in the absence or after addition of CideA. This system was used to evaluate whether the interaction between the two proteins was direct or indirect.

For this purpose UCP1 was isolated from interscapular brown adipose tissue of cold acclimated mice and purified using a hydroxyapatite column, whereas CideA was heterologously expressed in *E. coli*, purified and refolded from inclusion bodies. As CideA was sequestered in inclusion bodies and tended to precipitate upon reconstitution, not only the entire CideA was expressed but also the N-terminal part and the C-terminal part separately. Isolated UCP1 was reconstituted into liposomes and its function assessed upon addition of purified CideA.

### 2.2.1 Purification and reconstitution of mouse UCP1

In order to obtain sufficient amounts of UCP1 protein, the interscapular BAT from several cold acclimated mice was dissected, mitochondria were isolated and UCP1 was solubilised and purified from the mitochondrial fraction.

#### 2.2.1.1 *Isolation of BAT-mitochondria*

For the isolation of BAT mitochondria, the interscapular BAT depots of mice, which had been acclimated to 4°C for one week, were dissected and frozen at -20°C. Tissue was homogenised in Tris-buffer with a glass-teflon potter and the homogenate was centrifuged at 200 g for 10 min. The supernatant was transferred to a new tube and centrifuged again at 200 g for 10min. The new supernatant was again transferred to another tube and centrifuged at 11,000 g to pellet mitochondria. This also led to release of free fat, which could be removed from the top of the supernatant. The pellet was resuspended and mitochondria were pelleted once more at 11,000 g for 10 min. The resulting pellet was resuspended in 1 ml of buffer and protein concentration of the suspension was quantified with BCA assay.

#### *Tris-buffer*

(10 mM Tris, 200 mM sucrose, 0.16 mM EDTA pH 7.0)

#### 2.2.1.2 *Solubilisation and purification of UCP1*

The suspension buffer for the mitochondria was subsequently exchanged by a MOPS buffer and mitochondria were pre-solubilised with 3.2 % lubrol, by shaking for 30 min on ice. The solubilised mitochondria were separated by ultracentrifugation for 1 h at 100,000 g and 4°C, which resulted in 3 phases: a dark protein phase, a brighter membrane phase and liquid supernatant and lipids. The supernatant was removed and the other phases were solubilised for a second time with 2 % (v/v) Triton X100, shaking for 1 h on ice. After a second ultracentrifugation for 1 h at 100,000 g and 4 °C the supernatant was removed, the pellet washed once and supernatant and wash fraction were used for purification with a hydroxyapatite column (Bio-Rad). 0.5 ml of sample solution were loaded on 1.25 ml MOPS-buffer-equilibrated column material. UCP1 was recovered in the first flow-through fractions. UCP1 fractions were further purified with a sepharose column and bound to beads carrying a UCP1 antibody in order to remove detergent and lipids. After 2 h incubation at RT beads were recovered and UCP1 was eluted from the column with a 100 mM Glycin solution at pH 2.5. This was

immediately neutralised by a pH 8 Tris-solution preset in the collection tubes. Presence of UCP1 protein in elution fractions was tested with a SDS gel, which was stained with Coomassie.

#### *MOPS-buffer*

(20 mM MOPS, 20 mM Na<sub>2</sub>SO<sub>4</sub>, 0.16 mM EDTA)

### 2.2.2 Heterologous expression and purification of Cidea in *E.coli*

For heterologous expression in *E.coli* the full length CideA cDNA sequence or the N- or C-terminal half of it was inserted into the vector pHis17, which was replicated in bacterial cultures and subsequently induced for expression of the inserted cDNA sequence by addition of IPTG to the culture.

#### 2.2.2.1 *Transformation and bacterial culture*

Different CideA vectors were transformed into a bacterial strain, which had been selected for expression of mitochondrial carrier proteins (#41) (Miroux and Walker, 1996). This strain allowed the production of sufficient amount of protein, due to a higher membrane content which reduces toxicity of huge protein amounts in the cytosol of the cells.

For a large scale bacterial culture bacteria were first transformed with the vector of interest, by adding about 400 ng of plasmid to 50 µl of bacterial culture. After 20 min incubation on ice cells were heat-shocked at 42°C, 1 ml of pre-warmed SOC-medium was added and bacteria were incubated agitating for 1 h at 37°C. 200 µl were streaked onto a LB-agar plate containing 50 µg/ml ampicillin. In order to perform a large scale liquid culture a 50 ml pre-culture of LB medium containing ampicillin was inoculated with a transformed bacterial colony and incubated overnight shaking at 37°C. The next morning 2 l of pre-warmed LB were infected with 20 ml of pre-culture and growth of the culture was monitored by assaying optical density at 600 nm. Cultures were induced for protein expression at a density of OD<sub>600</sub> = 0.4-0.6 and grown for a further 2 h. Afterwards bacteria were collected by 15 min centrifugation at 2,000 g and 4°C. The supernatant was discarded and the pellet frozen at -20°C.

#### *LB-medium*

(0.5 % (w/v) yeast extract, 1 % (w/v) trypton, 0.5 % NaCl pH 7 sterile)

#### *SOC-medium*

(2 % (m/v) trypton, 0.5 % (m/v) yeast extract, 0.05 % (m/v) NaCl, 10 mM MgCl<sub>2</sub>, 10 mM MgSO<sub>4</sub>, 20 mM glucose)

### 2.2.2.2 Isolation and purification of CideA from bacteria

The bacterial pellet was resuspended and washed in buffer A and cells were pelleted again by 15 min centrifugation at 2,000 g 4°C. This pellet was resuspended in buffer A including PMSF and cells were disrupted by sonification. Inclusion bodies were separated by 15 min centrifugation at 10,000 g 4°C. The supernatant was subjected to ultracentrifugation to separate soluble fraction and membranes at 100,000 g for 1 h at 4°C (Beckmann, rotor Ti70). Soluble fraction, membranes and inclusion bodies were quantified with the BCA assay and tested for expression of CideA on a SDS gel which was stained with Coomassie.

As CideA was mainly located in the inclusion body fraction, this fraction was used for further purification and isolation. Inclusion bodies were washed by several steps of resuspension and centrifugation to remove intact cells and proteases. This was performed twice in buffer A containing 2 % TritonX and twice in buffer A. Subsequently inclusion bodies were quantified and frozen in 50 mg aliquots.

50 mg of inclusion bodies were solubilised by 30 min incubation at RT with 10 ml of buffer A containing 3 % (w/v) sarcosyl. Solubilised proteins were separated from the rest by centrifugation at 10,000 g. The resulting supernatant was separated by ultracentrifugation for 30 min at 100,000 g 4°C, yielding solubilised protein fraction and membrane fraction. The soluble fraction was diluted to 0.3 % (w/v) sarcosyl with buffer A and solubilised CideA was recovered from the clear supernatant with a nickel-sepharose column. CideA was also refolded on this column by slowly exchanging buffer A with sarcosyl to pure buffer A or to buffer A with 0.1 % FC12. Refolded CideA was eluted with increasing concentrations of imidazole, which was removed by a desalting column before the sample was concentrated with a centricon tube (millipore).

As full length CideA had a bad solubility and was located to inclusion bodies the N- (AA 1-110) and C- (AA 111-217) terminal part of the protein were expressed separately, in order to facilitate the isolation and purification process. Furthermore testing the effect of entire CideA, N-terminal CideA and C-terminal CideA could help to clarify which part of the protein interacts with UCP1. The N-terminus of CideA was indeed in the soluble fraction after disruption and separation of bacterial cells, whereas the C-terminal part was located in the inclusion body and the membrane fraction and precipitated during all attempts to refold and concentrate the protein.

#### *Buffer A*

(0.3 M NaCl, 50 mM phosphate ( $\text{Na}_2\text{HPO}_4/\text{NaH}_2\text{PO}_4$ ), pH 7.5)

### 2.2.3 Analysis of UCP1 function in liposomes

#### 2.2.3.1 *Reconstitution of purified UCP1 in liposomes*

Liposomes were generated as described previously (Mozo et al., 2006a). Phosphatidylcholine, phosphatidylethanolamine and cardiolipidin were mixed in chloroform, which was subsequently evaporated under nitrogen. The lipid film was resuspended in sulfate-buffer and liposomes were formed by sonication. UCP1 was added in the presence of TritonX which was removed afterwards by incubation with Biobeads. After dialysis against sucrose buffer liposomes were ready for analysis.

#### *Sulfate buffer*

(5 mM  $\text{KH}_2\text{PO}_4$ , 70 mM  $\text{K}_2\text{SO}_4$  pH 6.8)

#### *Sucrose buffer*

(200 mM sucrose, 0.5 mM HEPES, 0.5 mM EDTA pH 6.8)

#### 2.2.3.2 *Analysis of UCP1 transport activity in liposomes*

UCP1 activity in liposomes was determined by diluting liposomes in measurement buffer in a 1 ml cuvette which was placed in a photometer. Samples were stirred constantly and changes in Safranin O absorbance at 520 nm were recorded over time. As liposomes were formed in the presence of potassium but analysed in potassium free medium, this concentration gradient provided the driving force for the assay (**Figure 4A**). After a baseline recording nigericin was added to the liposomes, which resulted in the exchange of  $\text{H}^+$  and  $\text{K}^+$ . This exchange was electroneutral, but could lead to polarisation of liposomes if there was a second transport mechanism for protons back out of the liposomes. This could be either an artificial uncoupler like CCCP or a regulatable proton transporter like UCP1 (**Figure 4 C and D**). The proton translocation activity could be seen as the rate of decrease in Safranin O absorbance after addition of nigericin. CCCP was added in the end of each measurement to control for liposome volume and integrity. This measurement was performed with liposomes containing or not containing UCP1 and in the presence of known activators and inhibitors, as well as in the presence of isolated and purified full length CideA and the N-terminal part of CideA.

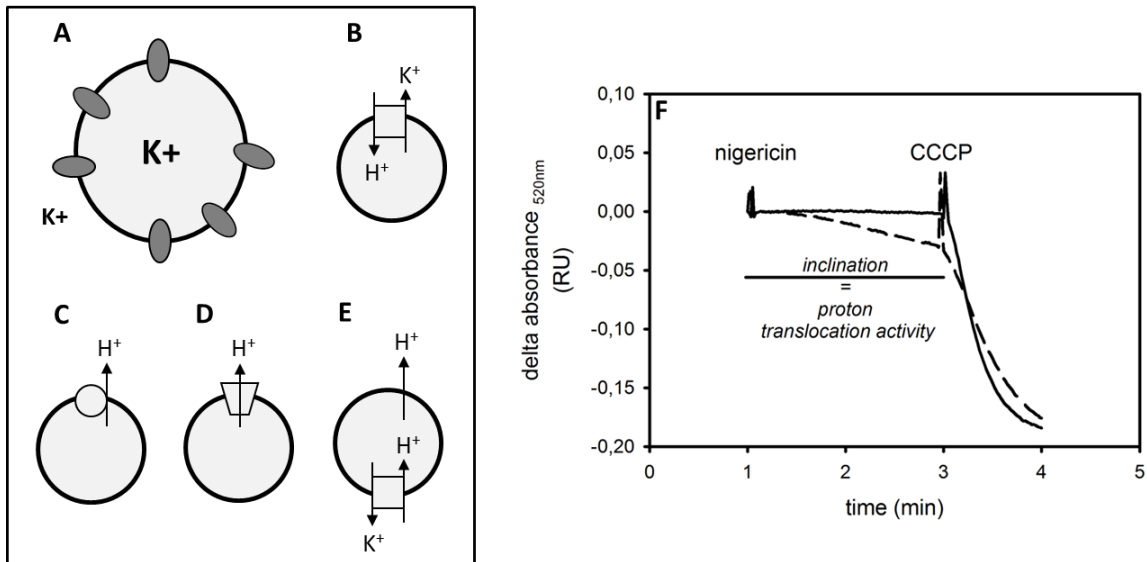


**Figure 4** Principle of liposome assay for UCP1 function.

Liposomes are membrane vesicles, into which membrane proteins can be inserted. (A) The inside of the vesicles contains high amounts of potassium compared to the measurement buffer, this concentration difference is the driving force for the functional assay. (B) In the presence of nigericin K<sup>+</sup> can be exchanged against H<sup>+</sup>, no polarisation occurs. (C) An uncoupler like CCCP allows unregulated proton translocation, leading to polarisation of the vesicle. (D) A regulatable proton translocator like UCP1 can lead to proton translocation and polarisation, depending on activation status. (E) Presence of nigericin and a proton translocating process leads to polarisation at a fixed rate, as long as the exchange of K<sup>+</sup> and H<sup>+</sup> provides enough protons for transport (modified after (Mozo et al., 2006a)) (F). The rate of polarisation after nigericin addition is a measure for the proton translocating activity of the reconstituted protein, addition of CCCP leads to full polarisation.

#### *Liposome measurement buffer*

(100 mM choline chloride, 40  $\mu$ M Safranin O pH 6.8)

## 2.3 Cell culture

### 2.3.1 Cultivation of HEK293 and HEK293 UCP1 cells

#### 2.3.1.1 *Seeding*

Cells were taken from cryoconservation in liquid nitrogen, thawed and washed with 5 ml prewarmed growth medium. Afterwards they were pelleted by 3 min centrifugation at 500 g, the supernatant was removed, cells were resuspended in 7 ml growth medium and put on a 10 cm culture dish. Cells reached confluency after 2-3 days and were transferred to new culture dishes or used for experiments.

*Growth medium HEK293*

(DMEM high glucose, 10 % (v/v) FBS superior, 50 µg/ml gentamicin)

*2.3.1.2 Proliferation*

For passage and dilution of a confluent 10 cm culture dish, growth medium was removed and the cell layer was washed with 2-3 ml prewarmed PBS. After removal of PBS cells were detached from the plate with 2 ml trypsin solution. Cells were resuspended in 5 ml growth medium, transferred to a falcon tube and pelleted by 3 min centrifugation at 500 g. The supernatant was removed and cells were resuspended in a suitable volume of growth medium and distributed on new culture dishes. If one confluent dish was diluted to seven new dishes, cells reached confluency again after 2-3 days.

*2.3.1.3 Cryoconservation*

Cell aliquots were stored in liquid nitrogen. For transfer of cells into this storage growth medium of a confluent 10 cm culture dish was removed, cells were washed with PBS and detached using trypsin solution. Afterwards cells were resuspended in 5 ml growth medium, transferred to a falcon tube and pelleted in a precooled centrifuge (3 min, 500 g, 4°C). The cell pellet was resuspended in 4 ml cryomedium, and prefrozen at -80°C in 1 ml aliquots before they were transferred into the liquid nitrogen.

*Cryomedium HEK293*

(10 % (v/v) DMSO, 81 % (v/v) DMEM high glucose, 9 % (v/v) FBS superior, filtered sterile 4°C)

**2.3.2 Transient or stable calcium-phosphate-mediated transfection**

DNA can be transfected into cells by generating a DNA-calcium co-precipitate, which is then added to the culture dish and subsequently taken up by endocytosis (Chen and Okayama, 1988). Part of such treated cells will introduce the DNA into the nucleus where encoded genes can be transcribed. Transfections like this lead with a maximum probability of  $10^{-4}$  to an insertion of the DNA into the genome of the cell, which would prevent degradation of the DNA and allow stable expression of the protein.

This method of transfection was on the one hand applied to introduce CideA and GFP expression vectors transiently into HEK293 and HEK293 UCP1 cells for subsequent analysis at the Clark

electrode. On the other hand it was also used to generate HEK293 UCP1 and HEK293 tag UCP1 cells showing stable protein expression. pcDNA3.1 and pcDNA 4 were used as vectors to transmit the gene of interest, the mouse UCP1 gene (NM 009463) into the genome of HEK293 cells. 24 h before the transfection cells were seeded onto new culture dishes at a number leading to a confluency of 60-70 % at the time of transfection. 1 h prior to transfection cells were supplied with fresh growth medium.

Plasmid DNA was mixed with CaCl<sub>2</sub> and water in the quantities given below, and the mixture was added dropwise to 2x HBS solution, while shaking the tube. Reagents were taken from a commercially available Kit (ProFection Mammalian, PROMEGA). The Mixture was incubated for 20 to 30 minutes at RT to allow the formation of precipitates.

Each 10 cm cell culture dish was treated with 1 ml of DNA-precipitate, which was added dropwise and distributed in the medium by gently swirling the plate. Cells were incubated for 8-16 h until the medium was aspirated and cells were washed with PBS to remove precipitates which had not been taken up by the cells. Afterwards cells were supplied with 7 ml fresh growth medium.

Cells with stable integration of the construct were selected by a 2 week treatment using the antibiotic geneticin. Resulting clonal colonies of cells which had stably integrated the vector were transferred to multwell plates using small trypsin-buffer soaked membrane pieces. Cell lines were grown separately and tested for UCP1 expression by western blot. The cell line with the highest UCP1 expression was chosen for further characterising experiments.

#### *Plasmids (Appendix)*

##### *DNA-mix per plate:*

DNA	20 µg (x µl)
CaCl <sub>2</sub>	50 µl
H <sub>2</sub> O	450 µl – x µl DNA
2x HBS	500 µl

### 2.3.3 Cultivation of immortalised brown preadipocytes

#### 2.3.3.1 *Isolation und immortalisation*

In order to establish an immortalised cell culture line of brown preadipocytes, the interscapular brown fat of newborn mice was dissected, minced with scissors and digested with collagenase.



Separated single cells were washed by centrifugation steps and cultivated in an incubator. 3 days after the isolation cells were treated with a virus, carrying the large T antigen of SV 40, which interferes with the cell cycle and immortalises cells by inactivation of tumor suppressor genes. After selection of cells which had integrated the virus and treatment against mycoplasma, aliquots were stored in liquid nitrogen for subsequent cultivation and experiments.

#### 2.3.3.2 *Cryo-conservation*

Cryo-conservation of brown preadipocytes was performed as described for HEK293 cells (2.3.1.3), only with HEPES-containing cryomedium.

##### *Cryomedium BFC*

(10 % (v/v) DMSO, 81 % (v/v) DMEM, 20 mM HEPES, 9 % (v/v) FBS superior, sterile 4°C)

#### 2.3.3.3 *Proliferation*

Brown preadipocytes were grown on 10 cm culture dishes in 7 ml growth medium. When reaching confluence they were diluted on new culture dishes, according to the protocol described for HEK293 cells.

##### *Growth medium BFC*

(DMEM high glucose, 20 mM HEPES, 10 % (v/v) FBS superior, 50 mg/ml gentamicin)

#### 2.3.3.4 *Differentiation*

In order to differentiate immortalised preadipocytes into mature brown fat cells, the growth medium of an 80 % confluent plate was exchanged with induction medium, containing indomethacin, dexamethason and IBMX. Cells were incubated in this medium for 48 h and were kept in differentiation medium for 4 further days until they were used for experiments.

##### *Differentiation medium BFC*

(growth medium BFC, 20 nM Insulin, 1 nM T3)

*Induction medium BFC*

(differentiation medium BFC, 500  $\mu$ M IBMX, 2  $\mu$ g/ml dexamethasone, 125  $\mu$ M indomethacin)

*2.3.3.5 Stimulation of the thermogenic gene expression*

In order to stimulate thermogenic adaptation and thereby UCP1 expression, differentiated brown adipocytes were stimulated for 48 h with modified differentiation medium.

In order to achieve an optimal stimulation different substances were tested for their effect on UCP1 expression. The  $\beta$ -adrenergic agonist isoproterenol, the PPAR $\gamma$ -agonist rosiglitazone and the RXR ligand retinoic acid were added alone and in combination to the differentiation medium. After a 48 h incubation period cells were washed with PBS and frozen at  $-80^{\circ}\text{C}$ . Mitochondria were isolated from the cells and tested for expression of UCP1 by western blot.

*Stimulation medium BFC*

(differentiation medium BFC, 10  $\mu$ M isoproterenol, 1  $\mu$ M retinoic acid, 20  $\mu$ M rosiglitazone)

*2.3.3.6 Viral transfection of brown preadipocytes*

One of the aims of this thesis was to analyse the possible interaction of CideA and UCP1. How overexpression of CideA in brown fat cells changes their physiology was tested by overexpressing CideA in adipocytes with the help of a viral system. The virus was a modified version of the retrovirus *moloney murine leukemia virus* and the modification both freed up space for expression of a gene of interest as well as guaranteed that the virus could only be produced in helper cells, containing the Gag, Pol Env genes. By that and by using the ecotrophic PlatE helper cell line, viral supernatants of BSL S1 were generated. Consequently the first step for adipocyte transduction was to produce virus in Plat E cells. Therefore Plat E cells were transfected with the viral vector pMXS using the calcium phosphate method (2.3.2). Plat E cells were maintained as described for HEK293 cells.

24 h after transfection the culture medium containing released virus was collected, mixed with BFC growth medium and 2.5  $\mu$ g/ml polybrene, filtered sterile and used for infection of preadipocytes. The virus could only be used for transduction of preadipocytes as it depended on cell division for integration in the cellular genome. Integration would initiate the expression of proteins of which the sequence had been integrated into the pMXS vector. After 24 h incubation with the virus the medium was replaced by induction medium and differentiation of preadipocytes to mature adipocytes was carried out as described for untransfected cells. GFP-transfections were used as

controls to distinguish between transfection- and CideA expression-mediated effects. Expression normally starts 36 to 48 h after addition of the supernatants.

#### 2.3.4 Analysis of lipid storage and lipolysis

As CideA was suggested to be a lipid droplet protein and to be regulating lipid storage, this effect of its overexpression on BFC was investigated by staining cells with Oil Red O solution, taking images with a microscope and measuring lipid droplet number and size using the Image J software. In a second approach pictures of unstained cells were taken and analysed with software offered by the company Wimasis, also giving number and size of individual droplets.

##### 2.3.4.1 *Lipid staining with Oil Red O*

In order to stain cells grown in 6well plates with the lipophilic dye Oil Red O, medium was removed and cells were washed with 1 ml PBS. After removal of PBS cells were fixed with 1 ml of 3.7 % formaldehyde for 30-60 min at RT. The formaldehyde was discarded and the cell layer was washed again with 1 ml of PBS. After removing PBS cells were incubated with 2 ml of Oil Red O working solution for 1 h at RT. Oil Red O solution was aspirated and cells were washed once with water and kept in water for taking microscopic pictures.

##### *Stock solution*

0.5 % (w/v) Oil Red O in Isopropanol (p.a.)

##### *Working Solution*

(40 % (v/v) DI water, 60 % (v/v) stock solution, filtered)

##### *Fixation Solution*

(3.7 % formaldehyde solution in DI water)

##### 2.3.4.2 *Quantitative analysis of lipid droplets with Image J*

Microscopic images of Oil Red O-stained BFC were analysed with Image J software to determine the number and size of lipid droplets. Therefore an additional plugin was added to the software which allowed setting threshold values for colours. Unstained areas were thereby excluded and residual areas which represented lipid droplets were transformed into a black and white image, which the program could analyse with respect to particle number and size.

### 2.3.4.1 Quantitative analysis of lipid droplets with Wimasis software

As it seemed that the staining procedure and subsequent automatic counting of particles did not reflect what had been observed by eye with the light-microscope, another method to count and measure lipid droplet size was applied. Light-microscopic images were uploaded on the Wimasis homepage and the company returned results describing number and size of particles, defined as lipid droplets. Mean particle number, size and the total lipid area (the product of number and size) were compared for BFC overexpressing GFP or CideA and treated either with retinoic acid or retinoic acid and isoproterenol.

### 2.3.4.2 Analysis of glycerol release

The release of glycerol into the medium of transfected BFC cells was determined with a commercial kit for glycerol detection (R-Biopharm) according to the manufacturer's instructions, except that all volumes were reduced to 25 %, resulting in a final volume of 755  $\mu$ l. Glycerol is detected by three coupled reactions which lead to the consumption of NADH, which is determined photometrically by measuring the absorbance at 340nm.

- 1) glycerol  $\rightarrow$  glycerol-P + ADP (glycerol-kinase)
- 2) ADP + PEP  $\rightarrow$  pyruvate + ATP (pyruvate-kinase)
- 3) pyruvate + NADH  $\rightarrow$  lactate + NAD<sup>+</sup> (lactate-dehydrogenase)

First the sample is mixed with all components for reactions 2 and 3, and then baseline absorbance is determined ( $A_1$ ). Afterwards glycerol-kinase is added and NADH breakdown proportional to glycerol content is measured ( $A_2$ ). Glycerol content in the sample was calculated from  $A_1$ - $A_2$  with:

$$C = \frac{V * MW}{\epsilon * d * v * 1000} * (A_1 - A_2)$$

V: final volume (ml), v: sample volume (ml), MW: molecular weight of substance to be assayed, d: light path,

$\epsilon$ : extinction coefficient of NADH; at 340 nm: 6.3 l\*mmol<sup>-1</sup>\*cm<sup>-1</sup>

BFC were seeded on 6well plates for the glycerol assay, transduced with virus leading to the expression of either GFP or CideA and then induced to differentiate into mature adipocytes. 4 days after induction, the thermogenic phenotype of cells was stimulated, either with isoproterenol and

retinoic acid, as done for proton leak measurements, or with retinoic acid alone. This additional condition was chosen as cells were supposed to be acutely stimulated with isoproterenol for the glycerol release assay. Medium samples were taken for analysis after the 48 h of stimulation and then 1 ml fresh medium with different concentrations of isoproterenol (0, 10 nM, 1  $\mu$ M, 10  $\mu$ M) was added to the cells. After 2 h incubation at 37°C medium samples were taken and analysed with the kit. In order to normalise glycerol release to cell number in the well, cells were washed with PBS and then frozen at -80°C for later extraction of proteins with RIPA-buffer. The results of BCA quantification of protein extracts were used to adjust the values of glycerol release.

## 2.4 Isolation of mitochondria

### 2.4.1 Isolation of HEK293 mitochondria

For isolation of mitochondria from HEK293 cells two culture dishes with a growth area of 625 cm<sup>2</sup> each were used for one day. First the medium was removed and then the cell layer was washed with 10 ml of STE 1 % BSA (fatty acid free (FAF) (Sigma A3803)). Afterwards cells were scraped in 10 ml STE 1% BSA<sub>FAF</sub>, transferred into a centrifuge tube and pelleted for 3 min at 500 g. This and all other centrifugation steps were carried out at 4°C, all other steps were performed on ice. The supernatant was discarded and the cell pellet was homogenized in a 40 ml loose fitted glass-glass douncer (Wheaton) in 20 ml buffer by applying 7 strokes. The homogenate was centrifuged for 10 min at 1,000 g to separate cell debris and intact cells. The supernatant was transferred to a new centrifuge tube and filtered through 250  $\mu$ M gauze. The pellet was homogenised with 7 strokes in fresh buffer and centrifuged at 1,000 g. First and second supernatant were centrifuged for 10 min at 10,400 g to pellet mitochondria and heavy membrane fraction. The supernatant was discarded, the pellets resuspended in STE, combined and recentrifuged at 10,400 g. the supernatant was carefully removed and the mitochondrial pellet was resuspended with a brush in a small buffer volume. The resulting mitochondria suspension was transferred into an eppendorf tube and protein content was determined using the biuret method.

*STE*

(250 mM sucrose, 5 mM Tris, 2 mM EGTA, pH 7.4 at 4°C)

#### 2.4.2 Isolation of mitochondria from cultured brown adipocytes

For isolation of mitochondria from BFC cells two culture dishes with a growth area of 625 cm<sup>2</sup> each were used for one day. First the medium was removed and the cell layer of each dish was washed with 10 ml IsoA. Afterwards cells were scraped in 10 ml IsoA, transferred into a centrifuge tube and pelleted for 5 min at 950 g. The cell pellet was homogenized in a 15 ml glass-teflon potter in 15 ml IsoA by applying 5 strokes. The subsequent centrifugation of the homogenate for 10 min at 8,700 g separated organelles, cell debris and intact cells from free fat, which floated on top. The fat was removed along with the supernatant, the pellet was resuspended in IsoB and re-centrifuged at 950 g for 10 min. This centrifugation separated cells and cell debris from the mitochondria, which remained in the supernatant. This supernatant was transferred to a new centrifuge tube and the pellet was homogenised again and subjected to the two centrifugation steps as described for the first homogenate. First and second supernatant were centrifuged at 8,700 g to pellet the mitochondria, which were resuspended in IsoC, combined and pelleted once more at 8,700 g for 10 min. The supernatant was carefully removed and the mitochondrial pellet was resuspended with a brush in a small buffer volume. The resulting mitochondria suspension was transferred into an eppendorf tube and protein content was determined with the biuret method.

##### *IsoA*

(250 mM sucrose, 10 mM TES, 1 mM EDTA-Na<sub>2</sub>, 2 % BSA<sub>FFA</sub>)

##### *IsoB*

(250 mM sucrose, 10 mM TES, 1 mM EGTA, 1 % (w/v) BSA<sub>FFA</sub>)

##### *IsoC*

(100 mM KCl, 10 mM TES, 1 mM EGTA, 0.4 % (w/v) BSA<sub>FFA</sub>)

#### 2.4.3 Isolation of mitochondria from brown adipose tissue

For isolation of mitochondria from brown adipose tissue, animals were anaesthetised and killed with carbon dioxide and BAT depots were dissected and transferred into cold IsoA. The tissue was minced with scissors and homogenised with a glass-teflon potter in 15 ml IsoA by applying 4 strokes. Centrifugation steps were carried out as described in 2.4.2 except that the pellet of the slow centrifugation was not homogenised for a second time.

## 2.5 Measurements of mitochondrial and cellular bioenergetics

Mitochondrial and cellular bioenergetics, with a special focus on mitochondrial proton leak, were studied in isolated mitochondria, trypsinised cells and adherently growing cells. For isolated mitochondria the parallel determination of membrane potential and leak respiration was applied to obtain curves describing the kinetic behaviour of proton leak. Furthermore basal, phosphorylating and maximum respiration were determined. These respiration states were also determined for trypsinised and adherently growing cells. In trypsinised cells additionally the fatty acid sensitivity of leak respiration was tested whereas in adherently growing cells the non-mitochondrial respiration was determined. A Clark-electrode was used to analyse oxygen consumption of isolated mitochondria and trypsinised cells, a TPMP<sup>+</sup> electrode was applied to measure membrane potential of isolated mitochondria. A Seahorse XF96 flux analyser allowed the analysis of oxygen consumption in adherently growing cells.

### 2.5.1 Determination of proton leak kinetics of isolated mitochondria

It is possible to determine proton leak kinetics for isolated mitochondria by parallel measurements of oxygen consumption and membrane potential. ATP-synthesis is blocked by addition of the inhibitor oligomycin and different steady energetic states are titrated by varying substrate supply. Plotting leak respiration against membrane potential results in a curve which describes the kinetic behaviour of proton leak and illustrates the non-linear dependence between the two variables, especially at high membrane potentials (e.g. **Figure 15**).

#### 2.5.1.1 *Analysis of oxygen consumption of isolated mitochondria*

The oxygen consumption of mitochondrial suspensions was determined with a Clark-type electrode (RANK BROTHERS). This electrode consists of a platinum cathode and a silver-anode which are connected by a 3 M potassium chloride solution. The sample is incubated in a chamber with a built-in water jacket, which allows measuring at a defined and constant temperature. It is separated from the electrode base with an oxygen permeable teflon membrane (YSI model 5794) and the chamber is sealed from the atmosphere with a fitted plunger, containing a small hole that is used to inject materials with a syringe.

When voltage is applied a current develops between the two electrodes, which depends linearly on the oxygen concentration with which the electrode is in contact. A calibration of the electrode to 100 % (equilibrated measurement buffer) and 0 % oxygen concentration (end of respiratory control ratio (RCR) analysis) was performed on every measurement day. Oxygen concentrations in the

measurement chamber were plotted by Powerlab software (CHART for Powerlab) as a function of time. Therefore the slope of the curve represented oxygen consumption of the incubated sample.

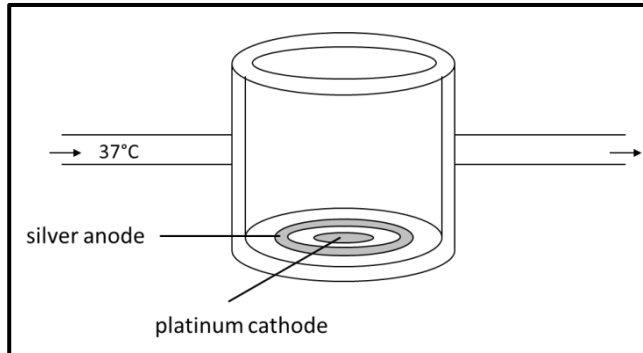


**Figure 5 Clark-electrode.**

Oxygen consumption of a sample which is incubated in the temperature controlled measurement chamber is detected as current between silver anode and platinum cathode. Current is proportional to oxygen concentration.

Absolute oxygen consumption rates were calculated by adjusting the value to min instead of s and assuming an oxygen concentration of 406 nmol O/ml at 37°C (Reynafarje et al., 1985). Considering the protein concentration in the measurement chamber values in nmol O\*min<sup>-1</sup>\*mg protein<sup>-1</sup> could be generated.

$$J_o \text{ (nmol O} \cdot \text{min}^{-1} \cdot \text{mg protein}^{-1}) = \frac{\% / \text{min} \cdot \text{nmol O} / \text{ml}_{\text{buffer}}}{(100 \cdot \text{mg protein} / \text{ml})}$$

$J_o$ : oxygen consumption, 100: units for oxygen consumption, nmol O/ml<sub>buffer</sub>: oxygen-solubility in measurement buffer (Reynafarje et al., 1985)

### 2.5.1.2 Analysis of membrane potential of isolated mitochondria

The membrane potential of isolated mitochondria was determined using the lipophilic cation TPMP<sup>+</sup>, as described by Brand (Brand, 1995). This ion was added to mitochondrial suspensions in the measurement chamber of the Clark-electrode, where it distributed between solution and organelles dependent on the energetisation status of the mitochondria. If the mitochondria maintained a high membrane potential, TPMP<sup>+</sup> accumulated inside of them, whereas at low membrane potential TPMP<sup>+</sup> stayed in the buffer. The TPMP<sup>+</sup> concentration in the buffer was monitored with self-made TPMP<sup>+</sup> sensitive electrodes (2.5.1.3). The electrode consisted of a piece of PVC tubing, which was sealed with a tetraphenylboron-impregnated PVC membrane. The impregnation provided a negatively charged surface for the interaction with the cation. Voltage changes at the TPMP<sup>+</sup> electrode were detected with a platinum wire, which protruded into the 10 mM TPMP<sup>+</sup> solution within the tubing. These changes were compared to a KCl-reference electrode (Driref 5, World precision instruments) which was like the TPMP<sup>+</sup> electrode connected to a pH amplifier (ADinstruments) which was connected to a Powerlab (ADinstruments). Voltage changes at the TPMP<sup>+</sup> electrode could be assigned to defined TPMP<sup>+</sup> concentrations in the medium (TPMP<sup>+</sup><sub>ext</sub>) by performing an internal calibration at the beginning of each measurement. For this calibration TPMP<sup>+</sup>



was added to the measurement buffer in 5 steps of 0.5  $\mu\text{M}$  TPMP<sup>+</sup>, yielding a final concentration of 2.5  $\mu\text{M}$ . The voltage at this concentration was set as zero ( $V_0$ ) and the voltage for the other concentrations was expressed as difference from  $V_0$ . Voltages for the calibration concentrations were plotted against the concentration values on a logarithmic scale, and if the coefficient of determination of the resulting standard curve was  $R^2 \geq 0.99$ , the calibration was used for estimation of extra-mitochondrial TPMP<sup>+</sup> concentrations (TPMP<sup>+</sup><sub>ext</sub>), reflecting mitochondrial energetisation during the measurement.

Voltage values which were recorded during a measurement were corrected for electrode drift and expressed as difference to  $V_0$  before they were used to calculate TPMP<sup>+</sup><sub>ext</sub> with the standard curve. Correction for electrode drift was based on the assumption, that if the uncoupler FCCP was added at the end of a measurement, all TPMP<sup>+</sup> would be released from the mitochondria and the resulting voltage detected by the electrode ( $V_{\text{FCCP}}$ ) should equal  $V_0$  again. The difference between  $V_{\text{FCCP}}$  and  $V_0$  was supposed to develop evenly over time, therefore voltage values could be corrected for drift by considering the timepoint between  $V_{\text{FCCP}}$  and  $V_0$  at which they were recorded.

$$\text{Correction for drift} = \frac{(V_0 - V_{\text{FCCP}}) * (t_{V_0} - t_x)}{(t_{V_0} - t_{\text{FCCP}})}$$

$V_0$ : voltage at the end of internal calibration (zero),  $V_{\text{FCCP}}$ : voltage after uncoupling with FCCP,  $t_{V_0}$ : timepoint at the end of internal calibration,  $t_x$ : timepoint of a recorded voltage during the measurement, reflecting a membrane potential,  $t_{\text{FCCP}}$ : timepoint after uncoupling with FCCP

$$\text{Value for estimation of TPMP}^+_{\text{ext}} \text{ with standard} = V_0 - (V_x - \text{correction for drift})$$

TPMP<sup>+</sup><sub>ext</sub>: extra-mitochondrial TPMP<sup>+</sup>-concentration,  $V_x$ : recorded voltage for a steady state in a measurement

Drift-corrected values, expressed as difference from  $V_0$  were used to determine TPMP<sup>+</sup><sub>ext</sub>. Calculation of membrane potential from TPMP<sup>+</sup><sub>ext</sub> was based on the Nernst equation, which describes the distribution of a monovalent cation until it reaches an equilibrium distribution as follows:

$$\Delta\psi = \left( \frac{RT}{F} \right) * \ln \left( \frac{[C^+_{\text{in}}]}{[C^+_{\text{out}}]} \right) \quad \text{at } 37^\circ\text{C: } \Delta\psi = 61,5 * \log \left( \frac{[C^+_{\text{in}}]}{[C^+_{\text{out}}]} \right)$$

R: electrical resistance, T: temperature, F: Faraday-constant,  $C^+_{\text{in}}$ : ion concentration inside,  $C^+_{\text{out}}$ : ion concentration outside

This equation allowed calculating membrane potential from a known extramitochondrial TPMP<sup>+</sup> concentration in the measurement chamber when literature values for mitochondrial matrix volume and TPMP<sup>+</sup>-binding to mitochondria were inserted. All calculations were performed with Excel software.

$$\Delta\psi \text{ (mV)} = \frac{61,5 \log (\text{TPMP}^+_{\text{vo}} - \text{TPMP}^+_{\text{ext}}) * B_{\text{TPMP}^+}}{(0,001 * \text{mg protein/ ml} * \text{TPMP}^+_{\text{ext}})}$$

$\Delta\psi$ : membrane potential, TPMP<sup>+</sup><sub>vo</sub>: added concentration of TPMP<sup>+</sup>, TPMP<sup>+</sup><sub>ext</sub>: extramitochondrial TPMP<sup>+</sup> concentration, B<sub>TPMP<sup>+</sup></sub>: correction factor for TPMP<sup>+</sup>-binding (skeletal muscle and HEK293 mitochondria 0.35 mg/ $\mu$ l (Rolfe et al., 1994), BAT and BFC mitochondria 0.4 mg/ $\mu$ l (Brand, 1995; Echtay et al., 2003)), 0.001: matrix volume

### 2.5.1.3 Construction of TPMP<sup>+</sup> electrodes

A TPMP<sup>+</sup> electrode consists of a piece of PVC-tubing, which is sealed at the bottom with a PVC membrane, which has been impregnated with tetraphenylboron. TPMP<sup>+</sup> electrodes were built according to the instructions published by Brand (Brand, 1995). The PVC membrane was first mixed and dried in glass petri dishes before it was connected to the tubing.

For the construction of the membrane tetraphenylboron and PVC were dissolved separately in tetrahydrofuran. Afterwards the solutions were mixed, dioctylphtalate was added and the mixture was poured onto glass petri dishes as a 1 mm thick layer. The layer was dried under the fumehood for 24-48 h. Approximately 7 cm long pieces of PVC-tubing with an evenly cut surface were produced, shortly submerged into tetrahydrofuran and put on the membrane. The tetrahydrofuran temporarily softened both materials and allowed their fusion. Electrodes were dried for further 24 h and were afterwards cut out of the petri dish. They were filled with 10 mM TPMP<sup>+</sup> solution and put onto the coaxial cable with the platinum tip and tested for reaction to additions of TPMP<sup>+</sup> to the measurement buffer. Functional electrodes were stored with the tip in 10 mM TPMP<sup>+</sup> solution.

### 2.5.1.4 Proton leak measurement

The determination of proton leak kinetics requires parallel measurements of oxygen consumption and membrane potential, performed in leak conditions for different steady energetic states. The setup for such a parallel measurement is illustrated in **Figure 6**.

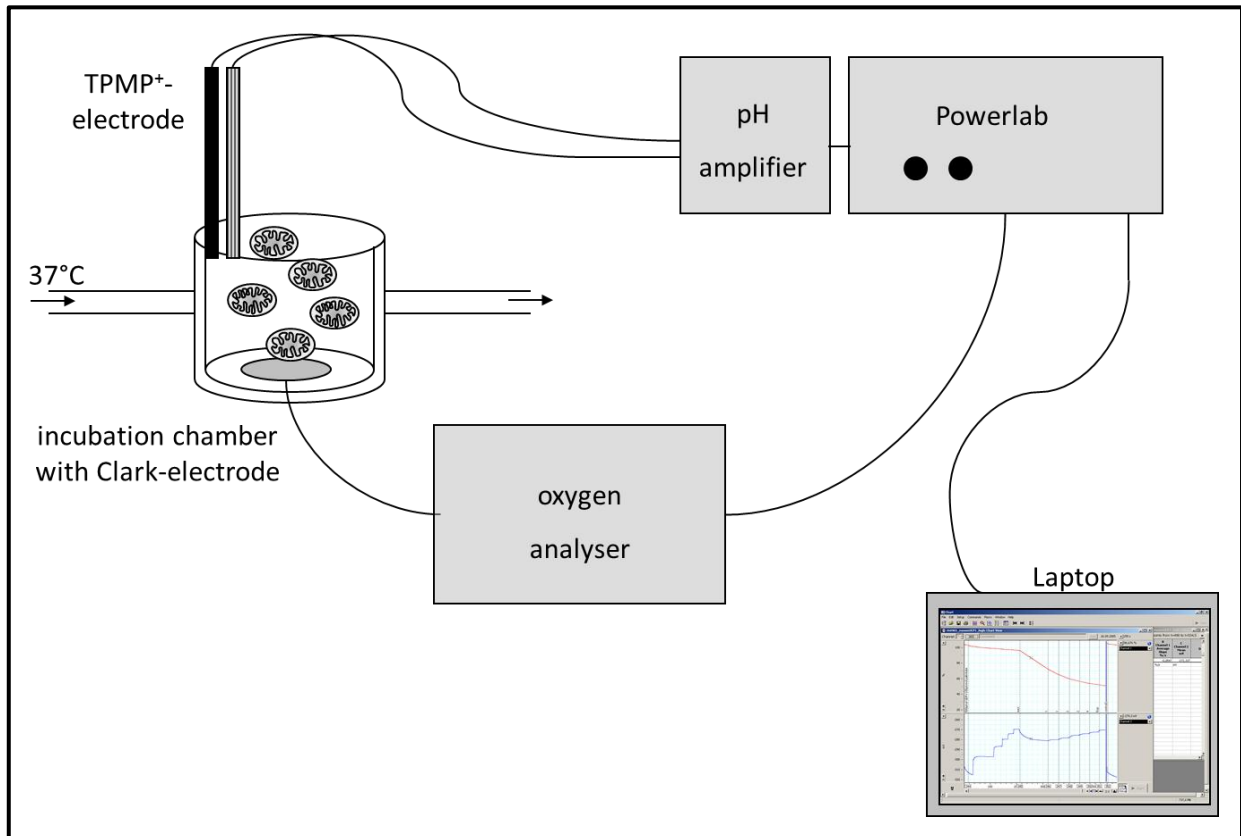


**Figure 6 Setup for proton leak measurements.**

A sample is incubated in the temperature-controlled measurement chamber and oxygen consumption is detected with a Clark-electrode. Membrane potential is recorded with a TPMP<sup>+</sup> sensitive electrode, both signals are amplified and collected with a Powerlab, which plots the data on a computer.

The sequence of titrations in such an experiment was the following:

A defined amount of mitochondria was diluted in measurement buffer in the incubation chamber (0.35 mg/ml; 2.5 ml volume) and leak respiration was established by the addition of 1 μg/ml oligomycin. As this blocked ATP synthesis, all residual respiration could be assigned to compensation of leak processes above the mitochondrial inner membrane, which is why the following recordings of oxygen consumptions could be used as a measure for proton leak of the incubated mitochondria. Endogenous substrate supply was blocked by inhibition of complex I with 5 μM rotenone and 80 ng/ml nigericin was added to convert the pH component of proton motive force into membrane potential. Thereby proton motive force could be fully detected by the membrane potential measurement. The chamber was closed with a fitted lid through which the TPMP<sup>+</sup>- and reference-electrode protruded into the measurement chamber. Air-bubbles were removed and the measurement was started with the internal TPMP<sup>+</sup>-calibration. After the calibration mitochondria were energised by the addition of the complex II substrate succinate (4 mM), which lead to the establishment of membrane potential at a steady oxygen consumption rate. In order to describe the kinetic behaviour of proton leak steady states of membrane potential and oxygen consumption were

now titrated by manipulating substrate supply via 5 stepwise additions of the succinate competitor malonate (up to 4 mM). After recording of several energetic states 1  $\mu$ M of the artificial uncoupler FCCP was added to the measurement, which abolished membrane potential and led to the release of TPMP<sup>+</sup> from the mitochondria, allowing correction of the measurement for electrode drift. The incubation chamber was cleaned with ethanol and water between different measurements to prevent contaminations with any of the substances. Measurement conditions were varied by addition UCP1 inhibitors or activators before closing the chamber with the plunger. Comparison of proton leak in their absence and presence enabled to conclude on the contribution of UCP1 to the detected proton leak. For the measurements of HEK293 cells GDP and a stock solution of palmitate in ethanol were diluted by injection into the chamber. For BAT and BFC measurements palmitate was equilibrated with BSA and diluted to the appropriate BSA and palmitate concentration within the measurement buffer. GDP was also added to the buffer and the pH for each of the measurement conditions was adjusted before starting the measurements.

#### *Measurement buffer KHE HEK293*

(120 mM KCl, 5 mM KH<sub>2</sub>PO<sub>4</sub>, 3 mM Hepes, 1 mM EGTA, 0.3 % BSA<sub>FFA</sub> pH 7.2 at RT)

#### *Measurement buffer KHE BFC*

(50 mM KCl, 4 mM KH<sub>2</sub>PO<sub>4</sub>, 5 mM Hepes, 1 mM EGTA, 0.4 % BSA<sub>FFA</sub> pH 7.2 at RT)

#### *2.5.1.1 Conjugation of palmitate to BSA*

For proton leak measurements of BAT and BFC mitochondria palmitate was conjugated with BSA to avoid its precipitation after injection into the measurement buffer. Palmitate was dissolved at 100 mM in 0.1 M KOH by melting it at 80°C. 677.5  $\mu$ l of this solution were added dropwise to a 9 % (w/v) BSA<sub>FAF</sub> solution in KHE, which was prewarmed to 37°C and stirred during the addition. This resulted in a stock solution with 6.77 mM palmitate, bound to BSA in a relation of 5:1. This stock solution was diluted to 0.4 % BSA and 300  $\mu$ M palmitate for the measurements by addition of KHE. Reference stock and buffer were generated in parallel, with 677.5  $\mu$ l of 0.1 M KOH, added to the 9 % BSA<sub>FAF</sub>-KHE solution. Aliquots of stock solutions were kept at -20°C.

#### *2.5.1.2 Comparison of proton leak kinetics at the highest common potential*

Proton leak curves for different mitochondria or different measurement conditions were compared by comparing leak respiration at the highest membrane potential that was reached in all single measurements which were supposed to be compared. Respiration could be used as a direct measure

for leak, as it was recorded in the presence of the ATP-synthase inhibitor oligomycin. Values of respiration for a defined membrane potential were calculated from the leak curves by linear interpolation between the two surrounding data points.

#### *2.5.1.3 Regression analysis of proton leak curves*

The comparison of different proton leak curves at single membrane potential values is limited and the estimation of leak respiration by linear interpolation is not completely accurate. Calculation of a regression allows the description and comparison of the kinetic behaviour of leak over a wide range of membrane potentials. Furthermore regressions can be subtracted to calculate the UCP1-dependent component of proton leak over a range of membrane potentials.

Therefore proton leak curves obtained for mitochondria from different test systems were subjected to a dynamic fit with Sigmaplot software. The function  $f(x) = ax + b \cdot \exp^{(cx)}$  ( $a > 0$ ;  $c > 0$ ) was applied (Jastroch et al., 2012) as it accounted for the linear dependence of leak and membrane potential at low potential values and the exponential dependence of the two variables at high membrane potential.

UCP1-dependent proton leak was calculated by subtracting the proton leak of HEK293 from UCP1-containing mitochondria in the same experimental conditions or by subtracting proton leak in a condition where UCP1 was inhibited (GDP) from proton leak in a condition where UCP1 was activated (palmitate) (BFC and BAT mitochondria).

#### *2.5.1.4 Titration of different respiration states- respiratory control ratio(RCR)*

Besides the determination of leak respiration and the kinetic dependence of leak on membrane potential also other characteristic respiration states of isolated mitochondria were assayed. Mitochondria were incubated in the Clark-electrode in the presence of rotenone and succinate and first basal respiration (state 2) was recorded. GDP was added to test whether UCP1 mediated leak had contributed to basal respiration. Next, ADP was added to allow ATP-production. Due to the high excess of ADP and succinate the rate of phosphorylating respiration (state 3) reflected the maximum phosphorylating capacity of the mitochondria. Subsequently leak respiration was established by the addition of oligomycin (state 4) and then maximum respiratory capacity of the mitochondria was tested by titration with FCCP. The ratios of FCCP/state 4 and of state 3/state 4 yield information about the quality of the mitochondrial sample. If leak respiration is far below the maximum respiratory capacity this hints towards a good mitochondrial preparation, which is also true for a high ratio of state3/state 4. Additionally this value illustrates the control of phosphorylation over

mitochondrial oxygen consumption and reports on the efficiency of ATP production in the respective mitochondrial sample.

### 2.5.2 Analysis of oxygen consumption of trypsinised cells

The bioenergetics of intact trypsinised cells was also determined using a Clark-electrode, but in a 4 ml incubation chamber. These measurements also gave information about the activity of the mitochondrial protein UCP1 as they were performed in the presence of oligomycin, which blocked ATP-synthesis-dependent oxygen consumption.

Cells of a confluent culture dish were trypsinised as described in 2.3.1.2 and resuspended in 4 ml DMEM containing 10 % FBS after centrifugation. Cellular respiration was determined for 1 ml aliquots and in duplicate for each cell culture dish. Cell number of one aliquot was determined with a hemocytometer and one aliquot was frozen at -20°C for later immunological analysis.

Basal respiration of the cells in the presence of DMEM (glucose) was determined in the closed incubation chamber, before leak respiration was established by injection of oligomycin. The sensitivity of leak to free fatty acids was tested by injection of 100-300 µM palmitate. Maximum respiratory capacity was determined by titration with the uncoupler FCCP at the end of the measurement. As FCCP provides a proton pathway into the mitochondrial inner membrane the respiratory tries to compensate this proton flux by increasing its activity, in order to maintain the same proton motive force across the membrane. This is possible up to a maximum capacity and thereafter a further increase in FCCP-mediated proton leak will cause a reduction in proton motive force and will destroy the mitochondria and thereby also reduce respiration.

### 2.5.3 Analysis of oxygen consumption of adherently growing cells

A recently developed method to measure oxygen consumption of adherently growing cells in multiwell format is applied by the Seahorse XF96 flux analyser (Seahorse Biosciences). The analysis is based on a fluorophore whose fluorescence is quenched by oxygen. In a second channel the extracellular acidification rate of cells can be determined in parallel with a proton sensitive fluorophore. Cells or mitochondria are fixed at the bottom of a well can be analysed in their normal growth conditions and after manipulation via two injection channels. Using this assay information on basal respiration, state 4 respiration, maximum respiratory capacity and non-mitochondrial respiration can be obtained.

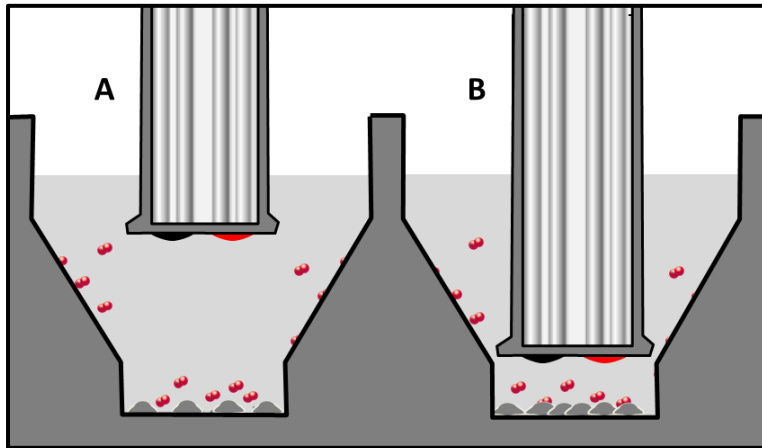


**Figure 7 Principle of Seahorse XF96 analysis.**

Cells are growing in a 96well plate and oxygen consumption or extracellular acidification rate can be determined with two fluorophores, which are quenched by oxygen and pH. They are spotted on the lid, which can be lowered during the measurement to form a microchamber at the bottom of the plate (B). Medium of the microchamber can be replenished by mixing with the residual medium in the well (A). This allows repeated measurements. The optics for excitation and detection are inserted in the lid and are not in direct contact with the medium in the wells.

Seahorse 96well plates have a slightly lower growth area as common 96well plates, as they taper towards the bottom (**Figure 7**). Three plastic spots on the bottom provide the border for the measurement chamber which is repeatedly formed during the analysis by lowering the lid (cartridge) of the plate. The cartridge has 96 cones, which fit into the wells of the plate and the oxygen and pH sensitive fluorophores are spotted on top of the cones. The light-optics for excitation and detection of light emission from the fluorophores are inserted into the inside of the cartridge cones and are not in direct contact with the wells. The formation of a little measurement chamber at the bottom of the plate allows replenishing the medium above the cells by mixing with the residual medium in the chamber. Therefore repeated analyses with the same starting values for oxygen concentration and pH can be performed in one well. Additionally, there is the possibility to perform two injections during a seahorse-measurement, which enables the user to perform repeated analyses of respiration rate and extracellular acidification rate in three different conditions per well. A common experiment would include determination of basal respiration in the beginning, subsequent injection of oligomycin and determination of state 4 respiration, followed by either FCCP injection to analyse maximum respiratory capacity or followed by antimycin/rotenone injection to determine non-mitochondrial respiration, which the other respiration rates have to be corrected for.

Seahorse analysis was applied to for basal characterisation of HEK293 and HEK293 UCP1 cells, as well as of CideA and GFP expressing HEK293 and HEK293 UCP1 cells. Furthermore BFC were compared after different stimulatory treatments.

#### 2.5.3.1 Seahorse measurement with HEK293 and HEK293 UCP1 cells

For a Seahorse measurement with HEK293 and HEKUCP1 cells 10.000 cells were seeded into each well of a 96well plate in a volume of 80  $\mu$ l, 24 h before the analysis. Furthermore a Seahorse

cartridge was hydrated during the night in the CO<sub>2</sub>-free incubator at 37°C. On the day of the analysis growth medium was exchanged with 180 µl unbuffered measurement medium and cells were incubated at 37°C and atmospheric CO<sub>2</sub>. In the meantime the cartridge was loaded with the injection substances (20 µl for the first and 22 µl for the second injection) and was afterwards equilibrated in the incubator for further 10 min before it was inserted into the analyser to start the measurement. After 20 min of calibration of the fluorophore spots on the lid the cells were put into the analyser and the programmed measurement and injection cycles were performed. Basal respiration, leak respiration, maximum respiration and non-mitochondrial respiration were recorded, and normalised to basal respiration. Non-mitochondrial respiration was subtracted from the other rates and the increase of maximum above basal respiration (spare respiratory capacity) and the contribution of leak to basal respiration were calculated.

#### *Measurement buffer*

(XF Assay medium/modified DMEM, 10mM glucose, 4 mM glutamine, 2 mM pyruvate, 0.1 % BSA<sub>FAF</sub>)

#### *Reagents*

(1 µM oligomycin, 0.6 µM FCCP, 1µM rotenone, 5 µM antimycin, stock solutions at 2.5 mM in DMSO)

#### *2.5.3.2 Seahorse measurement with BFC cells*

For a Seahorse analysis with BFC, 10.000 cells were seeded in a volume of 80 µl to well of a 96well plate. One day later cells were treated with induction medium and were differentiated as described in 2.3.3.4. The cells in some of the wells were stimulated with either retinoic acid alone or isoproterenol and retinoic acid 48 h before the Seahorse analysis, the measurement itself was conducted exactly as described for HEK293 and HEK293 UCP1 cells.

## **2.6 Statistical analysis**

Experimental data are presented as means with standard deviation (SD) or standard error mean (SEM) as measure for the variance. Leak respiration data were tested for dependence on the variables cell type (HEK293, HEK293 UCP1) or treatment (control, palmitate, GDP, isoproterenol, retinoic acid,...) with OneWay- or TwoWay-ANOVA. In order to fulfil the criteria of normal distribution and homogeneity of variance, data were log-transformed before the analysis. Post-hoc tests for significant differences between groups were Holm-Sidak, Bonferroni or Tukey test. Data on UCP1 protein expression, lipid accumulation or glycerol release in BFC and were tested with



OneWay-, TwoWay- and ThreeWay-ANOVA and Holm-Sidak test. The level of significance was set to  $p < 0.05$  and the analysis was performed with SigmaPlot 10.0 and SigmaStat 3.5 software.

### 3 Results

This thesis aimed to characterise UCP1 and CideA function in two mammalian cell lines. Results are presented in two parts, with the first part describing the function of UCP1 alone in different test systems and trying to evaluate the suitability of the two mammalian cell lines for research on UCP1. Additional experiments in other test systems, liposomes and isolated mitochondria from mouse BAT, helped to interpret and evaluate the results obtained for the cell lines.

The second part illustrates how the presence of CideA, which had been published as an inhibitor of UCP1, affects the function of UCP1 in the test systems. These experiments were supposed to underline the advantages of the cell culture models and tried to reproduce and understand the interaction between UCP1 and CideA.

#### 3.1 UCP1 activity in liposomes, HEK293 cells, immortalised brown adipocytes and isolated BAT mitochondria

The major aim of the following experiments was to characterise the HEK293 UCP1 cell culture system, which had been generated in the laboratory previously to this work and the BFC line, which had been provided by the laboratory of Bruce Spiegelman. Parameters which were determined are the expression level of UCP1, the regulation of its activity by known activators and inhibitors and the absolute catalytic activity of UCP1. These parameters were compared with results obtained in native mitochondria to evaluate if these test systems are suitable to answer open questions on the mechanistic function of UCP1 or to identify new modulators or regulators of the protein. UCP1 activity is also presented for liposomes as they were applied as test system for an interaction between UCP1 and CideA in the second part of the thesis. Results are first presented in order of lowest to highest complexity of the test systems and then compared to each other.

##### 3.1.1 UCP1 activity in liposomes

Liposomes are membrane vesicles which allow analysis of transport activities of membrane proteins in a setting where the proteins are directly accessible to possible activators or inhibitors and where influences of other proteins/factors or cellular processes can be excluded. Measurement conditions can be completely defined, which allows manipulation of membrane composition or identification of the transported substrate for example.

For the analysis of UCP1 activity in liposomes, which was carried out during a research visit to the laboratory of Bruno Miroux at the Université Paris V, UCP1 protein was purified from brown adipose

tissue mitochondria of cold acclimated mice and inserted into liposomes. Insertion required the presence of detergent, which was removed by incubation with biobeads and dialysis steps. Activity readout in the liposome assay was the absorbance of Safranin O, which associated with polarising liposomes, resulting in reduced absorbance. Polarisation of the liposomes could be detected as a decrease in absorbance at 520 nm and occurred only if liposomes contained a proton translocating moiety (see measurement principle; **Figure 4**). The rate of polarisation was a measure for the proton translocating capacity (**Figure 8**).

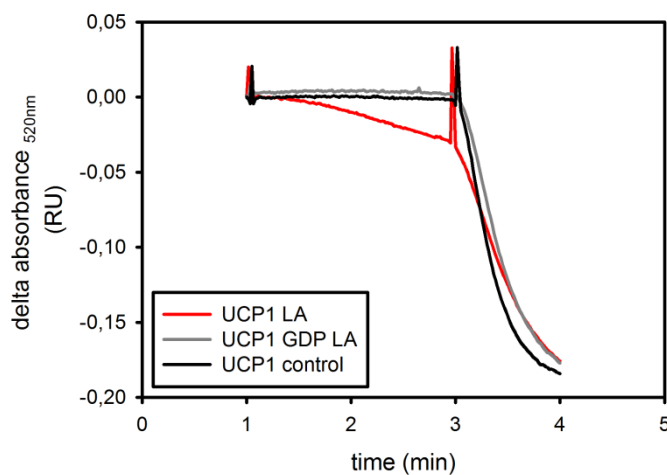


**Figure 8 Analysis of UCP1 activity in liposomes.**

Safranin O absorbance at 520 nm is plotted against time. The rate of the absorbance decrease after nigericin addition (min 1) is a measure for proton transport activity. Full polarisation after addition of CCCP (min 3) serves as quality control. Lauric acid (LA) induces polarisation, which is dependent on proton transport, GDP prevents this activation.

The value for polarisation rate provides relative information and allows comparison of this rate for different measurement conditions applied on one set of liposomes. As the final content of UCP1 protein in the liposomes was not determined, an absolute catalytic activity, which could be compared to other systems, was not calculated.

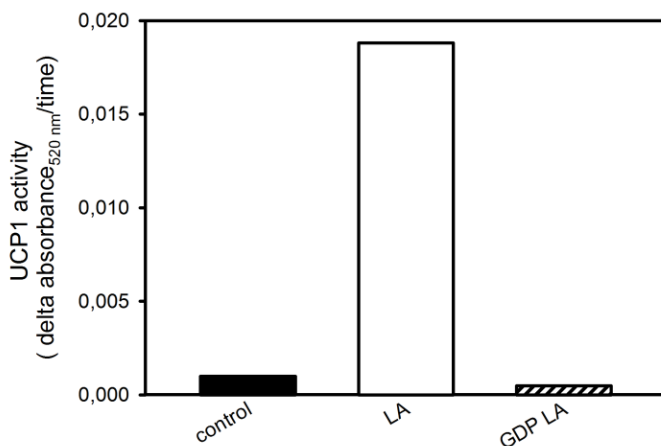


**Figure 9 Regulation of UCP1 activity in liposomes.**

Bars represent the polarisation rate of liposomes containing UCP1. Polarisation is dependent on proton transport activity and increased by addition of lauric acid (LA), whereas coincubation with GDP prevented the LA-induced activation of the protein.

The absorbance at 520 nm of measurement buffer with UCP1 containing liposomes was stable in the beginning of an experiment and did not change upon nigericin addition (**Figure 8**). CCCP addition led to full polarisation of the liposomes and served as control for their intactness. When lauric acid was added to the measurement, the addition of nigericin induced polarisation of liposomes at a constant rate which was largely increased by addition of CCCP which led again to full polarisation. The fact that lauric acid did not have an effect on the polarisation of liposomes not containing UCP1 and that addition of GDP prevented lauric acid-induced polarisation, indicated that polarisation reflects the activity of UCP1 (**Figure 9**).

### 3.1.2 UCP1 activity in HEK293 cells

Isolation and purification of a protein, as it is necessary for liposome assays, can affect protein integrity and is difficult to judge in such artificial test systems. Furthermore some of the protein will insert into the membrane in the wrong orientation, as import is mechanistically in the presence of detergent and not driven by coordinated import machinery. Cellular models which can be transfected to express proteins of interest have the advantage that the protein is produced in and stays in the cellular environment. HEK293 cells are a mammalian cell culture model which is easy to cultivate and can be modified by simple transfection methods. Furthermore HEK293 cells do not endogenously express UCPs, which allows the comparison of different UCPs in the same cellular background without overlaying activity from endogenous protein. HEK293 cells with stable expression of UCP1 had been generated and initially characterised before in the laboratory (Hirschberg, 2006) and this characterisation was extended with the following experiments. They aimed to demonstrate regulation by the known activator palmitate and inhibitor GDP in the test system and were supposed to exclude that UCP1 displayed an uncoupling artefact due to improper folding or insertion in the HEK293 cell mitochondria, a drawback which had been reported in the yeast system (Stuart et al., 2001b). Furthermore the catalytic activity of UCP1 in these cells was determined and compared with other test systems.

#### 3.1.2.1 *Detection of heterologously expressed UCP1 in HEK293 cells*

After generation of the HEK293 UCP1 cell line the success of the stable transfection had been verified qualitatively by western blot (Hirschberg, 2006). Now further immunological analyses of UCP1 expression were performed, confirming the subcellular localisation of the protein and its exact expression level.

Mitochondrial localisation was assessed by immunocytochemistry and by immunological detection of UCP1 in different cell fractions, which were obtained by differential centrifugation. Immunological detection of UCP1 in fixed HEK293 UCP1 cells (**Figure 10B**) revealed a similar staining pattern as the

one obtained for mitotracker in fixed HEK293 cells (**Figure 10A**), suggesting mitochondrial localisation of the heterologously expressed protein. Western blot analysis of HEK293 UCP1 cell fractions yielded an immunological signal only in the mitochondrial fraction, confirming that heterologously expressed UCP1 was correctly targeted to the mitochondria (**Figure 10C**).

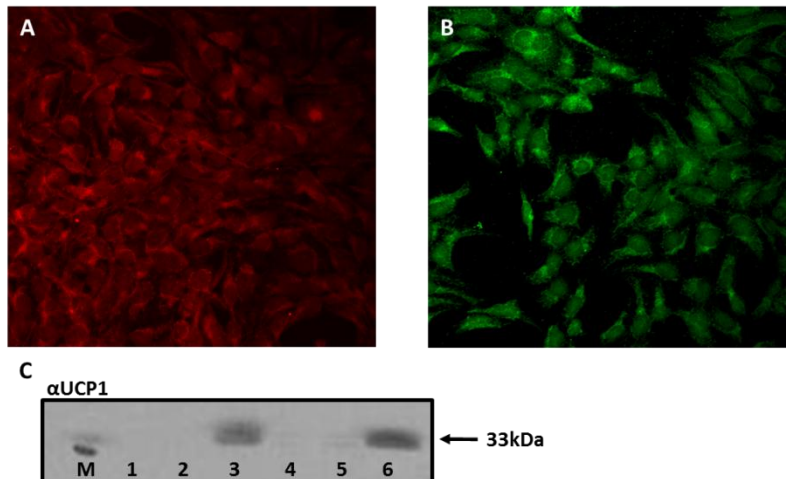


**Figure 10** Subcellular localisation of UCP1 in HEK293 UCP1 cells.

Mitochondria of HEK293 cells were stained with mitotracker (A) and UCP1 was detected immunologically in fixed HEK293 UCP1 cells (B). The similar distribution of signal suggests mitochondrial localisation of UCP1 in HEK293 UCP1 cells. This was confirmed by western blot analysis of cellular fractions (C). HEK293 UCP1 cell homogenate (lane 1, 4), the cell fractions pelleted by slow centrifugation (lane 2, 5) and the mitochondrial fraction pelleted by fast centrifugation (lane 3, 6) were used and UCP1 could only be detected in the mitochondrial fraction.

### 3.1.2.2 Calibration of a recombinant UCP1 protein standard

After confirmation of mitochondrial targeting, the expression level of UCP1 in HEK293 UCP1 mitochondria was determined. Knowing the amount of UCP1 per mg mitochondrial protein was a prerequisite for the calculation of UCP1 transport activity in the test system and enabled comparisons of the expression level to those reached in BAT and other test systems. UCP1 content was quantified with a recombinant mouse UCP1 standard. The protein had been expressed in *E. coli* and purified from inclusion bodies (provided by Bruno Miroux). The standard was used to generate a standard curve, relating intensity of immunological signals to UCP1 protein amounts. Therefore the UCP1 concentration in the standard had to be determined and it was calculated by correcting the Lowry quantification of the standard solution for its purity. The purity was determined by separation of a sample of standard solution on a SDS-PAGE and subsequent staining with Coomassie (**Figure 11A**). The intensity of the prominent UCP1 band at 33 kDa was divided by whole lane signal intensity. This was done for 3 different loading amounts of the standard and resulted in an average estimation of purity of 60.7 %. According to the corrected concentration of the UCP1 standard solution it was possible to load defined amounts of UCP1 protein on a SDS-PAGE and perform immunological detection of the protein after transfer on a nitrocellulose membrane (**Figure 11B**). Signals were detected with the Odyssey system (LICOR) and quantified with the manufacturer's software. Signal intensity analyses of 5 independent blots were each normalised to the intensity value of the highest

standard loading amount. Mean normalised signal intensities were plotted against UCP1 amount, resulting in a standard curve (**Figure 11C**), which demonstrated linearity of immunological signal per UCP1 amount. Therefore it was possible to quantify UCP1 amount in mitochondrial samples of HEK293 UCP1 cells with the chosen amounts of standard.

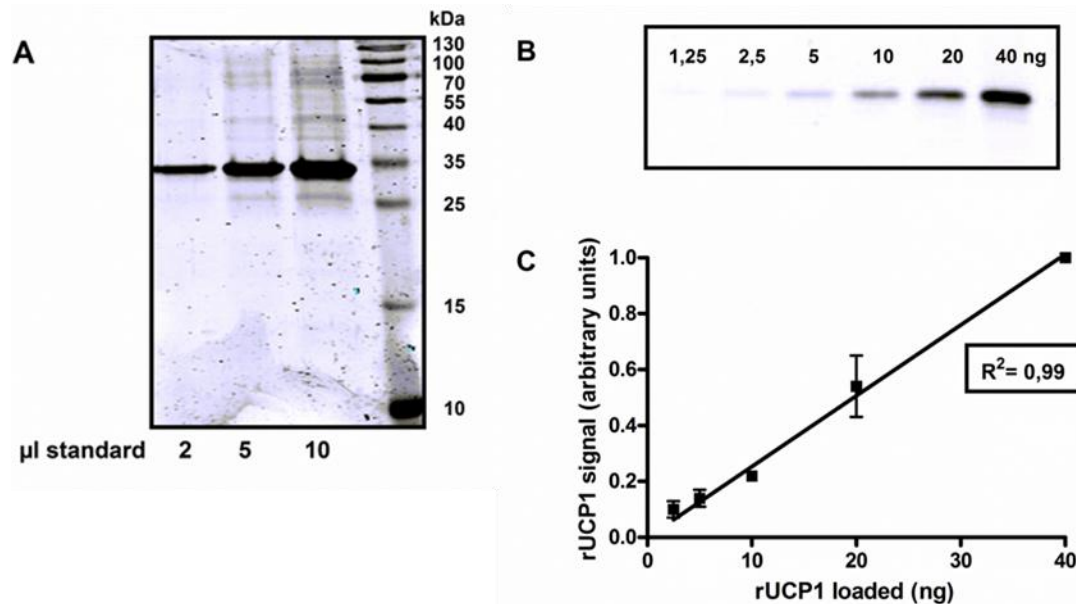


**Figure 11** Quantification of UCP1 standard solution and generation of a standard curve for UCP1 immunological signals.

The purity of recombinant UCP1 standard solution was analysed by separation on an SDS-PAGE and subsequent Coomassie staining (A). Defined amounts of UCP1 protein were used for western blot analyses and detected with an antibody against UCP1. (B) The mean intensity of immunological signals was plotted against the amount of loaded UCP1, resulting in a standard curve (C).

### 3.1.2.3 Quantification of UCP1 protein content in HEK293 mitochondria

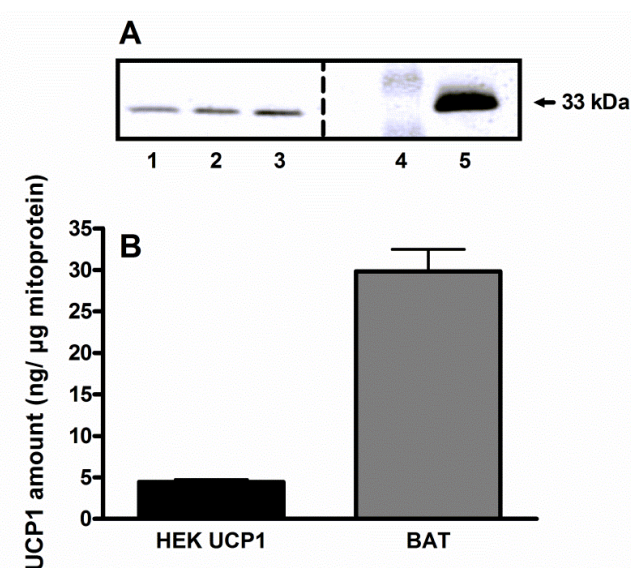


**Figure 12** Abundance of UCP1 protein in HEK293 UCP1 mitochondria and BAT mitochondria from RT-acclimated mice.

Exemplary immunological detection of UCP1 in mitochondria isolated from HEK293 UCP1 cells (lane 1-3) and from RT-acclimated mice (lane 5) (A). The correct size of immunological signal was controlled with a mass standard (lane 4). The amount of UCP1 protein per mitochondrial protein in HEK293 UCP1 cells and in BAT from RT-acclimated mice was determined by densitometric analysis of immunological signals and interpolation of the standard curve, generated with recombinant protein (B). Bars represent means  $\pm$  SEM; n= 3-5.

Mitochondrial samples from HEK293 UCP1 cells were analysed by western blot to determine their content of UCP1 protein. With the help of the recombinant standard densitometric analyses of immunological signals could be related to an absolute UCP1 amount. HEK293 UCP1 mitochondria contained 4.8  $\mu\text{g}$  UCP1/mg mitochondrial protein (**Figure 12**). UCP1 content in BAT mitochondria from RT-acclimated mice was determined as a reference and was 29.8  $\mu\text{g}$  UCP1/mg mitochondrial protein.

#### 3.1.2.4 Regulation of proton leak in HEK293 UCP1 mitochondria

After verification of stable expression and mitochondrial targeting of heterologously expressed UCP1 in HEK293 cells the function of the protein was tested. As active UCP1 increases proton leak, the proton leak kinetics of isolated HEK293 and HEK293 UCP1 mitochondria were determined for control conditions, in the presence of palmitate, which is known to activate UCP1, and in the presence of the UCP1 inhibitor GDP and palmitate at the same time.

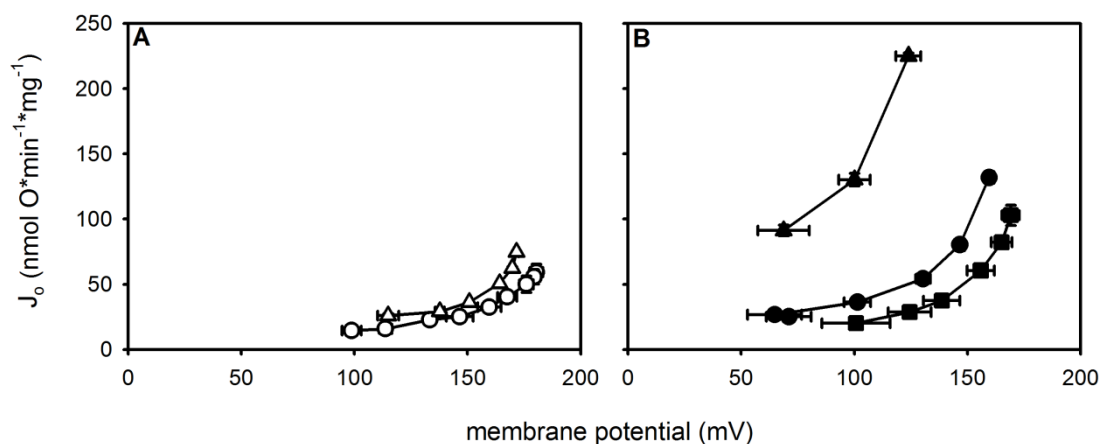


**Figure 13 Proton leak kinetics of mitochondria isolated from HEK293) and HEK293 UCP1 cells.**

Proton leak curves result from the plot of oxygen consumption ( $J_o$ ) in leak conditions against membrane potential. Mitochondria isolated from HEK293 cells (white symbols) did not change proton leak kinetics in the presence of palmitate (triangle) compared to control conditions (circle) (A). Proton leak of mitochondria isolated from HEK293 UCP1 cells (black symbols) was increased in the presence of palmitate, as indicated by the upwards shift of the curve compared to the control condition. This increase in proton conductance did not occur in the presence of GDP and palmitate (square) indicating that it reflected an activation of UCP1 (B). Values are means  $\pm$  SEM; n= 3-10.

Proton leak measurements were performed in the presence of oligomycin, which blocks ATP synthesis. Therefore the residual oxygen consumption reflected respiratory chain activity needed to maintain membrane potential against leak only, which is why oxygen consumption can be used to quantify the amount of proton leak. Therefore differences in proton leak between different mitochondria or incubation conditions at a certain membrane potential can be compared by looking

at leak respiration driving the maintenance of this membrane potential. Analysis of mitochondria from HEK293 cells demonstrated that changes in FFA level did not influence their proton leak kinetics as they were identical to control conditions (**Figure 13A**). During measurements with HEK293 UCP1 mitochondria the addition of palmitate increased proton leak, indicated by the upwards shift of the curve, whereas GDP prevented this increase and coupled mitochondria even stronger than under control conditions, indicated by the downwards shift of the curve (**Figure 13B**). Differences in proton leak were quantified by comparison of leak respiration of different mitochondria in different measurement conditions at the highest common potential, which was reached in all single measurements of the data set.

The highest common potential reached in the data set of mitochondria from HEK293 and HEK293 UCP1 cells was 117 mV. Mitochondria from HEK293 cells consumed 20 nmol O $\cdot$ min $^{-1}$  $\cdot$ mg $^{-1}$  to defend this membrane potential under control conditions and 25 nmol O $\cdot$ min $^{-1}$  $\cdot$ mg $^{-1}$  in the presence of 100  $\mu$ M palmitate. Mitochondria from HEK293 UCP1 cells needed almost the same amount of oxygen in the presence of 1 mM GDP and 100  $\mu$ M palmitate (24 nmol O $\cdot$ min $^{-1}$  $\cdot$ mg $^{-1}$ ), but exhibited increased respiration under control conditions, with an oxygen consumption of 44 nmol O $\cdot$ min $^{-1}$  $\cdot$ mg $^{-1}$  needed to maintain the membrane potential of 117mV. In the presence of 100  $\mu$ M palmitate mitochondria from HEK293 UCP1 cells increased the leak-dependent oxygen consumption further to 196 nmol O $\cdot$ min $^{-1}$  $\cdot$ mg $^{-1}$ , which is 4.5 fold as high as for control conditions (**Figure 14**).

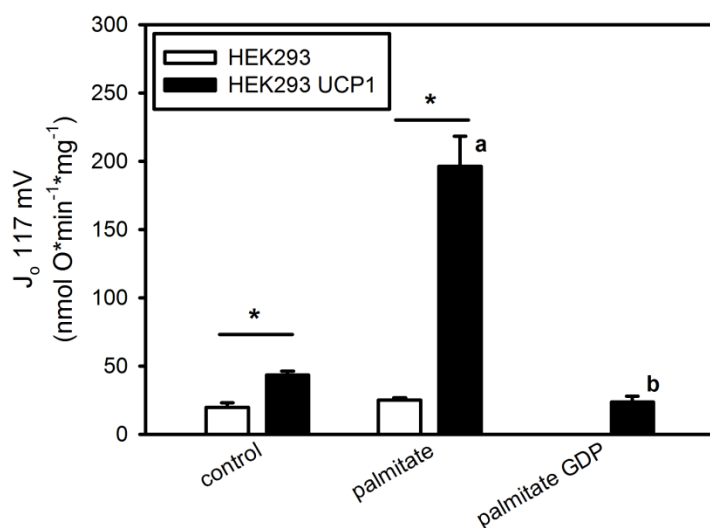


**Figure 14 Comparison of mitochondrial leak respiration for HEK293 and HEK293 UCP1.**

At 117mV, the highest common membrane potential reached in all measurements of the data set from Figure 13, mitochondria from HEK293 cells did not change leak respiration ( $J_o$ ) compared to control conditions after addition of palmitate. Mitochondria isolated from HEK293 UCP1 cells had significantly higher leak respiration than mitochondria from HEK293 mitochondria in control conditions which was further increased in the presence of palmitate. This increase did not occur if GDP was present at the same time. Bars represent means  $\pm$  SEM; n= 3-10; Asterisks indicate significant differences between cell types for one treatment, small letters indicate significant differences between treatments for one cell type.  $p < 0.05$ .

### 3.1.2.5 Basal proton leak of HEK293 and HEK293 UCP1 mitochondria

Proton leak in control conditions was clearly elevated in mitochondria from HEK293 UCP1 cells compared to mitochondria from HEK293 cells, displaying an almost 2 fold leak respiration at 117 mV (**Figure 14**). Therefore it had to be excluded that this represented an uncoupling artefact caused by



improper folding and insertion of the heterologously expressed protein into the mitochondrial membrane. This phenomenon has been reported for yeast, expressing UCP1 at a level higher than 0.9  $\mu\text{g}/\text{mg}$  mitochondrial protein (Stuart et al., 2001b). Such an artefact would reduce the suitability of the HEK293 cell system for identification of new modulators of UCP1 function and exclude its suitability for elucidation of its mechanistic function or the physiological role of the protein.

Therefore basal leak of mitochondria from HEK293 and HEK293 UCP1 cells was determined and directly compared in the presence of the UCP1 inhibitor GDP. As the overlaying proton leak curves in **Figure 15** demonstrate, the leak difference observed between the two cell lines in control conditions disappeared, excluding an uncoupling artefact caused by heterologous UCP1. Leak respiration at 117mV was 13  $\text{nmol O} \cdot \text{min}^{-1} \cdot \text{mg}^{-1}$  for HEK293 mitochondria in these conditions and 19  $\text{nmol O} \cdot \text{min}^{-1} \cdot \text{mg}^{-1}$  for HEK293 UCP1 mitochondria.

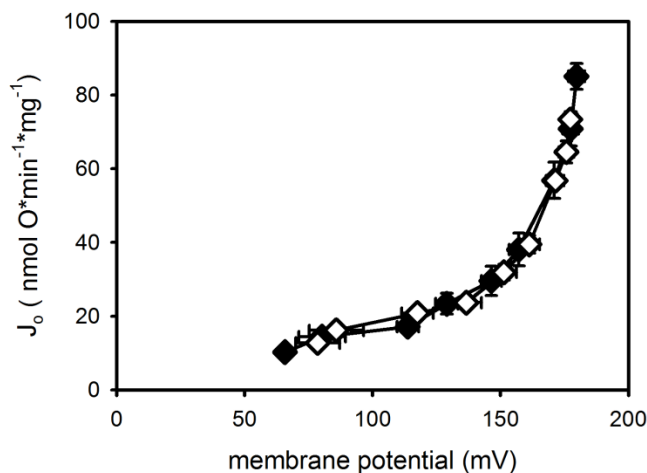


**Figure 15 Basal proton leak of mitochondria isolated from HEK293 and HEK293 UCP1 cells.**

The plot of oxygen consumption ( $J_o$ ) against membrane potential illustrates, that in the presence of 1mM GDP proton leak kinetics of mitochondria from HEK293 (white symbols) and HEK293 UCP1 cells (black symbols) were identical. This demonstrated that the heterologous expression did not cause an uncoupling artefact and that the presence of UCP1 alone did not contribute to basal proton leak. Values are means  $\pm$  SEM; n= 6.

### 3.1.2.6 Respiration states of isolated HEK293 and HEK293 UCP1 mitochondria

In addition to proton leak kinetics, which is the combined information of membrane potential and leak respiration (state 4, no ATP synthesis) in different steady states, basal respiration (state 2), phosphorylating respiration (state 3) and maximum respiration of mitochondria from HEK293 and HEK293 UCP1 cells were determined. Mitochondria from HEK293 UCP1 cells displayed a higher basal respiration with 102  $\text{nmol O} \cdot \text{min}^{-1} \cdot \text{mg}^{-1}$  compared to HEK293 mitochondria consuming 50  $\text{nmol O} \cdot \text{min}^{-1} \cdot \text{mg}^{-1}$ . Addition of GDP increased basal respiration in HEK293 mitochondria to 65  $\text{nmol O} \cdot \text{min}^{-1} \cdot \text{mg}^{-1}$  and reduced it in HEK293 UCP1 mitochondria to 76  $\text{nmol O} \cdot \text{min}^{-1} \cdot \text{mg}^{-1}$ , which still represented a significant difference between the two cell lines (**Figure 16**).

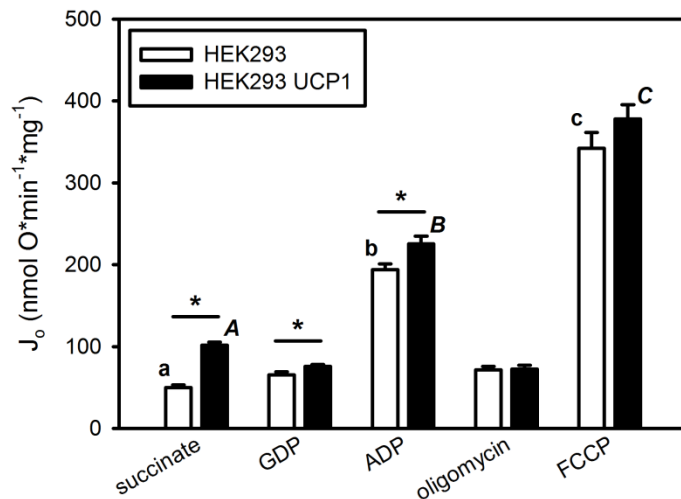


**Figure 16** Respiration ( $J_o$ ) of mitochondria isolated from HEK293 and HEK293 UCP1 cells.

Different respiratory states of mitochondria isolated from HEK293 (white bars) and HEK293 UCP1 cells (black bars) were determined with a Clark-electrode. Basal respiration (succinate), basal respiration in the presence of the UCP1 inhibitor GDP, phosphorylating respiration (ADP), leak respiration (oligomycin) and maximum respiratory capacity (FCCP) were subsequently titrated. Basal respiration in the absence and presence of GDP and phosphorylating respiration were significantly higher in mitochondria isolated from HEK293 UCP1 cells compared to mitochondria from HEK293 cells. Bars represent means  $\pm$  SEM;  $n = 11-12$ . Asterisks indicate significant differences between cell types for one treatment, small and italic letters indicate significant differences between treatments for one cell type.  $p < 0.05$ .

Addition of ADP induced phosphorylating respiration, as ATP synthase could now generate ATP from ADP and phosphate, which was supplied in the measurement buffer. In this condition both types of mitochondria increased respiration approximately to the 2.5 fold value of basal respiration and the mitochondria from HEK293 UCP1 cells still displayed significantly higher respiration than mitochondria from HEK293 cells. Leak respiration in the presence of oligomycin was about  $70 \text{ nmol O} \cdot \text{min}^{-1} \cdot \text{mg}^{-1}$  and not different between the two types of mitochondria, reflecting the finding from proton leak measurements (**Figure 15**). Maximum respiratory capacity, measured after addition of the chemical uncoupler FCCP, was also not changed by heterologous expression of UCP1 in HEK293 cells and was around  $350 \text{ nmol O} \cdot \text{min}^{-1} \cdot \text{mg}^{-1}$  in both types of mitochondria, approximately 6 fold as high as basal respiration.

### 3.1.2.1 Expression of tagged UCP1 in HEK293 cells

In order to further explore the potential of the HEK293 expression system for comparison of UCP paralogs and orthologs, it was tested if expression of a tagged version of the protein would impair mitochondrial targeting or the regulation of its activity in the heterologous cellular background. The expression of tagged UCP versions in HEK293 cells could facilitate direct comparisons, as protein expression could be compared using one antibody. Otherwise standards for all different UCP versions would have to be generated, quantified and calibrated to obtain exact expression levels, which would have to be determined for calculation of catalytic activities.

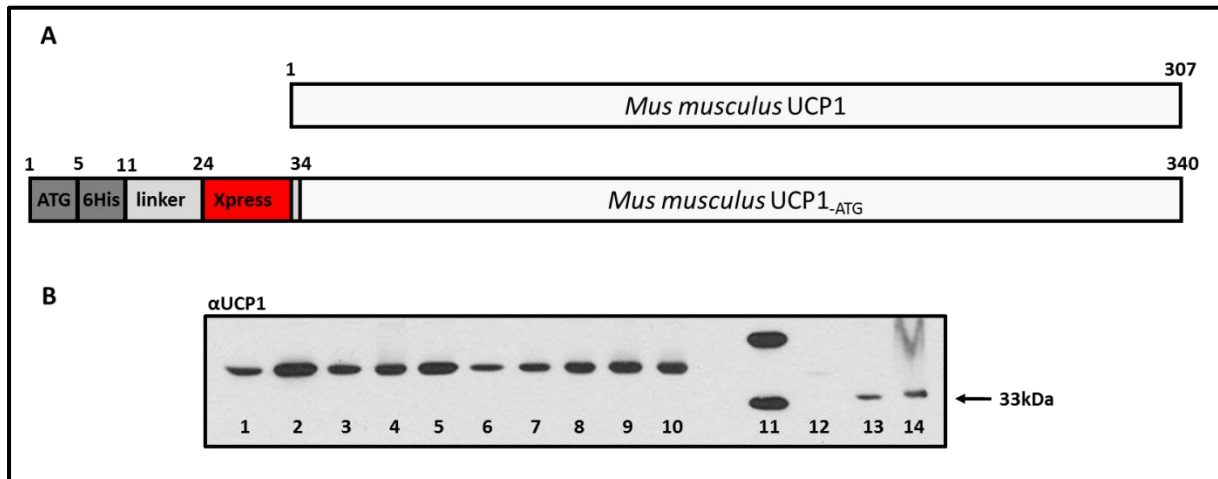


**Figure 17** Schematic illustration of Xpress-tagged UCP1 (tagUCP1) and immunological detection of tagUCP1 in mitochondria isolated from stably transfected HEK293 cells.

Schematic illustration of Xpress tag-modified UCP1, generated by expression of the protein from pcDNA4 vector (A). Xpress-tagged UCP1 was detected in mitochondria isolated from stably transfected HEK293 cells (lane 1-10) with an antibody against UCP1 (B). A mass standard was used as reference for the size of the protein (lane 11) and mitochondria from HEK293 Dr UCP1 (*Danio rerio* sequence, lane 12) HEK293 UCP1 cells (cell line with low expression level (lane 13) and mainly used cell line (lane 14)) were used as positive control. The tag induced a size shift of the immunological signal, but the signal was still found in the mitochondrial fraction.

Mouse UCP1 modified with an Xpress tag ( **Figure 17A**) could be detected in isolated mitochondria from stably transfected HEK293 cells with an antibody raised against hamster UCP1 and the signal was shifted to higher size, as expected due to the elongation of the protein by the 33 amino acid tag ( **Figure 17B**). Immunological signals for mitochondria from HEK293 tagUCP1 cell lines were even stronger than for HEK293 UCP1 mitochondria and BAT mitochondria which were used as positive controls on the same blot.

### 3.1.2.1 Regulation of proton leak in mitochondria isolated from HEK293 tagUCP1 cells

The function of Xpress-tagged UCP1 was tested by determination of proton leak kinetics of isolated mitochondria of one of the generated cell lines. The protocol was identical to the one used for mitochondria from HEK293 cells expressing the native protein version. Comparison of proton leak in control conditions, in the presence of palmitate and in the presence of GDP and palmitate at the same time demonstrated regulation of protein activity as found for the untagged protein (**Figure 18**). Palmitate increased proton leak compared to control conditions and this could be prevented by addition of GDP. In the presence of GDP proton leak was even lower than in control conditions.

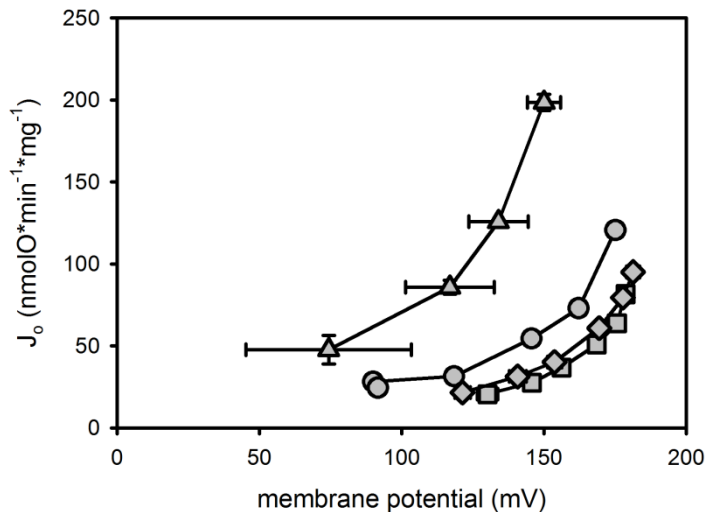


**Figure 18** Proton leak kinetics of mitochondria isolated from HEK293 tagUCP1 cells.

Oxygen consumption ( $J_o$ ) is plotted against membrane potential to illustrate the kinetics of proton leak. Addition of palmitate (triangle) increased proton leak of mitochondria from HEK293 tagUCP1 cells as indicated by the upwards shift of the curve, compared to control conditions (circle). GDP addition (square) prevented palmitate induced increase in proton leak and coupled mitochondria back to basal leak, which was identical to proton leak in the presence of GDP alone (diamond). The Xpress tag did not impair regulation of UCP1 by fatty acids and purine nucleotides. Values are means  $\pm$  SEM;  $n=2-3$ .

In order to quantify the regulation of proton leak by palmitate and GDP and to compare it to the regulation of unmodified UCP1 in HEK293 cell mitochondria the respiration needed to maintain the highest membrane potential found in all single measurements of the two data sets was estimated by linear interpolation of proton leak curve values. The highest common potential was 117mV and mitochondria isolated from HEK293 tagUCP1 cells needed between 15 nmol O\*min<sup>-1</sup>\*mg<sup>-1</sup> and 93 nmol O\*min<sup>-1</sup>\*mg<sup>-1</sup> to maintain this membrane potential, depending on incubation conditions. Absolute values of oxygen consumption reflecting leak respiration in different conditions were always lower than those determined for mitochondria from HEK293 cells expressing the native UCP1 protein under the same condition (**Figure 19A**), but regulation between conditions was almost identical in mitochondria from the two cell lines.

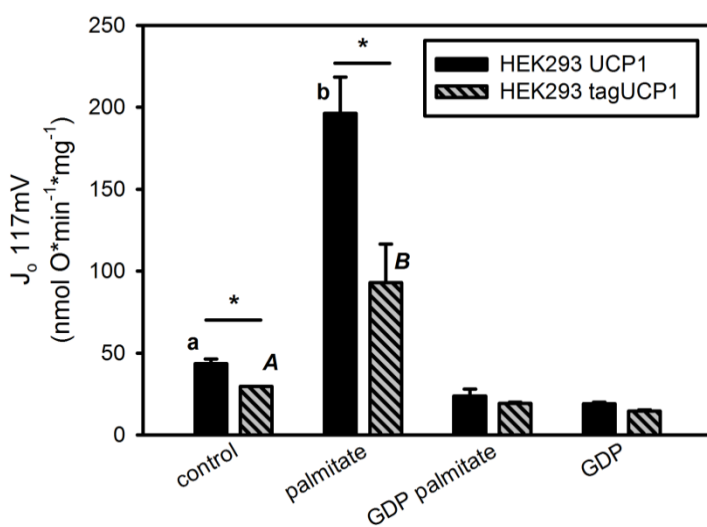


**Figure 19** Comparison of HEK293 UCP1 and HEK293 tagUCP1 mitochondrial leak respiration.

Proton leak curves describing proton leak kinetics of mitochondria isolated from HEK293 UCP1 and HEK293tag UCP1 cells were compared at the highest common potential which was reached in all single measurements and was 117 mV. Respiration ( $J_o$ ) which was needed to maintain this membrane potential against leak processes is plotted for different incubation conditions. Absolute leak respiration was higher in mitochondria from HEK293 UCP1 cells but the addition of palmitate increased leak in mitochondria containing native or tagged UCP1. Coincubation with GDP prevented this increase in leak respiration and lowered it

below control conditions. Bars represent means  $\pm$  SEM,  $n=2-9$ . Asterisks indicate significant differences between cell types for one treatment, small and italic letters indicate significant differences between treatments for one cell type.  $p < 0.05$ .

### 3.1.2.2 Oxygen consumption of trypsinised HEK293 cells

Even though UCP1 is a mitochondrial protein it might be regulated indirectly by processes taking place in other compartments of the cell. Only analysis of UCP1 function and proton leak in whole cells could detect such effects. Therefore analysis of UCP1 function in trypsinised intact HEK293 and HEK293 UCP1 cells was performed, also as basis for later analyses of the effects of interaction candidates. Such candidates could be transferred to the cells by transient transfection in small scale, avoiding large scale transfections which would be necessary to isolate enough mitochondria for subsequent determination of proton leak kinetics.

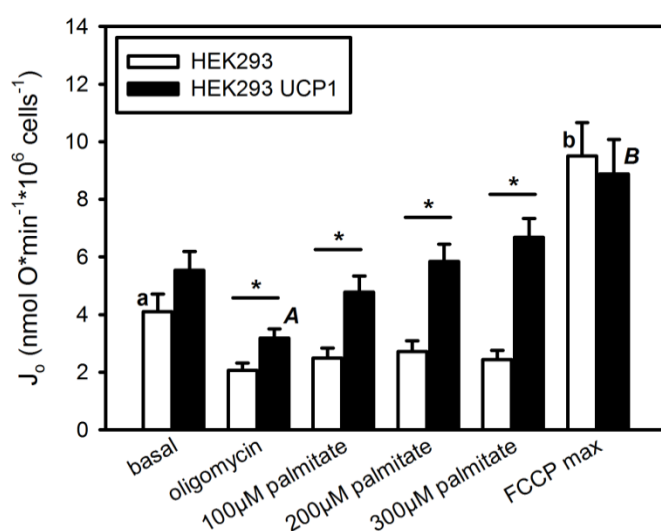


**Figure 20** Respiration of trypsinised HEK293 and HEK293 UCP1 cells.

Oxygen consumption ( $J_o$ ) of trypsinised HEK293 and HEK293 UCP1 cells was analysed with a Clark-electrode. After determination of basal respiration in the presence of glucose leak respiration was quantified after addition of oligomycin. A possible contribution of UCP1 to leak respiration was analysed by addition of different amounts of its activator palmitate. Maximum respiratory capacity was determined by addition of FCCP. Bars represent means  $\pm$  SEM;  $n=11-12$ . Asterisks indicate significant differences between cell types for one treatment, small and italic letters indicate significant differences between treatments for one cell type.  $p < 0.05$ .

Maximum respiration, induced by addition of the chemical uncoupler FCCP, was not different between HEK293 and HEK293 UCP1 cells, with mean values of 9.5 and 8.8 nmol O\*min<sup>-1</sup>\*10<sup>6</sup> cells<sup>-1</sup>, respectively. Respiration values for all other titrated states differed between the two cell lines and HEK293 UCP1 cells displayed about 0.5 fold to 3 fold increased oxygen consumption compared to HEK293 cells. Basal respiration of trypsinised HEK293 cells was at 4.1 nmol O\*min<sup>-1</sup>\*10<sup>6</sup> cells<sup>-1</sup> and decreased to a leak respiration of 2.1 nmol O\*min<sup>-1</sup>\*10<sup>6</sup> cells<sup>-1</sup> after addition of oligomycin. This value was almost unchanged in the presence of palmitate. HEK293 UCP1 cells had a basal oxygen consumption of 5.5 nmol O\*min<sup>-1</sup>\*10<sup>6</sup> cells<sup>-1</sup>, which decreased to a leak respiration of 3.2 nmol O\*min<sup>-1</sup>\*10<sup>6</sup> cells<sup>-1</sup> in the presence of oligomycin and increased stepwise upon the addition of palmitate to 6.7 nmol O\*min<sup>-1</sup>\*10<sup>6</sup> cells<sup>-1</sup> in the presence of 300 µM palmitate.

### 3.1.2.3 Oxygen consumption of adherently growing HEK293 cells

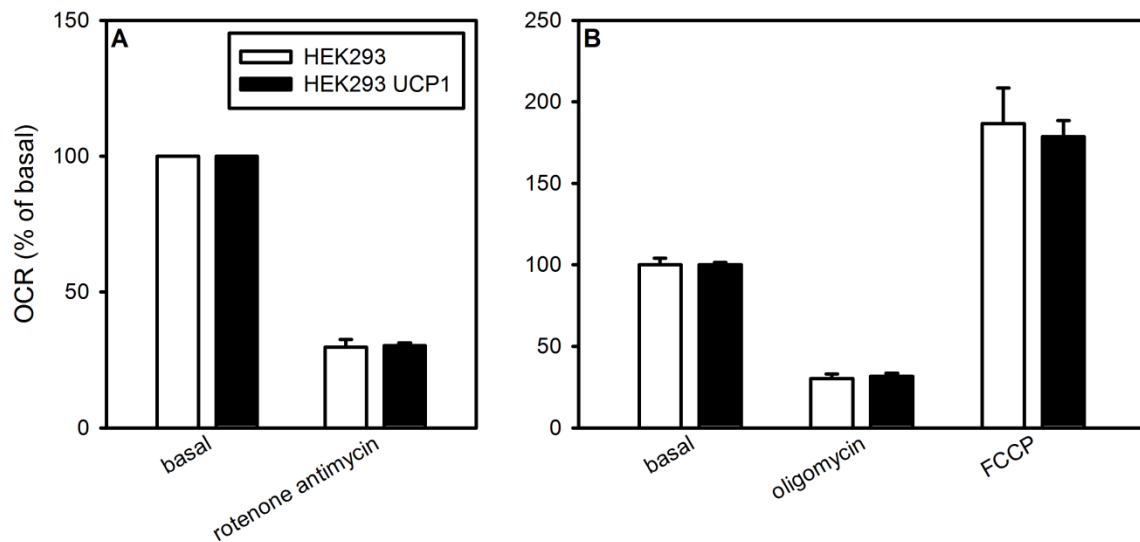


**Figure 21** Oxygen consumption rate (OCR) of adherently growing HEK293 and HEK293 UCP1 cells in different respiratory states.

HEK293 (white bars) and HEK293 UCP1 cells (black bars) were grown on 96well plates and analysed with a Seahorse XF96 flux analyser. Fluorescence based analysis of oxygen consumption allowed to determine basal oxygen consumption, leak respiration (oligomycin), maximum respiratory capacity (FCCP) and non-mitochondrial respiration (rotenone antimycin). The presence of UCP1 in HEK 293 UCP1 cells did not change cellular respiration in any of the analysed conditions compared to HEK293 control cells. Bars represent means  $\pm$  SEM of 7 plates with each 20 wells per condition.

Trypsinisation of usually adherently growing cells can be difficult to control and harm the cells as it changes their extracellular protein matrix and cells adopt to a round shape. Therefore the analysis of HEK293 and HEK293 UCP1 cells was also performed with Seahorse XF technology, allowing the determination of oxygen consumption of adherently growing cells. Oxygen consumption rates were determined first for basal conditions, then after addition of oligomycin (leak respiration) and after addition of FCCP, revealing maximum respiratory activity. As there are additional reactions in the intact cell which consume oxygen, these values were corrected for non-mitochondrial respiration, detected after injection of rotenone and antimycin.

In the chosen experimental conditions HEK293 and HEK293 UCP1 cells did not differ in any of the four analysed states (**Figure 21**). Non-mitochondrial respiration accounted for 25 % of basal respiration and was subtracted from basal, leak and maximum respiration. After this correction leak respiration accounted for 30 % of basal respiration and FCCP induced maximum respiratory capacity reached about 180 % of basal respiration.

### 3.1.3 UCP1 activity in immortalised brown adipocytes (BFC)

HEK293 cells were chosen as test system for UCP1 activity, as they are a well-established mammalian cell culture model, which does not endogenously express uncoupling proteins. This allows expression of different UCP paralogs or orthologs and comparison of their function in an identical mitochondrial or cellular background. The disadvantage of this system is that the cellular and mitochondrial environment might not contain all factors necessary to support an optimum function of uncoupling proteins. Differences in metabolism or the lack of cofactors might prevent a meaningful analysis of interaction candidates by knockdown or overexpression. Therefore, in addition to the HEK293 UCP1 cell line, a brown adipocyte cell culture model was characterised and compared to the HEK293 UCP1 cells.

#### 3.1.3.1 *Stimulation of endogenous UCP1 expression in BFC*

An established brown preadipocyte cell line (BFC), which had been provided by the laboratory of Bruce Spiegelman, was available in the laboratory. After differentiation of these cells according to the published protocol (Uldry et al., 2006) cells developed into mature adipocytes with multilocular lipid droplets (**Figure 22**), but showed only low or undetectable expression of UCP1.

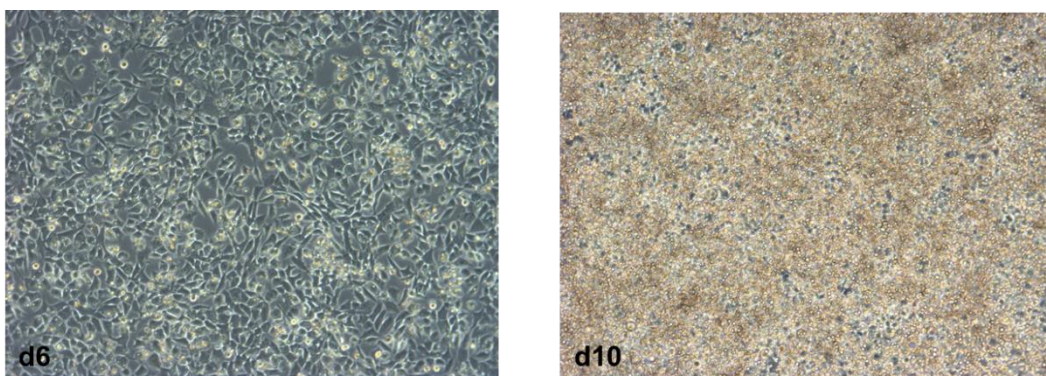


**Figure 22 Fat accumulation in BFC during differentiation.**

Lightmicroscopic pictures (Zeiss Axiovert 40 CFL, 10x magnification) of differentiating BFC illustrate fat accumulation in form of small lipid droplets between day 6 (d6, 2 days after induction) and day 10 (d10, fully differentiated cells).

The published protocol suggested different treatments to induce the thermogenic phenotype of the cell line and some of them were tested to find an optimum treatment to achieve a high UCP1 expression level in these cells. It was supposed that expression of UCP1 above a certain minimum would allow analysis of protein function in isolated mitochondria of these cells, which would represent a cell culture model with endogenous UCP1 expression. Tested stimulatory substances

were isoproterenol, retinoic acid and rosiglitazone and differentiated BFC were incubated with them for 48 h. Isoproterenol, retinoic acid and rosiglitazone alone each already induced UCP1 expression, with retinoic acid having the strongest effect. A maximum induction of UCP1 expression was achieved by adding a combination of isoproterenol and retinoic acid to the cells, reaching UCP1 amounts of 2.8 ng UCP1/ $\mu$ g mitochondrial protein. This was about 10 % of the UCP1 amount detected in BAT mitochondria from RT- acclimated mice and 60 % of the UCP1 amount detected in mitochondria of stably transfected HEK293 UCP1 cells (**Figure 23**).

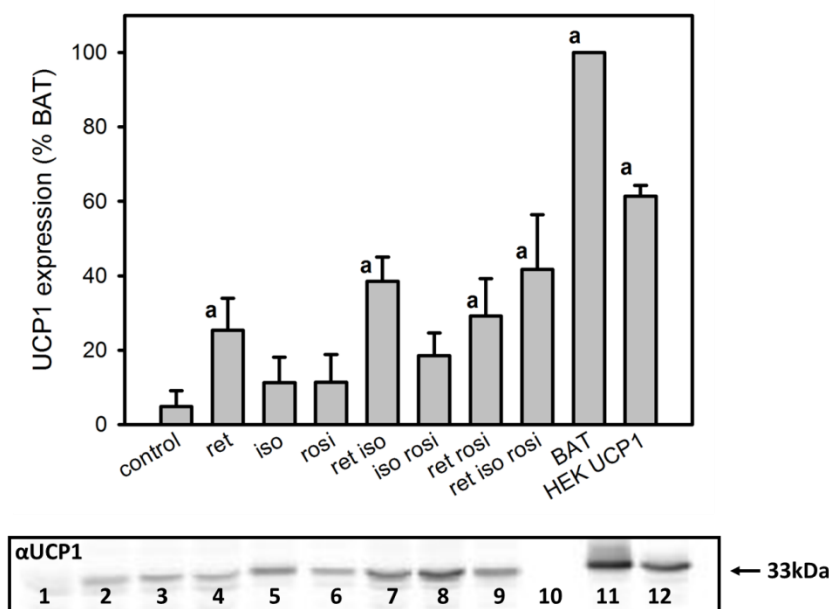


**Figure 23** Stimulation of UCP1 expression in differentiated BFC.

Differentiated BFC were treated with retinoic acid (ret; lane 2), isoproterenol (iso; lane 3), rosiglitazone (rosi; lane 4) and all possible combinations of the substances (ret/iso, lane 5; iso/rosi, lane 6; ret/rosi, lane 7; ret/iso/rosi, lane 8 and 9) or were just kept in differentiation medium (control, lane 1) for 48 h to induce expression of UCP1. Protein abundance was tested by western blot analysis of isolated mitochondria from stimulated cells. The size of the detected protein was controlled with a mass standard (lane 10) and signals were analysed densitometrically, normalised to a protein sample from brown fat

(BAT) and compared to a sample from HEK293 UCP1 mitochondria (lane 12). Treatment with a combination of isoproterenol and retinoic acid was most effective for stimulation of UCP1 expression. Bars represent means  $\pm$  SEM; n=3. **a** indicates a significant difference from control treatment.  $p < 0.05$ .

### 3.1.3.2 Generation of immortalised brown preadipocyte cell lines

In addition to the characterisation of the established brown preadipocyte cell line new cell lines were generated, aiming to isolate cell lines with higher potential to express UCP1 than found for BFC. Stromal vascular cells from the interscapular brown adipose tissue of 6 newborn mice were isolated and kept as 12 independent cell lines. They were transduced with pMXS LTA vector to express Large T Antigen fragments and were selected for successful treatment with puromycin. All cell lines survived this selection process and the further treatment against possible mycoplasma contamination. Cell aliquots were stored in liquid nitrogen and differentiation potential was tested. 10 cell lines were differentiated to test the expression level of UCP1 in mature adipocytes, but most of them showed high mortality during differentiation. Surviving cells were stimulated with a combination of isoproterenol and retinoic acid to induce the thermogenic phenotype. Western blot analysis of protein extracts demonstrated, that all cell lines expressed UCP1 and CideA after



stimulation (**Figure 24**), but due to the high mortality of cells during the differentiation process they were not used for further experiments on UCP1 function.

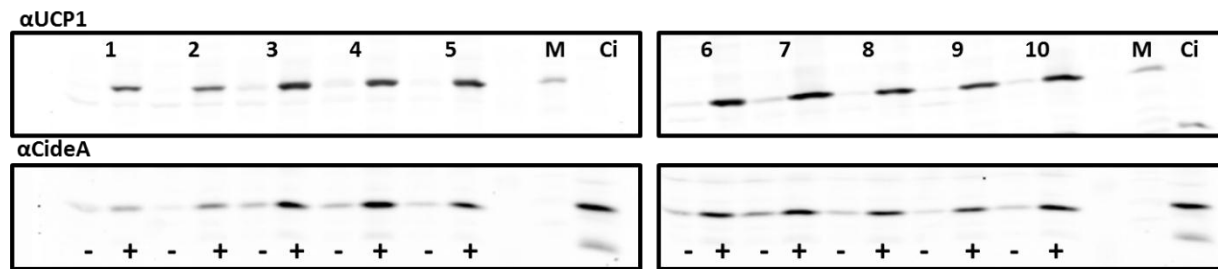


**Figure 24** Immunological detection of UCP1 and CideA in protein extracts from differentiated immortalised brown adipocytes.

Generated preadipocyte cell lines were differentiated and treated with isoproterenol and retinoic acid for 48 h (+) or kept in differentiation medium for 48 h (-). Whole cell protein extracts were generated and tested for the presence of UCP1 and CideA by western blot analysis. All analysed cell lines (1-10) showed clear immunological signals for UCP1 after stimulation, and some even a weak signal without stimulation. All cell lines expressed low amounts of CideA when kept in differentiation medium and this expression was further increased by the stimulation treatment.

### 3.1.3.1 *Effect of thermogenic stimulation on transcript levels of UCP1 and selected other genes in BFC*

In order to control the effect of the stimulation treatment on the expression of other genes, which might be relevant for the analysis of proton leak, BFC were differentiated and stimulated and RNA was isolated from the cells. RNA was transcribed into cDNA and the abundance of transcripts was determined with qPCR. Data were standardised to the expression of the housekeeping genes  $\beta$ -actin and Hsp90, which were unaffected by the different treatments. Afterwards data were normalised to the expression in control conditions.

UCP1 expression was strongly upregulated upon stimulation treatment of BFC, with a more than 60 fold increase of transcript amount after treatment with isoproterenol and retinoic acid. This huge increase compared to control can probably in part be explained by the lack of expression in control conditions. Isoproterenol alone and the combination of retinoic acid and rosiglitazone lead to an 10 fold increase of expression compared to control, whereas the treatment with all three substances in combination lead to a 30 fold expression level. CideA was regulated by the treatments to a smaller extent, with maximum fold changes of transcript level of about 4. This strongest regulation was also detected after treatment with isoproterenol and retinoic acid, although rosiglitazone alone already lead to a 2.5 fold increase of expression (**Figure 25**).

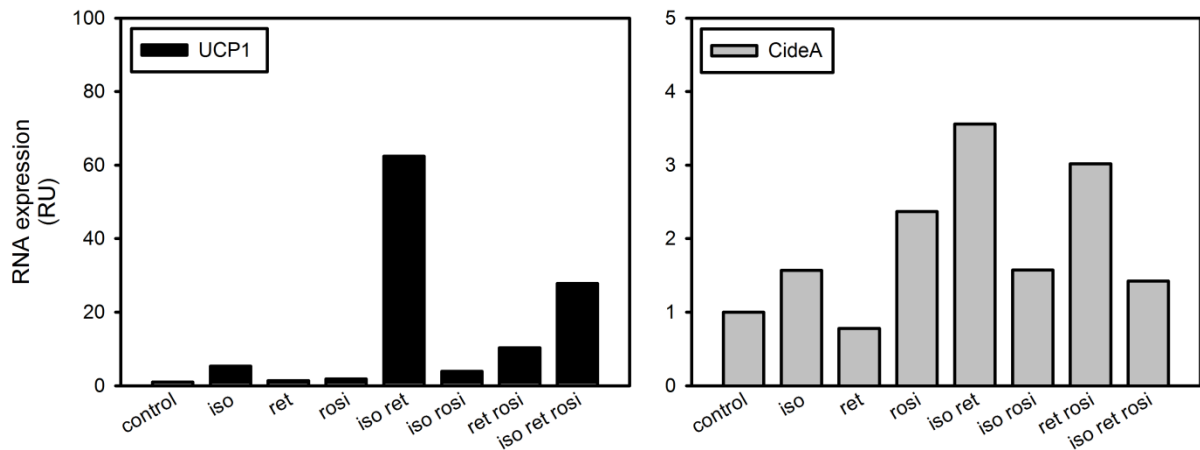


**Figure 25** Expression of UCP1 and CideA transcripts in differentiated and stimulated BFC.

BFC were differentiated and stimulated with isoproterenol (iso), retinoic acid (ret) and rosiglitazone (rosi) alone and in different combinations to induce UCP1 expression. UCP1 and CideA mRNA were quantified, confirming strongest expression of UCP1 after treatment with isoproterenol and retinoic acid and demonstrating that CideA is slightly upregulated by the stimulation too. Bars represent the means of 3 technical replicates for 1 biological sample.

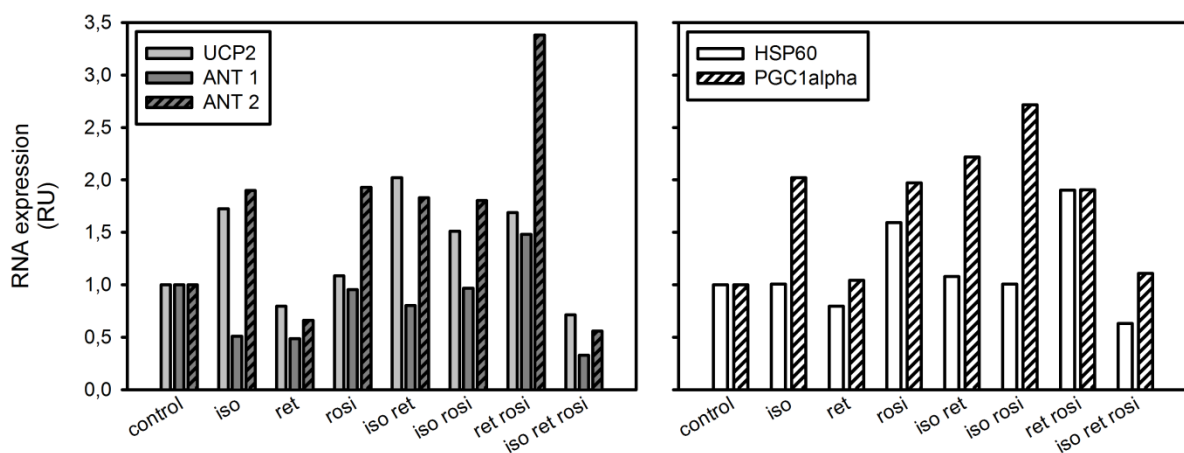


**Figure 26** RNA expression level of mitochondrial carriers and markers for mitochondrial proliferation in differentiated BFC after agonist treatments.

BFC were differentiated and stimulated with isoproterenol (iso), retinoic acid (ret) and rosiglitazone (rosi) to induce UCP1 expression. The transcripts of other mitochondrial and cellular proteins were tested for changed expression due to the treatment, in order to exclude secondary effects in BFC proton leak measurements. Bars represent the means of 3 technical replicates for 1 biological sample.

Besides the RNA expression level of UCP1 and CideA, the two proteins of main interest in this work, transcript regulation of other proteins of the inner mitochondrial membrane, which might contribute to proton leak was analysed. UCP3 could not be detected by qPCR and UCP2 expression was changed up to 2 fold by the treatments. The same was true for adenine nucleotide translocase 1 (ANT 1), whereas ANT 2 was about 3.5 fold upregulated after treatment with retinoic acid and rosiglitazone (**Figure 26**). Hsp60, a mitochondrial chaperone, was mostly unregulated but upregulated to 2 fold

expression by retinoic acid and rosiglitazone treatment (**Figure 26**). PGC1alpha, a coactivator important for the transcription of thermogenic genes was upregulated 2 fold compared to control conditions in almost all of the treatments.

### 3.1.3.2 Proton leak kinetics of isolated BFC mitochondria

After confirmation of UCP1 expression in the adipocyte cell line larger amounts of cells were differentiated and stimulated with isoproterenol and retinoic acid to isolate mitochondria for the analysis of UCP1 function. As the differentiated adipocytes contained lots of fat, isolation protocol and proton leak measurement conditions for BAT mitochondria were used. Fat was removed by a first fast centrifugation step and FFA were bound and removed during isolation by addition of BSA to the buffers. Isolation following this protocol yielded mitochondria which increased proton leak in the presence of palmitate. This increase could be prevented by coincubation with GDP but incubation with GDP alone coupled mitochondria even stronger, indicated by the downwards shift of the leak curve (**Figure 27**).

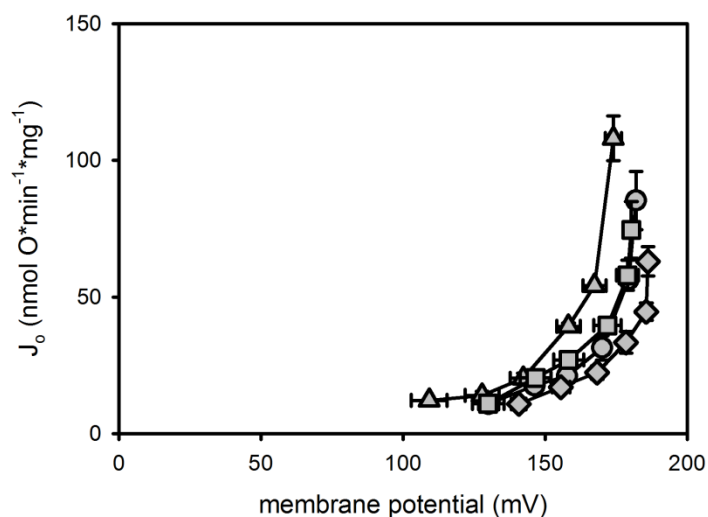


**Figure 27 Proton leak kinetics of mitochondria isolated from differentiated and stimulated BFC.**

Oxygen consumption ( $J_o$ ) was plotted against membrane potential to illustrate the kinetic behaviour of proton leak. Mitochondria isolated from BFC had an increased proton leak in the presence of palmitate (triangles), compared to control conditions (circles). This increase was prevented by coincubation with GDP (squares), in the presence of GDP alone proton leak was further reduced (diamonds). Values are means  $\pm$  SEM;  $n = 3$ .

Leak respiration of mitochondria isolated from differentiated immortalised brown adipocytes was quantified for the different incubation conditions by estimating respiration needed to maintain the highest common potential observed in all single measurements of the data set. This potential was 168 mV and mitochondria from differentiated immortalised brown adipocytes needed 30 nmol O\*min<sup>-1</sup>\*mg<sup>-1</sup> to defend this membrane potential under control conditions. In the presence of GDP alone this was reduced to 24 nmol O\*min<sup>-1</sup>\*mg<sup>-1</sup> but increased to 72 nmol O\*min<sup>-1</sup>\*mg<sup>-1</sup> in the presence of palmitate. Coincubation with GDP reduced this palmitate-induced leak respiration at 168 mV to 46 nmol O\*min<sup>-1</sup>\*mg<sup>-1</sup> but could not bring it down to the basal leak respiration in the presence of GDP alone.

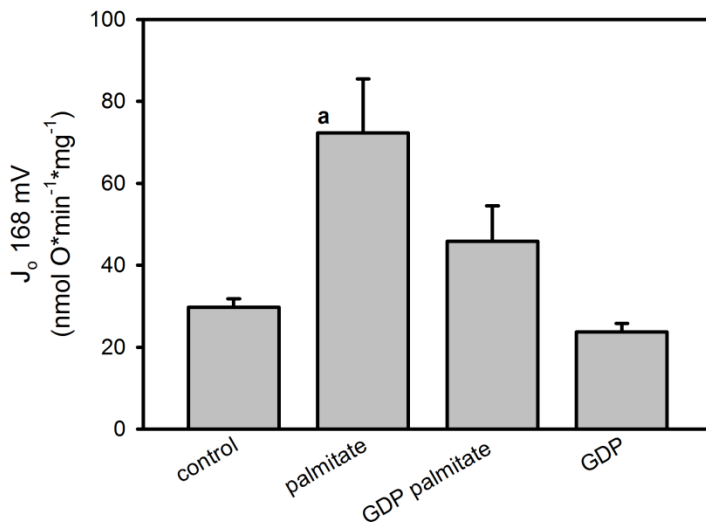


**Figure 28 Comparison of leak respiration of BFC mitochondria in different measurement conditions.**

Leak respiration ( $J_o$ ) of mitochondria isolated from BFC was compared between different measurement conditions. The respiration needed to maintain 168 mV, the highest potential which was present in all single measurements, is plotted for every incubation condition. Leak respiration in the presence of palmitate was almost 2.5 fold as high as in control conditions and 3.5 fold as high as in the presence of GDP. Incubation with palmitate and GDP at the same time lead to an intermediate level of leak respiration. Bars represent means  $\pm$  SEM;  $n=3$ . "a" indicates a significant difference from control and GDP condition,  $p<0.05$ .

### 3.1.3.1 Respiration states of isolated BFC mitochondria

In addition to the determination of proton leak kinetics, isolated BFC mitochondria were also characterised by titration of basal respiration (state 2), phosphorylating respiration (state 3), leak respiration (state 4) and maximum respiration (FCCP) (**Figure 29**).

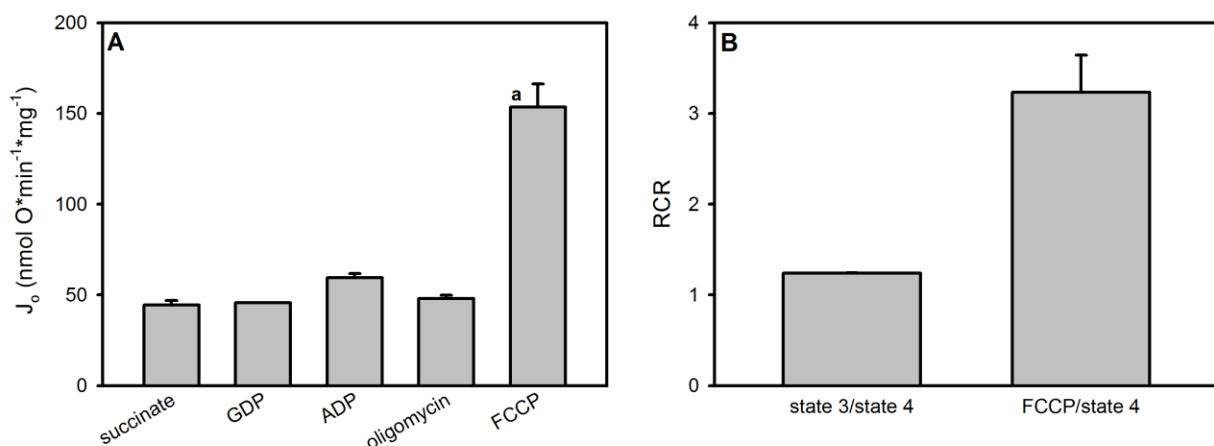


**Figure 29 Respiration states and respiratory control ratio of isolated BFC mitochondria.**

Isolated BFC mitochondria were characterised by titration of different respiratory states. Oxygen consumption ( $J_o$ ) in the presence of succinate was determined in the absence and in the presence of GDP. Phosphorylating respiration (state 3) was determined after addition of ADP and leak respiration (state 4) was induced by addition of oligomycin. Titration with FCCP allowed determination of maximum respiratory rate (A). Calculation of the respiratory control ratio revealed that BFC mitochondria had very low phosphorylating capacity but could increase respiration to a maximum value which was 2.5 fold higher than leak respiration (B). Bars represent means  $\pm$  SEM;  $n=3$ . "a" indicates a significant difference from the other conditions,  $p<0.05$ .

Basal respiration of isolated BFC mitochondria was  $54 \text{ nmol O}^* \text{min}^{-1} \text{mg}^{-1}$ , and was slightly reduced to  $50 \text{ nmol O}^* \text{min}^{-1} \text{mg}^{-1}$  by addition of GDP. Addition of ADP induced a state 3 respiration of  $59 \text{ nmol O}^* \text{min}^{-1} \text{mg}^{-1}$  and went down to  $51 \text{ nmol O}^* \text{min}^{-1} \text{mg}^{-1}$  leak respiration after addition of oligomycin. Maximum FCCP-induced respiration was  $122 \text{ nmol O}^* \text{min}^{-1} \text{mg}^{-1}$  (Figure 29A). Low phosphorylating capacity of the BFC mitochondria was reflected by the low respiratory control ratio of 1.2, but sufficient quality of the isolated mitochondria could be assumed due to the 2.4 ratio of FCCP respiration to leak respiration (Figure 29B).

### 3.1.3.2 Oxygen consumption of adherently growing BFC

With the availability of Seahorse technology in the laboratory first experiments were carried out to characterise UCP1 function in adherently growing BFC by analysis of cellular respiration. BFC were differentiated in 96wells and were either kept in differentiation medium the last 48 h before the experiment, or were stimulated with retinoic acid or with retinoic acid and isoproterenol to induce the thermogenic phenotype. Cells which had received these treatments were characterised by determination of basal respiration, leak respiration and maximum respiratory capacity in the presence of FCCP, all of which were corrected for non-mitochondrial respiration. Non mitochondrial respiration was determined after addition of rotenone and antimycin. For exploratory studies the assay conditions which had been optimised for HEK293 cells were also applied for BFC cells.

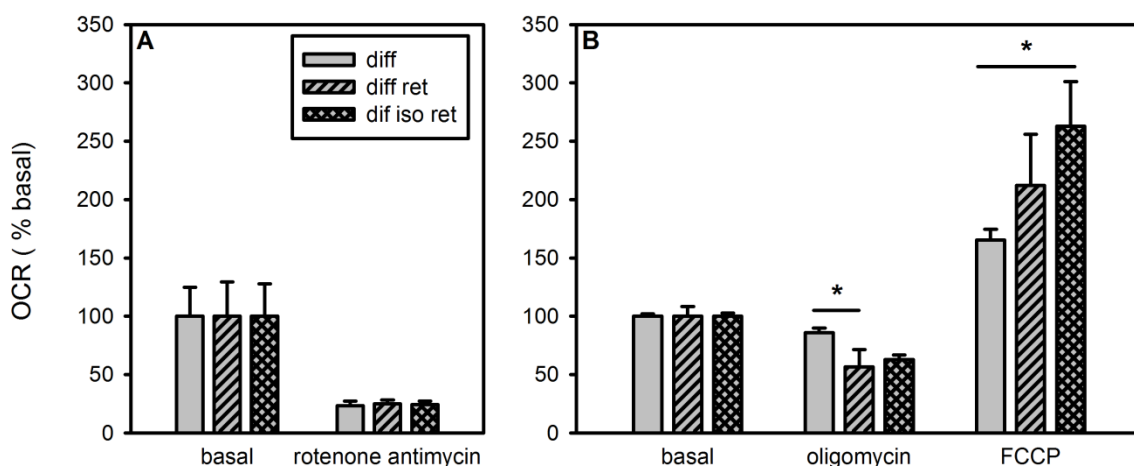


**Figure 30** Oxygen consumption rate (OCR) of adherently growing BFC.

Respiration states of differentiated and differently stimulated BFC were analysed in a Seahorse XF96 flux analyser. Cells had been kept in differentiation medium, or differentiation medium supplemented with retinoic acid (ret) or isoproterenol and retinoic acid (iso ret) 48 h before the measurement. Basal respiration, leak respiration (oligomycin) and maximum respiratory capacity (FCCP) were determined (B) and the values were corrected for non-mitochondrial respiration (rotenone antimycin, A). Bars represent means  $\pm$  stabw, n=3 plates with 12-16 wells per condition. Asterisks indicate significant differences between stimulation treatments in one measurement condition. p < 0.05.

Non-mitochondrial respiration in BFC cells accounted for almost 25 % of basal respiration, independent of treatment (**Figure 30A**). After correction for this value, leak respiration of BFC still contributed 60-85 % of basal respiration, with 85 % being reached by cells kept in differentiation medium prior to the assay and around 60 % being reached by cells which had been stimulated with retinoic acid or retinoic acid and isoproterenol. Maximum respiration in the presence of FCCP was 160 % of basal respiration in cells receiving only differentiation medium. Cells which had been stimulated with retinoic acid reached 210 % of basal respiration in the presence of FCCP and cells treated with retinoic acid and isoproterenol consumed even 260 % of basal respiration in the presence of FCCP (**Figure 30B**).

#### 3.1.4 UCP1 activity in mitochondria isolated from mouse BAT

In order to determine a standard for native UCP1 function, with which data from cell culture models could be compared, UCP1 function was analysed in isolated BAT mitochondria from mice acclimated to RT (22-24°C) or thermoneutral conditions (30°C). As the same setup was used as for the cell culture models it could be expected that comparability of these data was higher than for literature data. The acclimation of mice to different temperatures was supposed to result in two sets of BAT mitochondria with different content of UCP1 per mg mitochondrial protein and different proton leak.

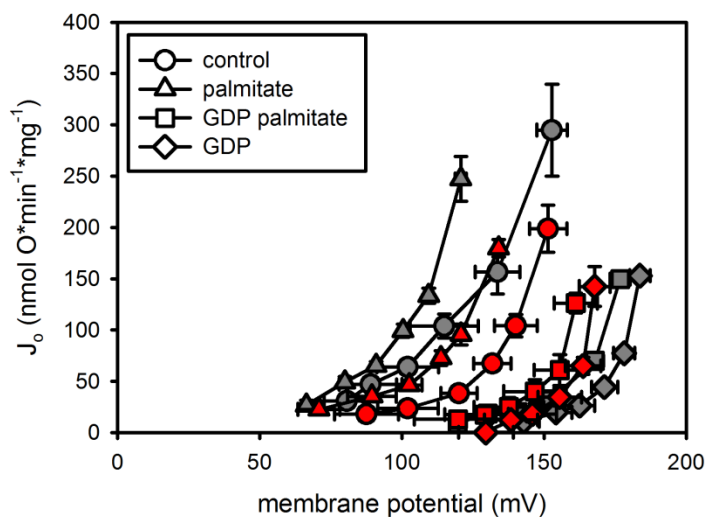


**Figure 31 Proton leak kinetics of BAT mitochondria isolated from mice acclimated to RT or 30°C.**

Proton leak kinetics were determined for BAT mitochondria isolated from mice acclimated to RT (22-24°C; grey symbols) or to thermoneutrality (30°C; red symbols) by parallel measurements of oxygen consumption ( $J_o$ ) and membrane potential. BAT mitochondria of mice from both acclimation temperatures increased proton leak in the presence of palmitate compared to control conditions. This could be prevented by conincubation with GDP, which lowered proton leak even below control conditions. In the presence of GDP acclimation temperature of the mice did not affect maximum leak respiration, but under control conditions

and in the presence of fatty acids mitochondria from mice kept at RT (grey symbols) showed a higher state 4 respiration than those from mice kept at 30°C (red symbols). Values are means  $\pm$  SEM; n= 2-4.

Proton leak of isolated mitochondria was determined for control conditions, in the presence of palmitate, in the presence of GDP and palmitate and after addition of GDP alone. BAT mitochondria from mice kept at both acclimation temperatures increased proton leak in the presence of palmitate compared to control conditions but could be recoupled to basal leak by addition of GDP and by

coincubation with GDP in the presence of palmitate (**Figure 31**). Respiration at basal leak was almost identical for mitochondria from both acclimation temperatures but served to maintain a lower membrane potential in mitochondria from 30°C acclimated mice, which can be interpreted as increased proton leak. These mitochondria had a lower proton leak in control conditions and in the presence of palmitate compared to mitochondria from mice kept at RT, as they maintained a higher membrane potential and consumed less oxygen, seen as a downwards shift of the proton leak curve.

Differences in mitochondrial proton leak resulting from incubation conditions of mitochondria or acclimation temperatures of mice were quantified by estimation of leak respiration at the highest membrane potential which was reached in all single measurements of the data set. Values for the incubation with GDP could not be determined as linear interpolation of the leak curves resulted in negative values. Respiration, reflecting respiratory chain activity needed to maintain the membrane potential of 118 mV against leak reactions, was about 9 nmol O<sub>2</sub>·min<sup>-1</sup>·mg<sup>-1</sup> in the presence of GDP and palmitate for both types of mitochondria. Under control conditions and in the presence of palmitate leak respiration was higher in mitochondria from mice kept at RT compared to mitochondria from mice kept at thermoneutrality. These consumed 49 nmol O<sub>2</sub>·min<sup>-1</sup>·mg<sup>-1</sup> to maintain 118 mV under control conditions, which was increased to the almost 2 fold value of 86 nmol O<sub>2</sub>·min<sup>-1</sup>·mg<sup>-1</sup> in the presence of palmitate. Mitochondria from mice kept at RT consumed 116 nmol O<sub>2</sub>·min<sup>-1</sup>·mg<sup>-1</sup> under control conditions which was also increased to an about 2 fold value of 224 nmol O<sub>2</sub>·min<sup>-1</sup>·mg<sup>-1</sup> in the presence of palmitate (**Figure 32**).

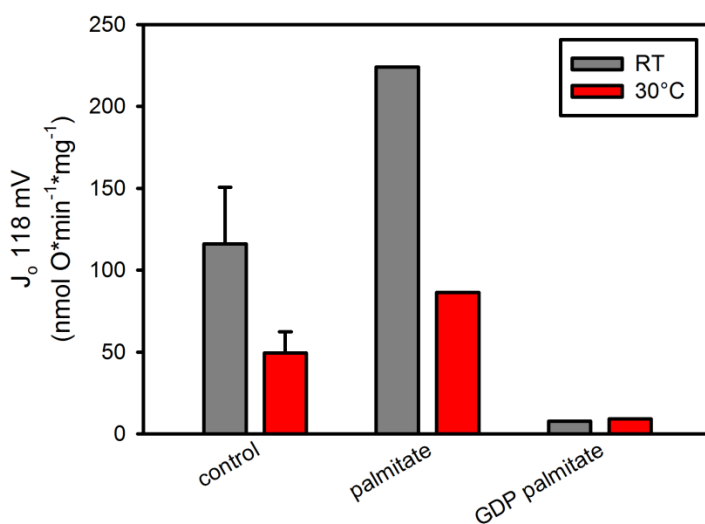


**Figure 32 Comparison of leak respiration of BAT mitochondria isolated from mice acclimated to RT or thermoneutrality.**

Proton leak of BAT mitochondria isolated from mice kept at RT (22-24 °C; grey bars) or at thermoneutrality (30°C; red bars) was compared at 118mV, the highest common potential of the data set in Figure 31. Oxygen consumption ( $J_o$ ) at this membrane potential was determined and did not differ between acclimation temperatures at basal leak, measured in the presence of GDP and palmitate. Both types of mitochondria had higher leak respiration compared to basal leak under control conditions and in the presence of palmitate. This effect was more pronounced in BAT mitochondria from RT-acclimated mice. Values are means  $\pm$  SEM; n= 2-4.

Mice were acclimated to different temperatures for these experiments, as this was supposed to alter the mitochondrial UCP1 content in BAT. These UCP1 expression levels were determined in order to

compare them and relate differences in palmitate-induced leak to UCP1 content. Calculation of UCP1 catalytic activity in mitochondria from differently acclimated mice could give an idea about the naturally occurring range of UCP1 catalytic activity in animals.

The expression level of UCP1 was determined in BAT mitochondria from mice acclimated either to RT or 30°C by western blot analysis. BAT mitochondria from mice acclimated to 30°C contained only half the amount of UCP1 of BAT mitochondria from mice kept at RT, but 2.5 fold as much UCP1 as mitochondria from the HEK293 UCP1 cell line (**Figure 33**).

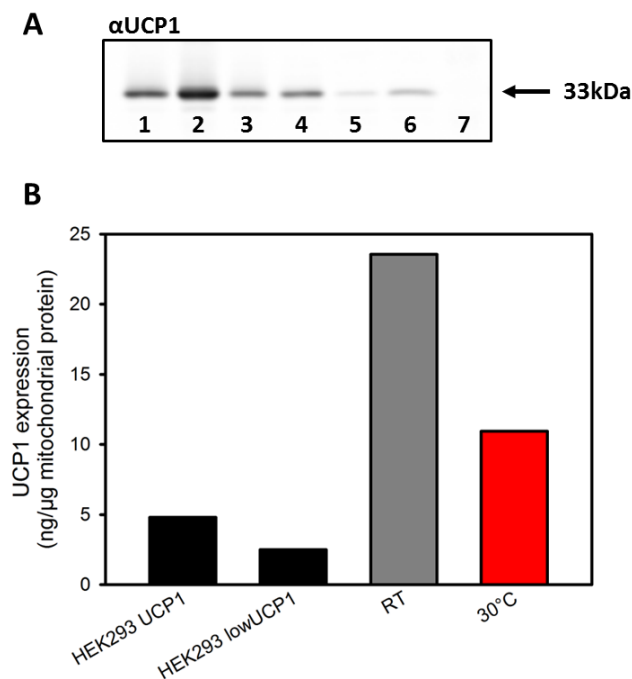


**Figure 33** UCP1 expression in BAT mitochondria from mice acclimated to RT or 30°C.

The UCP1 expression in BAT mitochondria from mice acclimated to RT (lane 1, 2) or 30°C (lane 3, 4) was determined by western blot analysis. A mitochondrial sample of HEK293 UCP1 cells (lane 6) and mitochondria from a HEK293 cell line with lower UCP1 expression (lane 5) were also blotted and a mass standard (lane 7) was used to control the correct size of the immunological signal (A). Results of densitometric analyses of signals were related to the sample of HEK293 UCP1 cells, which were known to express 4.8 ng UCP1/ $\mu$ g mitochondrial protein. UCP1 content of BAT mitochondria is reduced by 50 % compared to RT when animals are acclimated to thermoneutral temperature.

### 3.1.5 Comparison of UCP1-dependent proton leak and catalytic activity in different test systems

Linear interpolation can fail to estimate values for leak respiration, especially at lower values of membrane potential, as the example of the GDP leak curves for BAT mitochondria illustrated. The region of the proton leak curve where it changes from the mostly exponential part to the almost linear part might also be difficult to describe with this approach. On the other hand an accurate regression of the kinetic behaviour of proton leak would allow subtraction of regression curves and calculation of the UCP1-dependent proportion. Therefore a regression equation was applied which accounted for both, the linear and exponential characteristics of proton leak kinetics. Proton leak curves for all experimental systems were fitted to this equation with Sigma plot software and afterwards leak respiration for a condition where UCP1 was inactive or absent (GDP or HEK293) was



subtracted from leak respiration for a condition where UCP1 was active or present (palmitate or HEK293 UCP1). Resulting curves described the contribution of UCP1 activity to proton leak over a range of membrane potentials and could be adjusted to UCP1 amount in the respective experimental system, allowing comparison of UCP1 catalytic activity in the different test systems.

### 3.1.5.1 UCP1-dependent proton leak in HEK293 UCP1 mitochondria

UCP1-dependent proton leak in HEK293 UCP1 mitochondria could be determined for different experimental conditions, as the UCP1-dependent contribution could be calculated by comparison of mitochondria from HEK293 and HEK293 UCP1 cells. Maximum contribution of UCP1 to proton leak was  $98 \text{ nmol O} \cdot \text{min}^{-1} \cdot \text{mg}^{-1}$  in control conditions and  $177 \text{ nmol O} \cdot \text{min}^{-1} \cdot \text{mg}^{-1}$  in the presence of palmitate, representing an almost 2 fold increase. UCP1 activity was negligible in the presence of the UCP1 inhibitor GDP. When compared at 117 mV, the highest membrane potential still reached in the presence of palmitate, the contribution of UCP1 was almost 6 fold increased, from about  $28 \text{ nmol O} \cdot \text{min}^{-1} \cdot \text{mg}^{-1}$  in control conditions to almost  $161 \text{ nmol O} \cdot \text{min}^{-1} \cdot \text{mg}^{-1}$  in the presence of palmitate (Figure 34).

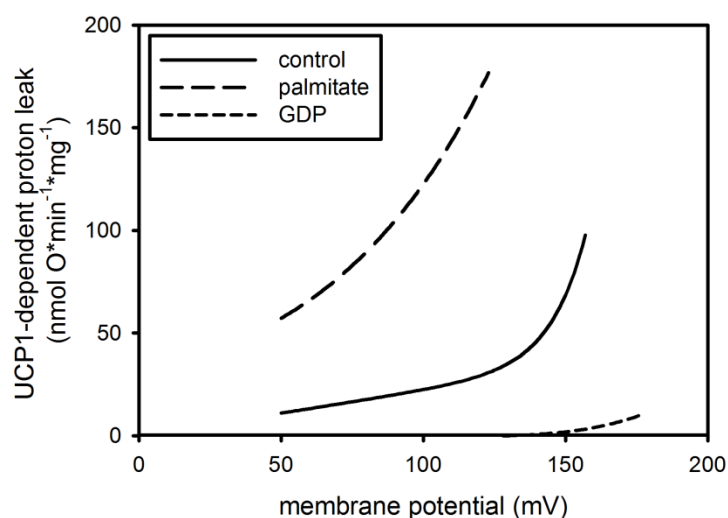


**Figure 34** UCP1-dependent proton leak in HEK293 UCP1 mitochondria.

UCP1 dependent proton leak in mitochondria from HEK293 UCP1 cells was calculated in the presence of palmitate (long dash line), for control conditions (solid line) and in the presence of GDP (short dash line) by subtracting leak respiration of HEK293 mitochondria from the value obtained for HEK293 UCP1 mitochondria in the same conditions. This resulted in curves describing the kinetics of UCP1-dependent leak, demonstrating the non-linear dependence of UCP1 activity on membrane potential and the huge impact of its regulators palmitate and GDP.

### 3.1.5.2 UCP1-dependent proton leak in BFC mitochondria

UCP1-dependent proton leak in BFC mitochondria was calculated by subtracting leak respiration in the presence of GDP and palmitate from the leak respiration in the presence of palmitate alone. Therefore only one curve describing UCP1 activity in BFC mitochondria could be generated. The maximum contribution of UCP1 to state 4 respiration was  $62 \text{ nmol O} \cdot \text{min}^{-1} \cdot \text{mg}^{-1}$  at 174 mV. The

change from linear to exponential conditions occurred much more rapid than in the HEK293 mitochondria, seen as clear bending of the curve at about 160 mV (**Figure 35**).

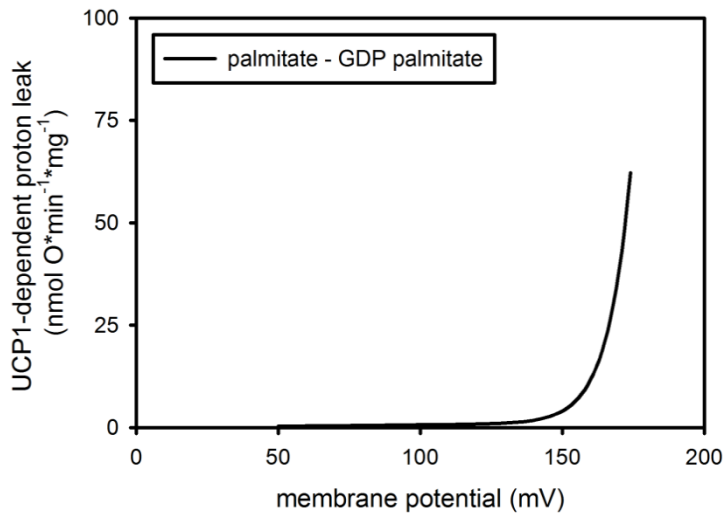


**Figure 35** UCP1-dependent proton leak in differentiated BFC cells.

A graph describing UCP1-dependent proton leak for mitochondria isolated from differentiated BFC was generated by subtracting the regression curve for leak in the presence of GDP and palmitate from the curve describing leak in the presence of palmitate alone. UCP1-dependent leak is very low from 50 to 150 mV and then increases steeply up to its maximum at 174 mV.

### 3.1.5.3 UCP1-dependent proton leak in mouse BAT mitochondria

UCP1-dependent proton leak in BAT mitochondria was determined for mitochondria from RT and 30°C- acclimated animals by subtraction of leak respiration in the presence of GDP and palmitate from the leak respiration in the presence of palmitate alone.

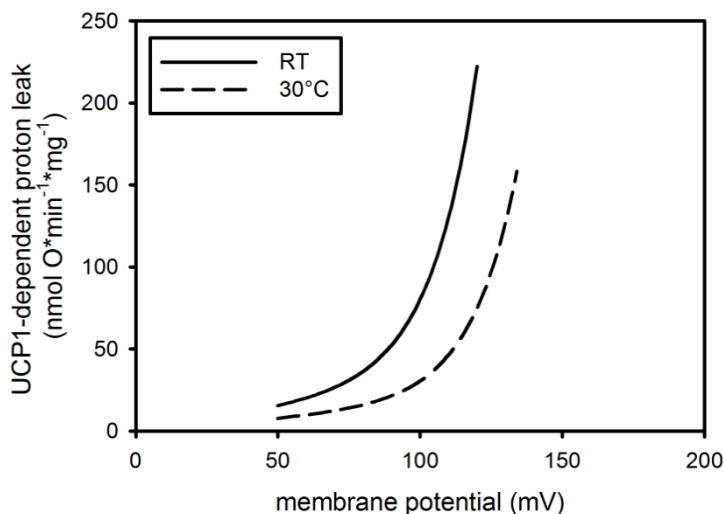


**Figure 36** UCP1-dependent proton leak in BAT mitochondria from mice kept at RT or at 30°C.

UCP1-dependent proton leak of BAT mitochondria isolated from mice kept at RT (22-24°C) or at thermoneutrality (30°C) was calculated by subtracting the regression curve for proton leak in the presence of GDP and palmitate from the curve describing leak in the presence of palmitate alone. UCP1-dependent leak increased exponentially with membrane potential and was higher in BAT-mitochondria from RT-acclimated mice.

The contribution of leak in different conditions could not be determined as there were no reference BAT mitochondria available lacking UCP1. This would have allowed calculations comparable to those

for HEK293 and HEK293 UCP1 mitochondria. The maximum UCP1-dependent contribution to leak respiration was  $158 \text{ nmol O} \cdot \text{min}^{-1} \cdot \text{mg}^{-1}$  in mitochondria from  $30^\circ\text{C}$ -acclimated mice and  $222 \text{ nmol O} \cdot \text{min}^{-1} \cdot \text{mg}^{-1}$  in mitochondria from RT-acclimated mice. Compared at  $120 \text{ mV}$ , the membrane potential which is maintained while UCP1 activity demands  $222 \text{ nmol O} \cdot \text{min}^{-1} \cdot \text{mg}^{-1}$  in mitochondria from RT-acclimated mice, UCP1 activity accounted only for  $75 \text{ nmol O} \cdot \text{min}^{-1} \cdot \text{mg}^{-1}$  in mitochondria from  $30^\circ\text{C}$ -acclimated mice, meaning that UCP1-dependent leak respiration in BAT mitochondria is reduced to approximately one third due to acclimation of mice to thermoneutrality.

#### 3.1.5.4 Comparison of UCP-dependent leak rate per $\mu\text{g}$ UCP1 in different test systems

Direct comparison of the values obtained for maximum UCP1-dependent leak rate in the different test systems implies that the maximum contribution of UCP1 to mitochondrial leak respiration is quite variable, ranging from  $62 \text{ nmol O} \cdot \text{min}^{-1} \cdot \text{mg}^{-1}$  to  $222 \text{ nmol O} \cdot \text{min}^{-1} \cdot \text{mg}^{-1}$ . But of course it has to be considered that the systems contain different amounts of UCP1/mg mitochondrial protein and contributions to leak respiration have to be adjusted for this value to allow judgement about possibly different catalytic activity of UCP1 in different mitochondrial backgrounds or at different expression levels in one background.

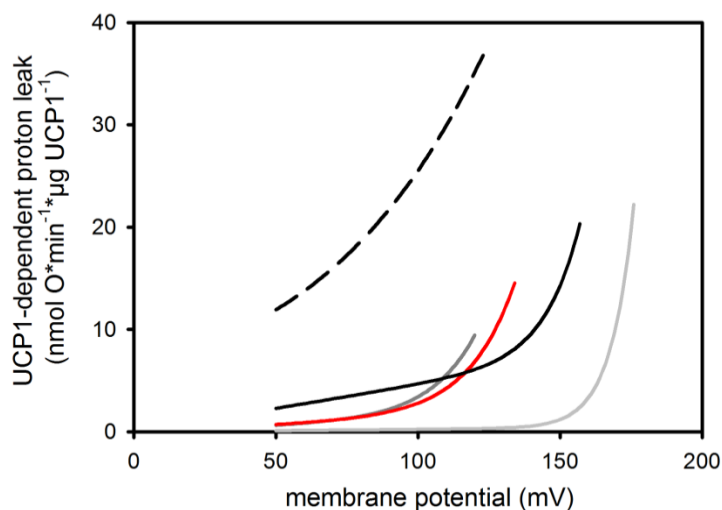


**Figure 37** Catalytic activity of UCP1 in different test systems, expressing UCP1 at different expression levels.

Catalytic activity of UCP1 in different test systems was calculated by dividing the UCP1-dependent leak respiration per mg mitochondrial protein by the UCP1 content in the respective test system. The resulting curves illustrate that UCP1 catalytic activity is similar between HEK293 UCP1 (black line), BFC (grey line) and BAT mitochondria (dark grey (RT) and red line ( $30^\circ\text{C}$ )) under control conditions, but is strongly increased in HEK293 UCP1 mitochondria in the presence of palmitate (dashed line).

After correction for UCP1 content in the mitochondria of HEK293 cells, immortalised brown adipocytes and BAT mitochondria from RT- and  $30^\circ\text{C}$ -acclimated mice all curves determined for catalytic activity under control conditions clustered, with maximum UCP1 dependent leak respiration between  $9 \text{ nmol O} \cdot \text{min}^{-1} \cdot \mu\text{g UCP1}^{-1}$  in mitochondria from RT-acclimated mice and  $22 \text{ nmol O} \cdot \text{min}^{-1} \cdot \mu\text{g UCP1}^{-1}$  in mitochondria from BFC (**Figure 37**). The lower the UCP1 expression level in the test system was, the further were the curves shifted to the right and the higher were the maximally reached catalytic activities. Clearly separated from the other curves was the curve describing the catalytic activity of UCP1 in HEK293 mitochondria in the presence of palmitate, with a maximum of  $37 \text{ nmol O} \cdot \text{min}^{-1} \cdot \mu\text{g UCP1}^{-1}$  at a membrane potential of  $120 \text{ mV}$ .



the serum of one animal in **Figure 39**. First reactivity at the expected molecular mass occurred after 2 months but increased strongly until month 4. All animals injected with the Cter peptide developed immunoreactivity, whereas only 1 out of 3 animals injected with the Ci 4 peptide did.

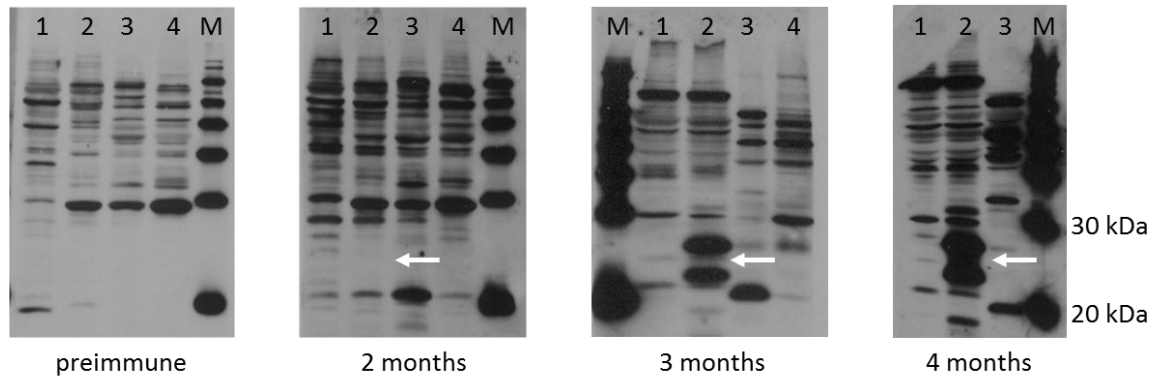


**Figure 39** Development of immunoreactivity with CideA protein in the serum of a rabbit immunised with the CideA peptide Cter.

Serum samples from rabbits were withdrawn before and during the process of immunisation against a peptide from mouse CideA and then analysed for reactivity with protein samples from HEK293 cells (1), HEK293 cells overexpressing CideA (2), and BAT tissue homogenate (3 cytosolic fraction, 4 membrane fraction). The size of immunoreactive signals was determined with a mass standard (M). Two immunoreactive bands (white arrows) between 20 kDa and 30 kDa developed after immunisation and got stronger over time, especially in the protein samples from HEK293 cells overexpressing CideA.

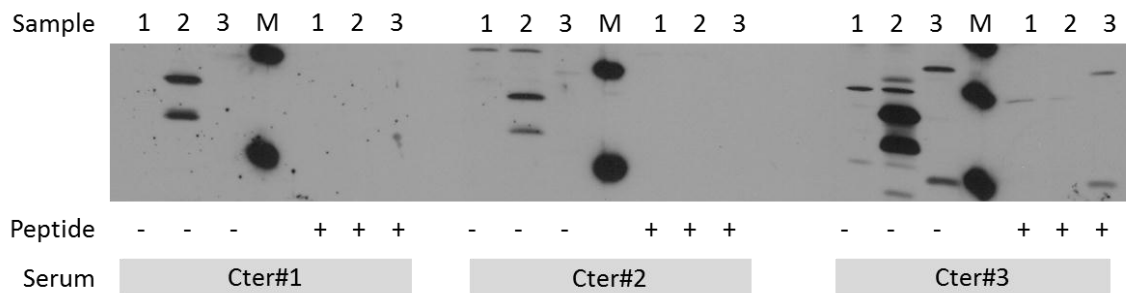


**Figure 40** Specificity of CideA- immunoreactive signal.

The specificity of the immunoreactive signal, which had developed during the immunisation period, was tested for the serum of 3 different animals (Cter #1-#3). Nitrocellulose membranes with protein samples from HEK293 cells (1), HEK293 cells overexpressing CideA (2) and from BAT (3) were incubated with serum alone (-) or serum and the peptide used for immunisation (+). The peptide was able to block the immunoreactive signal, indicating specificity of the signal.

Specificity of the immunological signal was finally confirmed by blocking it by coincubation with the CideA peptide, which had been used for immunisation of the animals. As shown in **Figure 40** for the serum from the animals injected with Cter-peptide, immunological signals which had developed during the immunisation period did not appear after coincubation of western blot membranes with serum and peptides, indicating specificity of the antibody. Serum of the animal with the strongest

immune reaction for the Cter peptide and the only animal with immune reaction for the Ci 4 peptide were taken and purified to be used as antibody solution during the following experiments.

### 3.2.2 CideA expression in mouse tissues

The CideA antibody was used to analyse the tissue specific expression of CideA in protein samples of various mouse tissues, which had been separated into cytosolic and membrane fraction. Immunoreactive signals at approximately 25 kDa appeared only in the samples of interscapular BAT, with a slightly stronger signal in the membrane fraction (**Figure 41**).

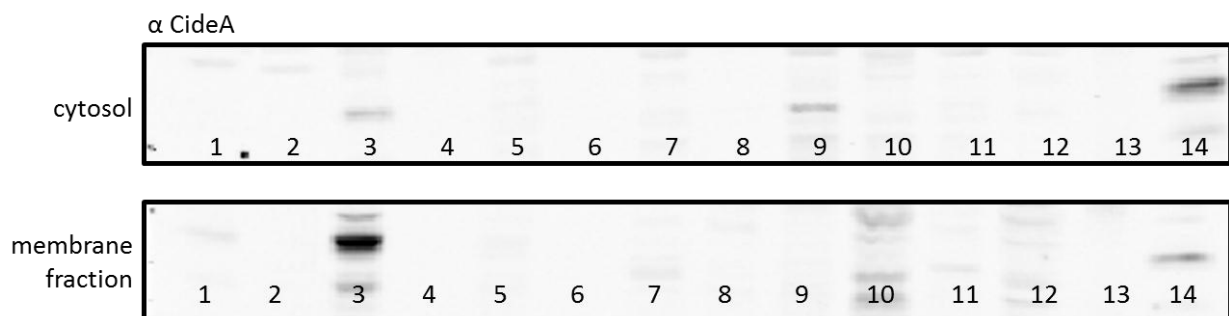


**Figure 41** Detection of CideA in different mouse tissues.

Protein extracts from mouse tissues were generated, separated into cytosolic and membrane fraction and subjected to western blot analysis. A mass standard (M) was used to confirm the correct size of the immunological signal for samples from heart (1), lung (2, 8), interscapular BAT (3), epididymal WAT (4), inguinal WAT (5), perirenal WAT (6), brain (7), spleen (9), pancreas (10), kidney (11), liver (12) and membrane fraction (upper panel)/cytosolic fraction (lower panel) of interscapular BAT (14). CideA was only detected in interscapular BAT.

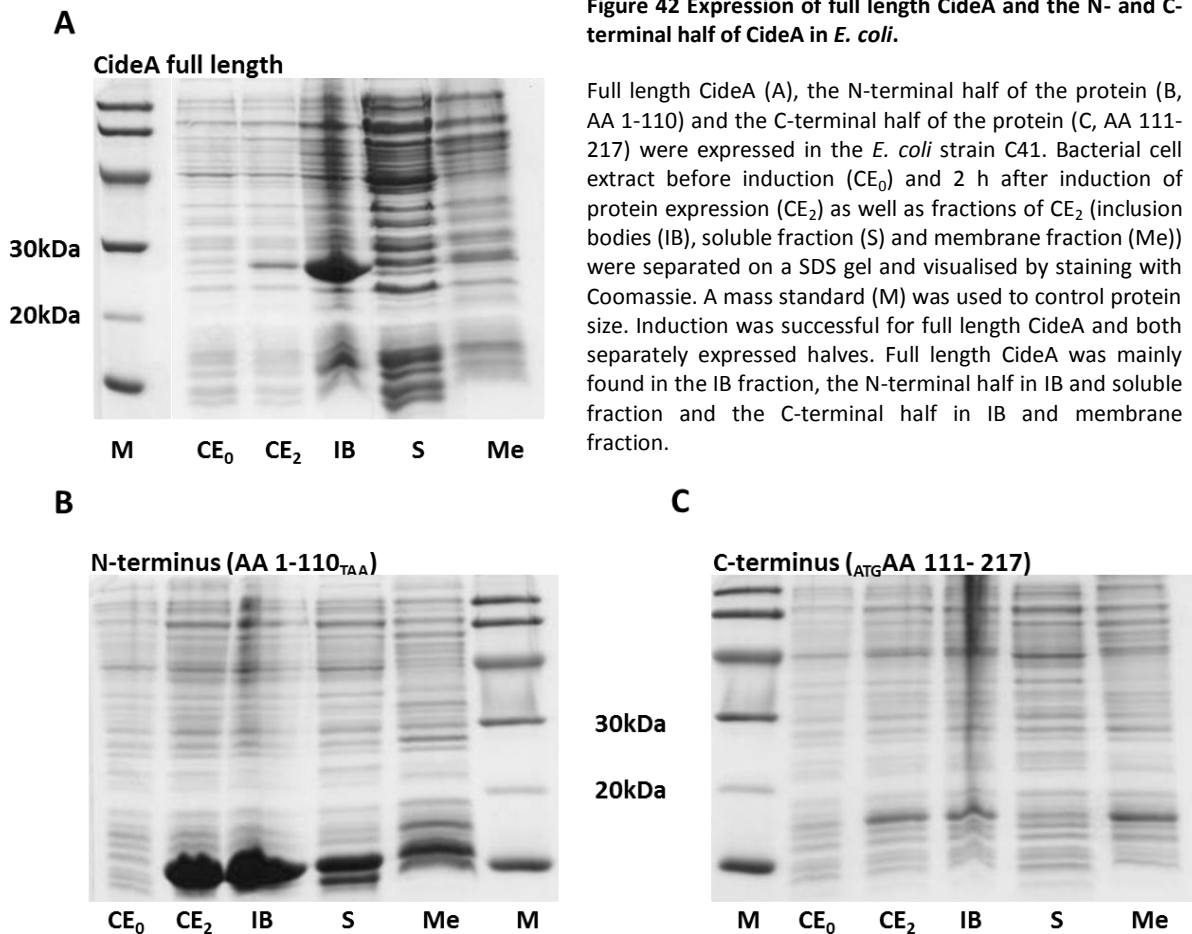
### 3.2.3 Interaction of CideA and UCP1 reconstituted into liposomes

The interaction of CideA and UCP1 was first analysed in liposomes. Only a direct physical interaction would be detectable in this system, as mediating cellular reactions do not take place and other proteins possibly mediating the interaction are not present. CideA had to be heterologously expressed and purified to be available for liposome experiments.

#### 3.2.3.1 *Heterologous expression of CideA in E. coli*

Heterologous expression of full length CideA and the N- or C-terminal half of CideA were performed in the bacterial strain C41, which had been established for the expression of membrane proteins (Miroux and Walker, 1996). After a 2 h induction of protein expression bacterial cells were pelleted and fractionated into inclusion body, soluble and membrane fraction. Samples of all fractions were

loaded on a SDS-PAGE and after electrophoretic separation the gels were stained with Coomassie dye to visualise protein bands. Full length CideA and the C- and N-terminal half were all properly expressed. Full length CideA was mainly recovered in the inclusion body fraction, the C-terminal half in inclusion body and membrane fraction and the N-terminal half in inclusion body and soluble fraction (Figure 42).



As full length CideA and the C-terminal half of the protein were isolated from inclusion bodies, they had to be renatured to be available for the liposome assay. Both proteins precipitated in the attempt to refold them by dialysis, which removed stabilizing detergents and salts. Therefore a strategy of purification and renaturation on a column was chosen. This strategy did not work for the C-terminal half but was successfully applied for full length CideA which could be eluted from the nickel-column as soluble protein (Figure 43).

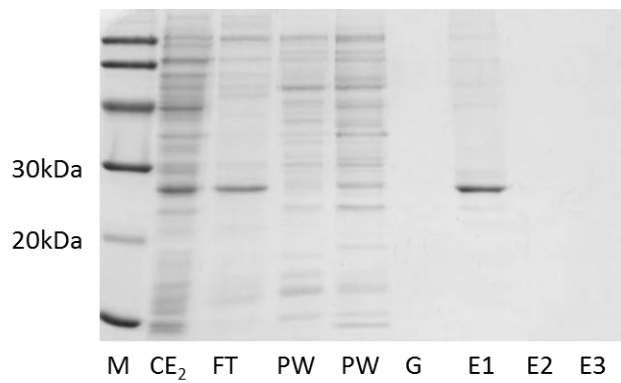


**Figure 43 Purification and refolding of full length CideA on a nickel-column.**

Solubilised inclusion bodies from *E. coli* expressing full length CideA were loaded onto a Nickel column. Flow-through (FT), washing (PW) and elution fractions (E1-3) were collected and analysed for the presence of protein by separation on a SDS gel and subsequent staining with Coomassie. Purified CideA was recovered in the first elution fraction.

The N-terminal half was purified from the soluble fraction of disrupted bacterial cells with a Nickel column, without the need to renature the protein.

### 3.2.3.2 Effect of CideA on UCP1 function in liposomes

The interaction of CideA and UCP1 was tested in liposomes which contained native UCP1 isolated from BAT of cold acclimated mice. CideA was heterologously expressed in *E. coli* and the full length protein was purified and refolded with the help of a His-tag on a nickel-column, whereas the N-terminal half of CideA was only purified. The N-terminal half of CideA is supposed to mediate interaction with other proteins and contains the sequence unique to CideA, which is not present in the other members of the Cide-family (Inohara et al., 1998b).

In the activity assay it is the decrease in Safranin O absorbance which reports liposome polarisation and it occurs only if there is H<sup>+</sup> translocating activity in the liposomes. Liposome-assays with UCP1 and CideA revealed that neither the addition of the N-terminal half, nor the addition of full length CideA affected the fatty acid activated and polarisation of the liposomes. Addition of CideA even seemed to enhance polarisation after nigericin addition (**Figure 44A**). Addition of the buffer alone revealed that this effect did not depend on the protein but on the buffer it was kept in (**Figure 44B**).



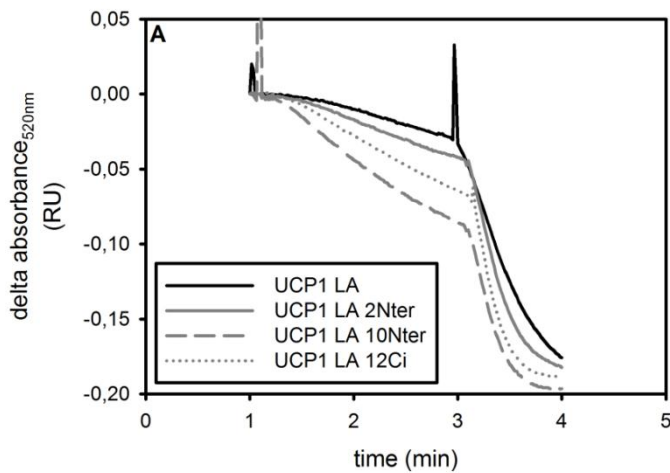
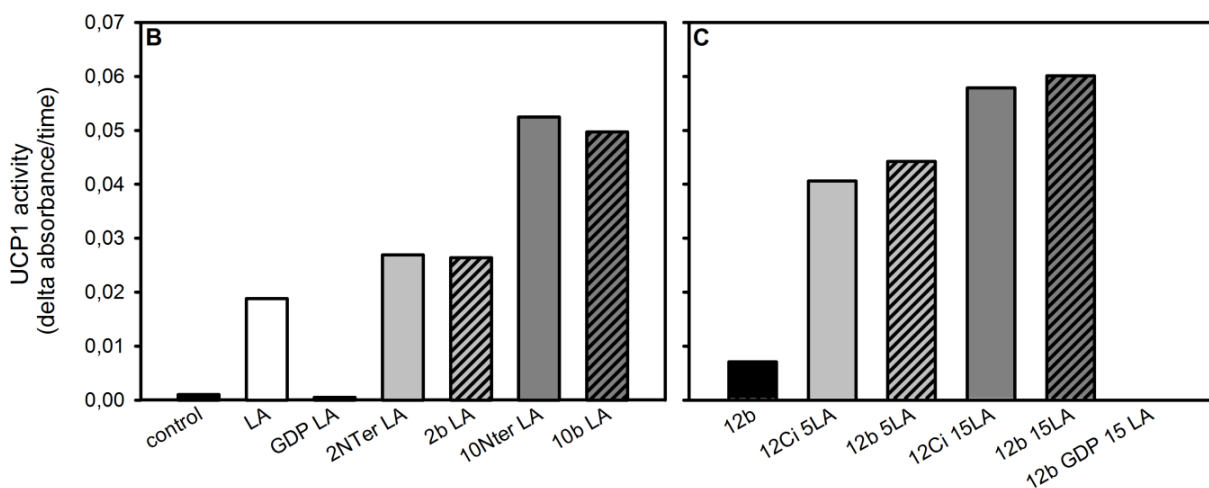


**Figure 44 Effect of Full length CideA and the N-terminal half of CideA on lauric acid-induced liposome polarisation.**

UCP1 activity in liposomes was monitored by the decrease of Safranin O absorbance over time (A). Lauric acid (LA) activated polarisation (white bar) seemed to be further enhanced by the addition of the N-terminal half of CideA (B, grey bars) or full length CideA (C, grey bars). Control experiments with additions of solubilisation buffer alone indicated that this effect could not be attributed to the purified proteins and their interaction with UCP1 but that it depended on the buffer of the protein solution (B and C, structured bars).



### 3.2.4 Interaction of CideA and UCP1 in HEK293 cells

Modulation of UCP1 activity by CideA was also tested in HEK293 and HEK293 UCP1 cells. This cell culture model allowed to evaluate the interaction of the two proteins in a cellular context, which might, different from liposomes, provide necessary cofactors. Both cell lines were transfected with empty pcDNA3 vector or pcDNA3 CideA and in a first experiment oxygen consumption of trypsinised cells was determined with a Clark-electrode. Additionally the respiration of transfected and still adherently growing cells was determined with a Seahorse XF96 Flux analyser.

#### 3.2.4.1 Oxygen consumption of trypsinised HEK293 and HEK293 UCP1 cells transiently expressing CideA

HEK293 and HEK293 UCP1 cells were trypsinised 24 h after transfection with empty pcDNA3 vector or pcDNA3 CideA and basal respiration in the presence of glucose and leak respiration after addition of oligomycin were determined with a Clark-electrode. Furthermore it was tested if the addition of palmitate increased leak respiration and then maximum respiration was induced by addition of FCCP.

FCCP-induced respiration, normalised to cell number, was not different between the 4 experimental groups (**Figure 45**), therefore the other respiratory states were expressed relative to FCCP respiration.

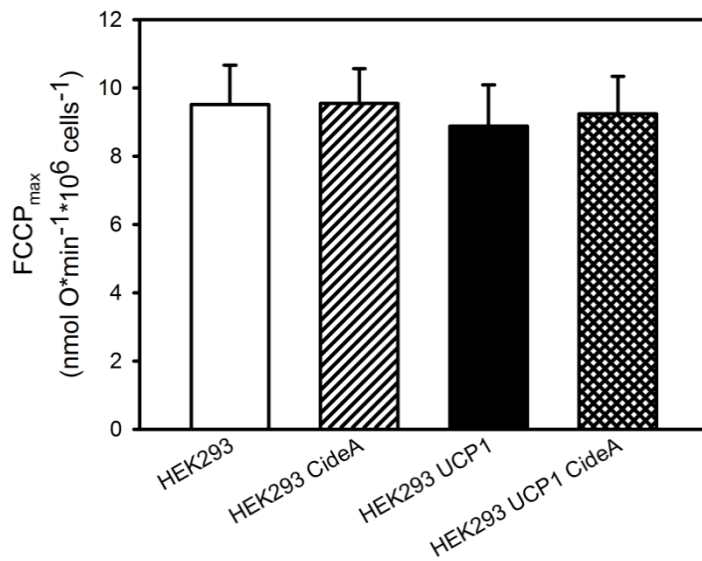


**Figure 45** Maximum respiratory capacity of trypsinised HEK293 and HEK293 UCP1 cells transfected with empty pcDNA3 vector or pcDNA3 CideA.

HEK293 and HEK293 UCP1 cells were transfected with empty pcDNA3 vector or pcDNA3 CideA and trypsinised for characterisation of basal, leak and maximum respiration in a Clark-electrode. Maximum FCCP induced respiration was not different between cell types or transfections. Bars represent means  $\pm$  SEM; n=11-12.

HEK293 cells used about 42 % of their maximum respiratory capacity under basal conditions and reduced respiration to 22 % of FCCP<sub>max</sub> when oligomycin was added and only leak processes at the mitochondrial inner membrane had to be compensated. Addition of palmitate did not affect leak respiration. HEK293 UCP1 cells had an elevated basal respiration, as they used already about 64 % of their maximum respiratory capacity under basal conditions. Leak respiration was also increased compared to HEK293 cells, as addition of oligomycin only lead to a reduction of respiration to 39 % of FCCP<sub>max</sub>. HEK293 UCP1 cells did increase leak respiration upon stepwise addition of palmitate, reaching a value of about 81 % of FCCP<sub>max</sub> in the presence of 300  $\mu$ M palmitate. Transfection with CideA did not affect any of the respiratory rates of HEK293 or HEK293 UCP1 cells in the chosen experimental conditions (**Figure 46**).

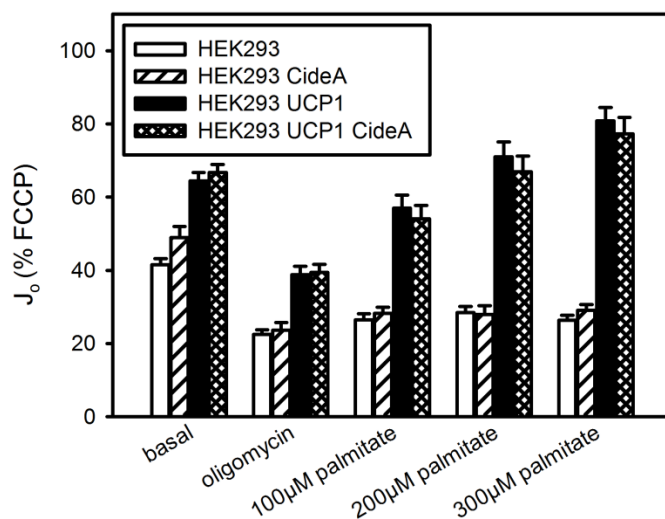


**Figure 46** Respiration of trypsinised HEK293 and HEK293 UCP1 cells transfected with empty pcDNA3 vector and pcDNA3 CideA.

HEK293 and HEK293 UCP1 cells were transfected with empty pcDNA3 vector or pcDNA3 CideA and 24 h after transfection cells were trypsinised and different respiratory states were determined in a Clark-electrode. Basal respiration was recorded in the presence of glucose and leak respiration after the addition of oligomycin. Fatty acid sensitivity of leak respiration ( $J_0$ ) was tested by addition of palmitate up to a concentration of 300  $\mu$ M. Values are expressed relative to maximum FCCP-induced respiration which was not different between groups (Figure 45). Bars represent means  $\pm$  SEM; n=11-12.

The fact that transfection of HEK293 and HEK293 UCP1 cells with pcDNA3 CideA did not affect basal respiration, leak respiration or maximum respiratory capacity of the cells could not be explained by endogenous CideA expression in cells transfected with empty vector or by lack of CideA expression from pcDNA3 CideA, as western blot analysis confirmed the absence of CideA protein in empty vector controls and a clear immunological signal in protein samples from cells transfected with the CideA expression vector (**Figure 47**).

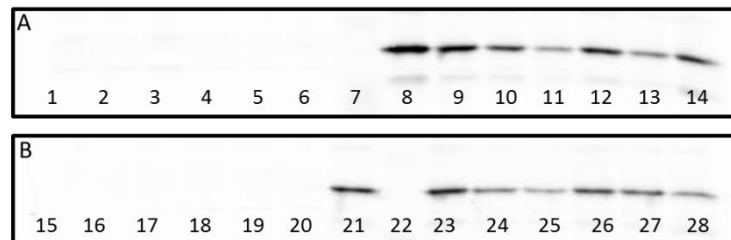


**Figure 47 Immunological detection of CideA in HEK293 and HEK293 UCP1 cells, transiently transfected with pcDNA3 or pcDNA3 CideA for analysis of cellular respiration.**

CideA was detected in protein extracts of HEK293 cells (A) and HEK293 UCP1 cells (B) which had been transiently transfected either with empty vector (lane 1-6 and 15-20) or pcDNA3 CideA (lane 8-13 and 21-27). A mass standard (lane 7 and 22) was used to verify correct size of the immunological signal, HEK293 protein extract from a previous transfection was used as positive control (lane 14 and 28). CideA was absent in cells receiving empty vector and was expressed to a similar extent in both cell types receiving pcDNA3 CideA.

#### 3.2.4.2 Oxygen consumption of adherently growing cells

The analysis of adherently growing HEK293 and HEK293 UCP1 cells for the characterisation of UCP1 function in this cell system gave different results from those obtained for trypsinised cells (**Figure 20**, **Figure 21**) and raised doubts about the integrity of the cells in the latter assay. As this might be a reason for the lack of effect of CideA expression on UCP1 function HEK293 and HEK293 UCP1 cells were grown on 96well plates for Seahorse XF analysis and transfected with pEGFP N1 as control vector and pcDNA3 CideA. In a first step respiratory states were titrated as performed for the characterisation of HEK293 UCP1 cells, which included basal respiration, leak respiration in the presence of oligomycin, maximum respiration induced by FCCP and as correction value non-mitochondrial respiration after the addition of rotenone and antimycin.

The modulation between basal respiration, leak respiration and maximum respiration of transfected HEK293 and HEK293 UCP1 cells seemed to be less flexible in transfected HEK293 and HEK293 UCP1 cells (**Figure 48**) compared to untransfected cells (see **Figure 21**). Oligomycin reduced respiration only to 40 % of basal respiration and the maximum respiration after FCCP addition represented 150 % of basal respiration. CideA expression did not affect respiration of HEK293 and HEK293 UCP1 cells in any of the analysed conditions.

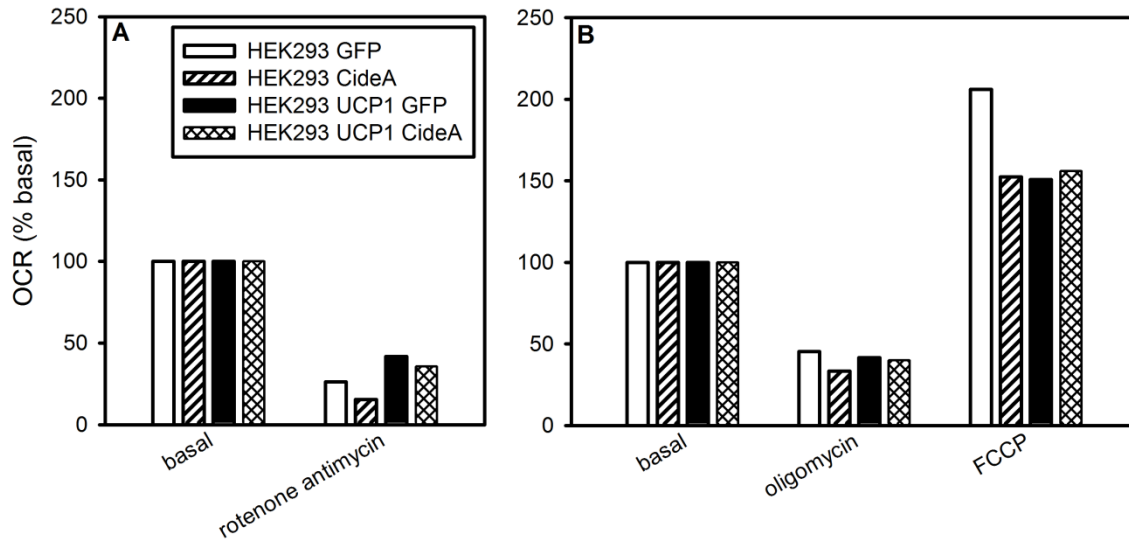


**Figure 48** Oxygen consumption rate (OCR) of adherently growing HEK293 and HEK293 UCP1 cells, overexpressing GFP or CideA.

HEK293 and HEK293 UCP1 cells were grown on 96well plates and transfected with pEGFP-N1 or pcDNA3 CideA. 24 h after transfection oxygen consumption of the cells was determined with the Seahorse 96XF flux analyser. Basal oxygen consumption was determined in the presence of glucose as main substrate, leak respiration after addition of oligomycin, maximum respiratory capacity after addition of FCCP and non-mitochondrial respiration after injection of rotenone and antimycin (A). Values were corrected for non-mitochondrial respiration and then normalised to basal respiration (B). CideA expression did not have an effect on the analysed respiratory states in HEK293 UCP1 cells. Bars represent means of 2 plates, each with 8-12 wells per condition.

### 3.2.5 Overexpression of CideA in immortalised brown adipocytes

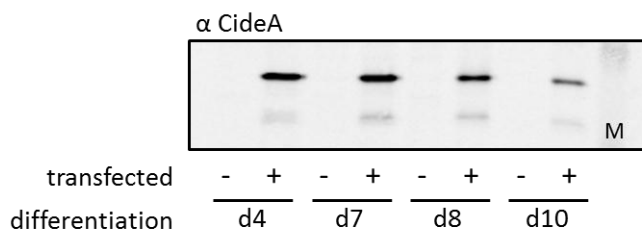


**Figure 49** CideA expression during differentiation of BFC after viral transduction as preadipocytes.

BFC were transduced with a virus containing the CideA sequence and then differentiated into brown adipocytes. CideA expression was monitored during differentiation and persisted from day 4 (induction, 1 day after transduction) until day 10 (mature adipocytes, timepoint for experiments). Immunological detection revealed CideA expression only in protein extracts from transduced cells (+).

CideA addition did not affect UCP1 function in liposomes, arguing against a direct physical interaction between the proteins. Furthermore the transient overexpression of CideA in HEK293 UCP1 cells did not affect UCP1 activity in trypsinised or adherently growing cells, although it has to be noted that adherently growing cells were not stimulated with fatty acids. In order to exclude that a cellular factor only present in brown fat cells is necessary to mediate the effect of CideA on UCP1 function, experiments were carried out in which CideA was overexpressed in the preadipocyte cell line BFC. A viral expression system was applied, and cells were transduced before induction of

differentiation, as the virus could only enter dividing cells. First it was demonstrated that treatment with the virus led to an overexpression of CideA, which persisted during differentiation (**Figure 49**).

### 3.2.5.1 Lipid droplet size of BFC overexpressing GFP or CideA

After the initial publication as direct inhibitor of UCP1 another group identified CideA as lipid droplet protein, regulating lipid accumulation (Puri et al., 2008). This function could also modulate UCP1 activity, by modulation of FFA levels, which directly control UCP1 activity and expression. Therefore the lipid accumulation and capacity for breakdown of lipids of GFP and CideA transfected BFC was determined.

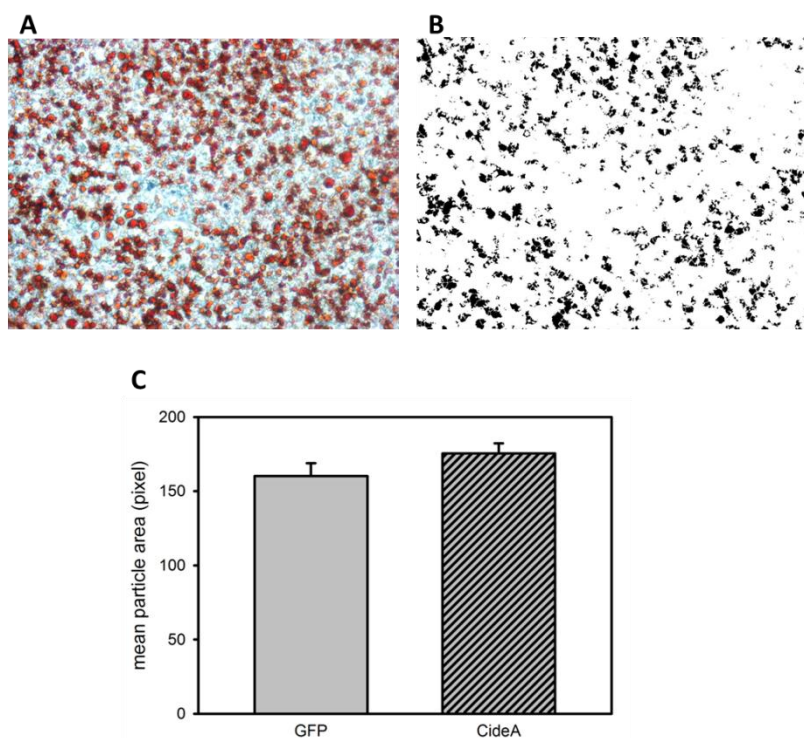


**Figure 50 Lipid accumulation in BFC expressing GFP or CideA.**

Differentiated BFC, transduced with viruses driving expression of GFP or CideA, were stained with Oil Red O to evaluate lipid accumulation. Microscopic images (A) were analysed with Image J software which counted the size of red particles, after they had been selected by exclusion of non-coloured areas and transferred to a black and white image (B). Mean particle size was not significantly different between differently transduced cells but tended to be higher in BFC expressing CideA. Bars represent means  $\pm$  SEM; n=5.

Lipid accumulation was assessed by Oil Red O staining and by analysis of lipid droplet size in microscopic pictures. BFC were transduced with viruses driving expression of GFP or CideA and then differentiated to mature brown adipocytes. After 6 days of differentiation cells were stained with Oil Red O to evaluate lipid accumulation. Microscopic pictures of the cells were taken and analysed with Image J software. Red lipid droplets were selected by exclusion of unstained areas and then the software calculated the number and size of the remaining particles in the entire picture.

Inspection by eye suggested that number and size of stained lipid droplets was very similar for both transductions and this observation was also confirmed by the Software. Mean particle size in pixel tended to be higher with 175 pixel in BFC expressing CideA, compared to a mean of 160 pixels in BFC expressing GFP, but was not significantly different (**Figure 50**).

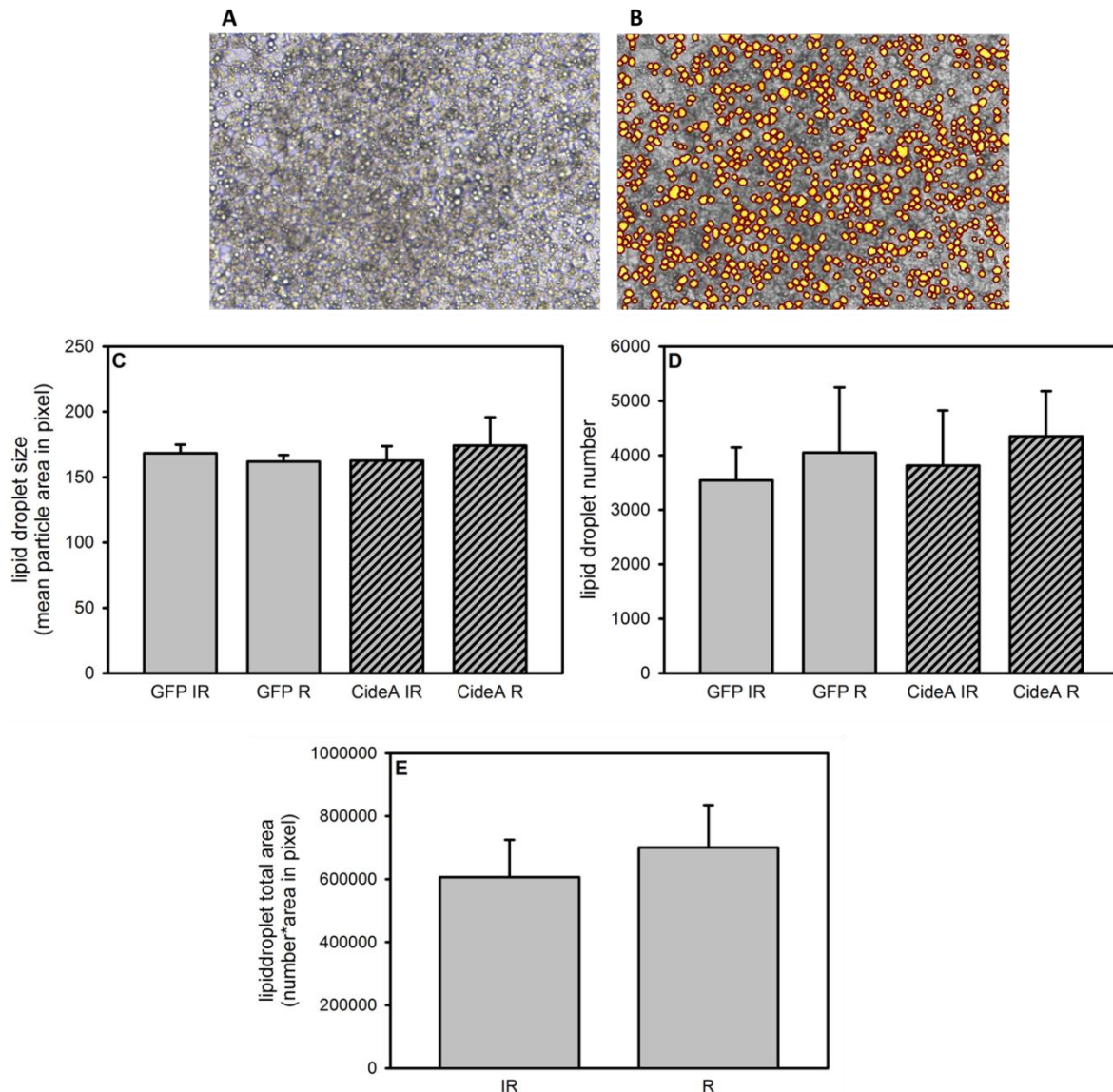


**Figure 51 Analysis of lipid droplet number and size after stimulation treatment in BFC expressing GFP or CideA.**

Lightmicroscopic image of differentiated BFC overexpressing CideA (A) and the same image with labelled particles, which were chosen by the Wimasis software for analysis (B). Lipid droplet mean area (C) and number (D) were calculated for BFC overexpressing GFP or CideA, treated with retinoic acid (R) or isoproterenol and retinoic acid (IR) for 48 h. Total lipid droplet area was calculated from number and mean area and compared for the two different stimulation conditions (E). Bars represent means  $\pm$  SD; n = 3 wells from independent experiments for each conditions, each with two image analyses.

As Oil Red O staining procedure and manual exclusion of unstained areas with the Image J software was prone to introducing much variation the analysis was repeated with the service of the company Wimasis, which allowed counting lipid droplets and analysing their size in lightmicroscopic images. Images of cells which had been transduced for glycerol release assays were taken before the assay,

therefore BFC overexpressing GFP or CideA, stimulated with retinoic acid or isoproterenol and retinoic acid were compared in this analysis.

Lipid accumulation, judged by either lipid droplet size (**Figure 51C**) or lipid droplet number (**Figure 51D**) was not different between cells expressing GFP or CideA. Total lipid droplet area was calculated from number and area and tended to be higher in cells treated only with retinoic acid, compared to cells treated with retinoic acid and isoproterenol (**Figure 51E**).

### 3.2.5.2 Basal and stimulated lipolysis of immortalised brown adipocytes expressing GFP or CideA

Oil-red O staining and lipid droplet size analysis were applied to test whether CideA expression in BFC affected lipid storage of the cells. Glycerol release after stimulation with isoproterenol was determined as further parameter reflecting the capacity of the cells to mobilise lipids.

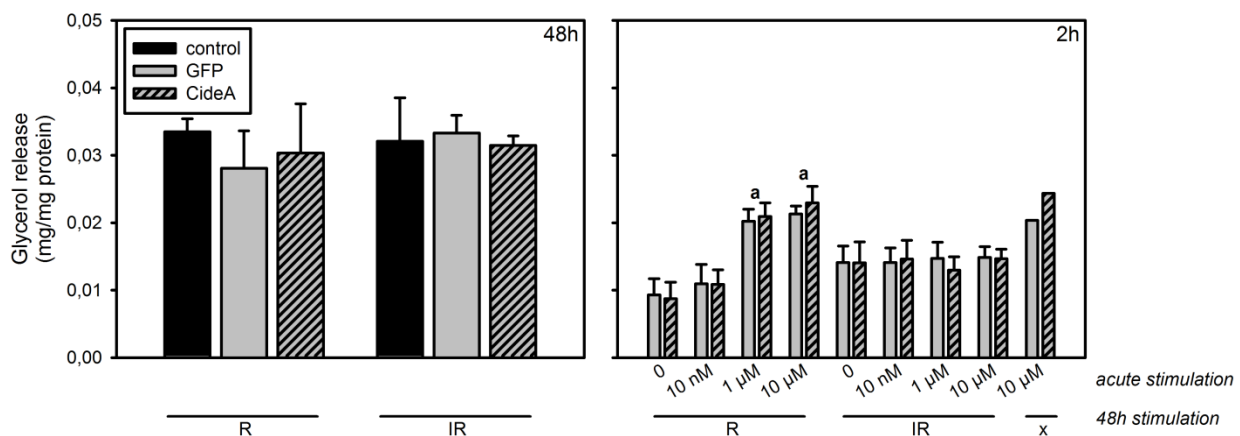


**Figure 52** Glycerol release during 48 h stimulation of thermogenic phenotype in BFC and upon subsequent acute 2 h stimulation with different isoproterenol concentrations.

BFC preadipocytes were transduced with viruses containing the GFP or CideA sequence or remained untreated and were then differentiated to mature adipocytes. Differentiated cells were stimulated with retinoic acid (R) or isoproterenol and retinoic acid (IR) for 48 h to induce the thermogenic phenotype of the brown adipocytes. Medium was exchanged and cells were acutely stimulated with different concentrations of isoproterenol (0, 10 nM, 1 μM, 10 μM) to test the lipolytic capacity of the adipocytes. Glycerol release was determined as measure for triglyceride breakdown during the 48 h period of thermogenic stimulation and during the 2 h period of lipolysis stimulation. Bars represent means  $\pm$  SEM, n=3. **a** indicates significant differences of the acute treatment from the other acute treatments.  $p < 0.05$ .

BFC preadipocytes were transduced with GFP or CideA and cells were induced and differentiated to mature adipocytes. As described for other experiments with BFC, some of the cells were stimulated at the end of the differentiation period with isoproterenol and retinoic acid to develop the thermogenic phenotype. But as isoproterenol was used for acute stimulation in the glycerol release assay a subset of cells was stimulated only with retinoic acid. Glycerol release was determined after the 48 h of stimulation of the thermogenic phenotype and after 2 h acute stimulation with different concentrations of isoproterenol. Values for glycerol release were compared between control BFC and BFC expressing GFP or CideA.

Analysis of glycerol accumulation in the 48h period of stimulation revealed that neither in the presence of retinoic acid, nor in the presence of isoproterenol and retinoic acid GFP and CideA expressing BFC behaved different from untransfected cells (**Figure 52**, 48 h). The results for the glycerol accumulation in the acute stimulation phase of 2 h revealed, that cells treated with isoproterenol in the 48 h period did not respond to the acute stimulus, releasing about 0,015 mg glycerol/mg of protein, independent of isoproterenol treatment (**Figure 52**, 2 h). Cells which had been kept in differentiation medium during the 48 h period released around 0,02 mg glycerol/mg of protein. This value was also reached by cells stimulated with retinoic acid in the 48 h period and with 1  $\mu$ M or 10  $\mu$ M isoproterenol in the 2 h period. Cells stimulated with retinoic acid for 48 h and with 0 or 10 nM isoproterenol during 2 h released about 0,01 mg glycerol/mg protein. Isoproterenol therefore induced a 2 fold increase of glycerol release in these cells. BFC expressing GFP or CideA did not differ in their reaction to acute isoproterenol stimulation.

Glycerol release per well in glycerol/ml was normalised to cell number by relating the values determined per well to the protein content of RIPA-extracts prepared from whole wells. CideA has also been reported to induce cell death (Inohara et al., 1998b), therefore it might have been possible that cell growth and protein content differed systematically depending on transfection. But this was not the case, as protein extracts from wells with untreated, GFP-or CideA-expressing BFC all contained about 6mg/ml protein (**Figure 53**).

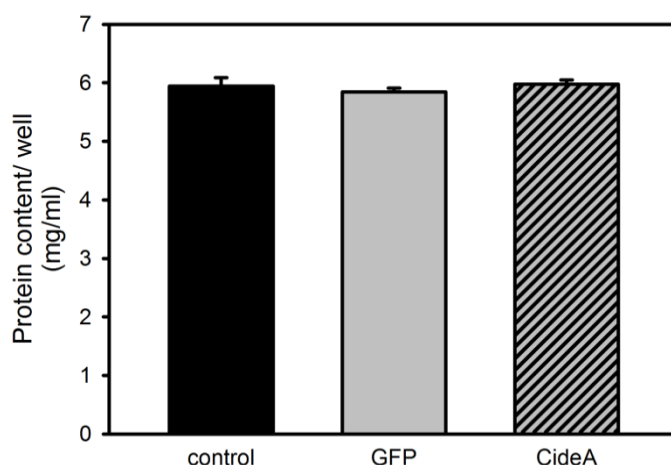


**Figure 53 Comparison of cell number in wells used for glycerol release assays and transfected with different viruses for expression of GFP or CideA.**

All cells of 6wells with normally differentiated BFC (control), or BFC expressing either GFP or CideA were collected and used for protein extraction. Protein content of these extracts was plotted as measure for cell number, which was controlled to exclude an effect of transduction on cell growth or cell death.



## 4 Discussion

The aim of this PhD thesis was to characterise the established cell line HEK293 as a test system for uncoupling protein function and to explore the potential of an immortalised brown adipocyte cell line to resolve mechanistic questions on UCP1 function. CideA, the putative inhibitor of UCP1 function, was expressed in both test systems to clarify how CideA might exert an inhibitory influence on UCP1 and BAT activity. Experiments with liposomes and BAT mitochondria isolated from mouse tissue were carried out to facilitate the integration of results from the two cell culture models.

### 4.1 Suitability of HEK293 cells and BFC as test systems for UCP function

A first parameter which determines the suitability of a test system for the analysis of uncoupling protein function is the correct expression and targeting of the protein to the mitochondrial membrane. This should be true for an expression level in the physiological range, which in case of UCP1 in BAT is very high. Furthermore the function of the protein should still be regulated as it is described for native mitochondria and the expression should not provoke an uncoupling artefact. Such an artefact would be an increased proton flux across the membrane which is not explained by controlled protein activity, but by improper folding and insertion into the membrane, allowing unregulated proton flux.

#### 4.1.1 Expression of UCP1 in HEK293 UCP1 and BFC

##### 4.1.1.1 *UCP1 is correctly targeted to mitochondria in HEK293 UCP1 cells*

HEK293 UCP1 cells express the protein from the CMV promoter of the stably integrated pcDNA3 vector. Despite constitutive heterologous expression the uncoupling protein was still targeted to the mitochondrial inner membrane. This was indicated by fluorescence microscopy, which resulted in similar staining patterns for HEK293 cells stained with mitotracker and the immunologically detected uncoupling protein in HEK293 UCP1 cells (see **Figure 10**). Further confirmation of this finding was the result of the western blot analysis of HEK293 UCP1 cell fractions, where UCP1 was detected only in the mitochondrial fraction. UCP1 is targeted to mitochondria via an internal signalling sequence and not with an N-terminal targeting sequence as found for most mitochondrial proteins (Neupert and Herrmann, 2007). The relevant region containing the signal for import into the inner mitochondrial membrane could be narrowed down to the central repeat of the tripartite structure of UCP1 in a mutational study (Schleiff and McBride, 2000). UCP1 is imported via the TIM22 pathway which starts by translocation of the protein from the cytosol to the intermembrane space by the TOM complex (translocase of the outer membrane). In the intermembrane space the protein interacts with small

TIM proteins, which shield the hydrophobic domains of the sequence to maintain the solubility of the protein until it reaches the TIM22 complex (translocase of the inner membrane), which mediates the insertion into the inner mitochondrial membrane (Neupert and Herrmann, 2007).

This internal signalling sequence is probably the reason why modification with the Xpress tag at the N-terminus does not affect targeting, and why tagUCP1 is still found in the mitochondrial fraction of HEK293 tagUCP1 cells ( **Figure 17**).

#### *4.1.1.2 UCP1 expression level in HEK293 UCP1 cells*

On the one hand it was necessary to determine UCP1 expression level for the calculation of protein catalytic activity in HEK293 UCP1 cells. On the other hand the expression level itself was a first criterion for the characterisation of the cell line. The physiological role of UCP1 is dependent on its high abundance in BAT mitochondria, where it can account for up to 8 % of mitochondrial protein mass, as had been calculated for cold acclimated rats and hamsters (Lin and Klingenberg, 1980). This enables considerable influence on the coupling state of mitochondria, which can lead to heat production. Mitochondrial concentrations of UCP1 protein, which have been reported for mouse BAT vary between an average of 6.3  $\mu\text{g}$  and 55  $\mu\text{g}$  per mg mitochondrial protein, depending on the acclimation temperature of the animals (see **Table 2**) (Stuart et al., 2001b). Therefore the UCP1 expression level of 4.8  $\mu\text{g}/\text{mg}$  mitochondrial protein is close to what is found in BAT mitochondria from mice kept at thermoneutrality. It is even within the physiological expression range, as it is above the expression level in thymus mitochondria, which can be calculated to be about 3  $\mu\text{g}$  per mg mitochondrial protein (Adams et al., 2010). UCP1 expression level in yeast can reach higher values than the one described here for HEK293 UCP1 cells, but it seems that expression above 0.9  $\mu\text{g}$  per mg mitochondrial protein leads to function artefacts (Stuart et al., 2001a). UCP1 amount in adipocyte cell lines has never been quantified and due to its low expression level mostly been tested on RNA level (Klaus et al., 1994; Mercader et al., 2010). In CHO cells, a mammalian cell culture model for UCP1 expression which had been established but never really used for research on UCP1 function, expression of 1  $\mu\text{g}$  UCP1 per mg mitochondrial protein was reported. But full functionality and exclusion of uncoupling artefacts have never been demonstrated (Casteilla et al., 1990; Mozo et al., 2006b). Therefore it seems that HEK293 cells are a promising test system for further research on uncoupling protein function, offering expression levels within the physiological range, close to values found in BAT mitochondria of thermoneutral acclimated mice.

**Table 2 UCP1 expression in different experimental systems, species and at different acclimation temperatures.**

data source	species/ test system	acclimation	amount UCP1 ( $\mu\text{g} \cdot \text{mg} \text{ mitoprotein}^{-1}$ )
this thesis (Jastroch et al., 2012) (Hirschberg et al., 2011)	HEK293 mouse	37°C	4.8
	mouse	24°C	29.8
	BFC	37°C	2.8
collected in (Stuart et al., 2001b)	rat	thermoneutral	13
	rat	cold, 5°C	56
	mouse	thermoneutral	6.3
	mouse	cold	55
assumed from (Neschen et al., 2008)	skm mouse	24°C	2.1
	CHO mouse	37°C	1
(Mozo et al., 2006b)	yeast 307	30°C	0.9*
(Stuart et al., 2001b)			

#### 4.1.1.3 Stimulation of UCP1 expression in BFC

Several attempts were made to derive a cell line from brown fat, which reflects the brown adipocyte characteristics, including a high level of UCP1 expression. For this purpose embryonic fibroblasts were subjected to serial passage (BFC-1, HB2), precursor cells from bone marrow were isolated (RBM-Ad, C3H10T1/2) or cells from brown fat tumors from SV40 transgenic mice were separated (HIB1B, T37i, e.g.) (Klein et al., 2002). These cell lines have largely increased the knowledge about proliferation, differentiation and the action of hormones on adipocytes, but none of them has been applied to test UCP1 function. Despite well detectable RNA expression, UCP1 protein was either only present at low level or not detectable in these cells. Recently SV40 treatment was applied to proliferating primary adipocytes, isolated from individual mice, leading to the generation of murine cell lines (Klein et al., 1999). These cell lines showed UCP1 expression which was responsive to adrenergic agonists, but so far they have not been used for functional analysis of the uncoupling protein.

Isoproterenol, retinoic acid and rosiglitazone were applied in this thesis to stimulate UCP1 expression in the BFC line. BFC cells had been generated as mentioned above by viral treatment of proliferating adipocytes. These three agonists, which are known to bind and/or stimulate factors involved in UCP1 transcription (**Figure 54**) were used, as BFC did not express UCP1 protein if they were only fully differentiated. Stimulation of UCP1 expression on the RNA and protein level by isoproterenol has also been demonstrated for the HIB1B cell line (Klaus et al., 1994). But here the sensitivity of the adipocytes to adrenergic agonists was different from what had been described in primary adipocytes, as HIB1B depended more on  $\beta_1/\beta_2$  adrenergic receptors than on  $\beta_3$  receptors (Klaus et al., 1991;

Rehmark et al., 1990). Retinoic acid and synthetic ligands for RAR and RXR have been shown to increase UCP1 expression in many *in vitro* and *in vivo* systems (Cannon and Nedergaard, 2004). Retinoic acid was even able to stimulate UCP1 expression in mouse embryonic fibroblasts (MEFs), a commonly used model for white adipocytes (Mercader et al., 2010). Rosiglitazone, which has been applied as antidiabetic drug and belongs to the thiazolidinedione class of drugs, acts on PPAR $\gamma$ , which has been shown to promote not only white but also brown fat differentiation, part of which is the expression of UCP1 (Cannon and Nedergaard, 2004; Barbera et al., 2001). PPAR $\gamma$  agonists have been shown to stimulate UCP1 expression in cultured human adipocytes (Digby et al., 1998).

For the BFC line isoproterenol, retinoic acid and rosiglitazone all already alone increased UCP1 expression compared to the level after control treatment and a combination of isoproterenol and retinoic acid resulted in the strongest induction. The effects were neither additive nor synergistic for the different combinations, as had been observed for the effects of insulin and T3 on HIB1B differentiation and UCP1 expression, for example (Klaus et al., 1991).

The positive effect on UCP1 expression of adrenergic treatment along with retinoids is not exclusively characteristic for brown adipocytes, as the above cited studies demonstrate, but the combined treatment was able to induce UCP1 expression at 2.8  $\mu\text{g}/\text{mg}$  mitochondrial protein. This is more than had been previously reported for immortalised brown fat cell lines and is only slightly below the physiological range as elaborated in 4.1.1.2.

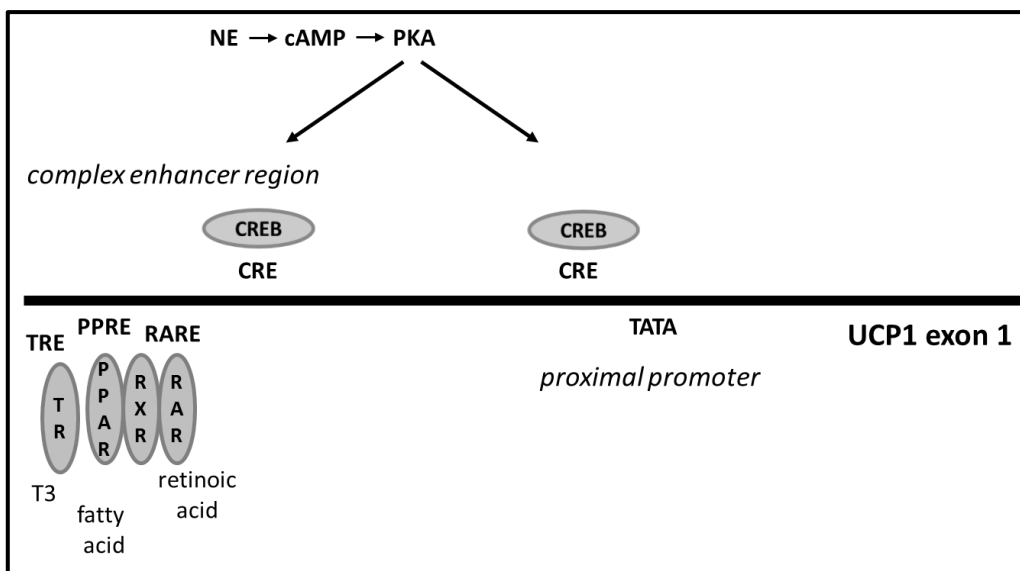


**Figure 54 Simplified illustration of the UCP1 promoter.**

UCP1 expression is controlled by a variety of transcription factors, acting in an upstream enhancer region or in the proximal promoter. Norepinephrine (NE) acts via protein kinase A (PKA) on cAMP responsive elements (CRE). T3 activates binding to thyroid hormone response elements (TRE), fatty acids and other effectors promote binding of PPARs to their response elements (PPRE) and retinoic acid interacts with RXR and RAR which then bind to retinoic acid response elements (RARE) (Adapted from (Cannon and Nedergaard, 2004)).

#### 4.1.2 Regulation of UCP1 activity in HEK293 UCP1 and BFC mitochondria

##### 4.1.2.1 *UCP1 can be activated and inhibited by its native regulators in the heterologous environment*

Determination of proton leak kinetics of HEK293 and HEK293 UCP1 mitochondria showed that fatty acids increased the leak of HEK293 UCP1 mitochondria and that this increase could be prevented by co-incubation with GDP (**Figure 13**). This reflects the native UCP1 function in mitochondria, which can be defined as fatty acid inducible increase in proton leakage, which is sensitive to purine nucleotide addition. Characterisation of fatty acid activation has shown that fatty acids with a chain length of 10 or more C atoms are potent activators of UCP1 (Rial et al., 1983). Palmitate, which has a chain length of 16 carbon atoms, is widely used in studies on UCP1 function, as it is a potent activator. Although it is most likely that ADP and ATP are the relevant inhibitors in tissue, it is GDP that is preferred *in vitro*, as it has a higher affinity to UCP1 (Nicholls, 1976; Nicholls, 2006).

The kinetics of fatty acid activation and inhibition by purine nucleotides are competitive (Shabalina et al., 2004), but UCP1 activator and inhibitor do not act on the same binding site (Rial et al., 1983). Experimental data fit a model in which UCP1 is inherently active, if not inhibited by purine nucleotides. This nucleotide inhibition, which would always occur at cellular levels of ATP and ADP (Nicholls, 2006), has to be overcome by FFA (Shabalina et al., 2004). Basal activity of UCP1 in HEK293 UCP1 cells in control conditions might be explained by the availability of residual fatty acids, which could not be removed during the isolation process and led to activation of the protein. Increasing the concentration of purine nucleotides by addition of GDP was able to prevent this activation. This supports the assumption of a basal fatty acid mediated activation in control conditions and is in accordance with the concept of competitive kinetics. An intermediate activation state in the presence of palmitate and 500  $\mu$ M GDP compared to full inhibition in the presence of 1 mM GDP (data not shown) provides further evidence and demonstrates that UCP1 in HEK293 UCP1 cells is regulated as in its native environment.

##### 4.1.2.2 *Native regulation of UCP1 function in BFC mitochondria*

In isolated BFC mitochondria the addition of GDP alone also reduced the proton leak below the leak detected for control conditions, similar to what was observed in HEK293 UCP1 mitochondria (**Figure 28**). Although these mitochondria were isolated in the presence of higher amounts of BSA (initial step 2 %) and also analysed in the presence of more BSA (0.4 %), it seems that still residual fatty acids were available for basal activation of UCP1. Addition of further fatty acids still increased proton leak compared to control conditions and this increase was sensitive to GDP. Therefore functional UCP1 with native regulation can also be assumed for this cell line.

The fatty acid induced increase in proton leak could not fully be inhibited by the addition of 1 mM GDP. In this condition the proton leak curve is overlaying with the one for control conditions instead of with the one representing basal leak, measured in the presence of 1 mM GDP alone (**Figure 27**). This could on the one hand mean that more GDP is necessary to compete with the amount of free fatty acids, which is very likely as more free fatty acids were supplied to activate BFC mitochondrial leak. On the other hand it is possible that at the concentration of 300  $\mu$ M palmitate, which was added in complex with BSA and resulted in a free fatty acid concentration of 97.9 nM, also other fatty acid sensitive pathways in the inner mitochondrial membrane were activated (Wojtczak and Wieckowski, 1999). Further measurements including carboxyatractylate, an inhibitor of ANT, could help to clarify that.

#### 4.1.3 UCP1 in HEK293 UCP1 and BFC: No uncoupling artefact or contribution to basal leak

The final proof that UCP1 displayed native activity in the heterologous HEK293 expression system was the demonstration that it could be completely inactivated by purine nucleotides. This was illustrated by the complete overlay of proton leak curves for HEK293 mitochondria and HEK293 UCP1 mitochondria in the presence of 1 mM GDP (**Figure 15**). On the one hand the result excludes the presence of an uncoupling artefact, as it has been reported for yeast mitochondria expressing UCP1 at an expression level above 0.9  $\mu$ g per mg mitochondrial protein (Stuart et al., 2001b). On the other hand this supports the idea that inactive UCP1 does not contribute to basal proton leak, a question which has recently been discussed (Parker et al., 2009; Shabalina et al., 2010). This is also of direct relevance for the potential of UCP1 and BAT as therapeutic target in humans. If UCP1 did not contribute to basal leak, than the mere presence of BAT would not be beneficial but it would have to be activated to reduce obesity and resulting diseases in humans. This would also further underline the importance of test systems like the HEK293 UCP1 system, which allow high throughput screening for activators and inhibitors of UCP1 function.

Although an uncoupling artefact due to stimulated endogenous UCP1 expression in BFC cells is not likely, it cannot be excluded with the data which were generated for this thesis. Comparisons of mitochondrial proton leak between differentiated and stimulated and differentiated non-stimulated cells or comparisons between BFC and a cell line derived from interscapular BAT of the UCP1 knockout mouse would have to prove that they are identical in basal proton leak. This might then, like the data for the HEK293 UCP1 cell line, also contribute to answer the question of an increased basal proton leak due to the presence of UCP1 in the mitochondrial membrane. On the other hand it could be questioned if the contribution of UCP1 to basal leak was detectable at the given expression amount in the cell lines. Parker and colleagues, however, detected at about 150 mV an approximately 6 fold higher basal proton leak in mitochondria from wildtype compared to mitochondria from UCP1 knockout animals, with a contribution of 3 nmol  $O^*min^{-1} \cdot mg^{-1}/\mu$ g UCP1

(Parker et al., 2009). Assuming linearity between UCP1 content and proton leak rate of inhibited protein, a contribution of about  $15 \text{ nmol O}^* \text{min}^{-1} \cdot \text{mg}^{-1}$  could be expected for the HEK293 UCP1 mitochondria and a contribution of  $9 \text{ nmol O}^* \text{min}^{-1} \cdot \text{mg}^{-1}$  for the BFC mitochondria. For the HEK293 UCP1 mitochondria this could have been resolved but can be excluded based on the results.

#### 4.1.4 Basal activity of UCP1 in the cellular context

Concerning the question if UCP1 is in a basal active state in the living cell, the two data sets on HEK293 UCP1 cell lines give different answers. In the literature it is assumed that UCP1 is normally inactive, due to inhibition by the high intracellular levels of purine nucleotides (mainly ADP and ATP) and this inhibition has to be overcome by the release of free fatty acids (Shabalina et al., 2004; Nicholls, 2006). In trypsinised cells analysed with the Clark-electrode, a different basal respiration between HEK293 and HEK293 UCP1 cells was detected. This difference persisted after the establishment of leak respiration and was even more pronounced after the addition of palmitate (**Figure 20**). Analyses of cellular respiration for adherently growing HEK293 and HEK293 UCP1 cells on the other hand did not detect any difference in basal or leak states (**Figure 21**). Leak in the presence of exogenously added free fatty acids was not assessed. This finding can possibly be explained by the use of growth medium (DMEM 10 % FBS) as substrate in the Clark-electrode assay while DMEM 0.1 % BSA was used for the Seahorse analysis. FBS might deliver the free fatty acids necessary to overcome nucleotide inhibition in the trypsinised cells.

The absolute values of cellular respiration determined with the Clark electrode are in the range of previously conducted studies on HEK293 cells transiently expressing uncoupling proteins or of studies determining cellular respiration of INS1E cells and myotubes (Affourtit and Brand, 2008). HEK293 UCP1 cells consumed  $6 \text{ nmol O}^* \text{min}^{-1} \cdot 10^6 \text{ cells}^{-1}$  in basal conditions, which was reduced to  $3 \text{ nmol O}^* \text{min}^{-1} \cdot 10^6$  in leak conditions. In a previous study the cellular respiration of HEK293 cells transiently expressing UCP1 had been determined with a Clark electrode and absolute values of respiration for all cells from a confluent plate were given in  $\text{nmol O}_2^* \text{min}^{-1}$ . Assuming that one plate contained about  $5 \cdot 10^6$  cells the given values could be translated into a basal respiration of  $16 \text{ nmol O}^* \text{min}^{-1} \cdot 10^6 \text{ cells}^{-1}$  and a leak respiration of about  $7 \text{ nmol O}^* \text{min}^{-1} \cdot 10^6 \text{ cells}^{-1}$  for cells which transiently expressed UCP1. Addition of palmitate increased leak respiration to  $10 \text{ nmol O}^* \text{min}^{-1} \cdot 10^6 \text{ cells}^{-1}$ . As exact cell number is not known these values can be regarded as very comparable to those determined for HEK293 UCP1 cells. This is also true for the relative proportions of basal and leak respiration relative to maximum FCCP-induced respiration ( $\text{FCCP}_{\text{max}}$ ). In this thesis and the previous study leak respiration accounted for 40 % of  $\text{FCCP}_{\text{max}}$  and was increased to 60 % of  $\text{FCCP}_{\text{max}}$  in the presence of 100  $\mu\text{M}$  palmitate. Basal respiration was increased in the previous study, reflecting 80 % of  $\text{FCCP}_{\text{max}}$ , whereas it only accounted for 60 % of  $\text{FCCP}_{\text{max}}$  in this study. This might have been caused by a reduced  $\text{FCCP}_{\text{max}}$  respiration in the previous study, which seemed to be repressed by the

expression of UCP1 compared to control cells. It might also result from high cell numbers (about  $5 \cdot 10^6$ ) in the Clark electrode, as it was found in this thesis, that above an optimum cell number the  $FCCP_{max}/\text{cell number}$  decreases (data not shown).

In a study on cellular respiration of INS1E cells and myotubes (after correction of oxygen consumption values for non-mitochondrial respiration) myotubes consumed about  $15 \text{ nmol O} \cdot \text{min}^{-1} \cdot 10^6 \text{ cells}^{-1}$  in basal conditions and  $2 \text{ nmol O} \cdot \text{min}^{-1} \cdot 10^6 \text{ cells}^{-1}$  in the presence of oligomycin. INS1E cells respired at  $8 \text{ nmol O} \cdot \text{min}^{-1} \cdot 10^6 \text{ cells}^{-1}$  in basal conditions, which was only reduced to  $6 \text{ nmol O} \cdot \text{min}^{-1} \cdot 10^6 \text{ cells}^{-1}$  by addition of oligomycin (Affourtit and Brand, 2008). Again the absolute values are in the range of values from this study. Comparison of HEK293 UCP1 cells with a cell model which is very ATP-efficient, with a low contribution of leak to basal respiration (myotubes, leak is 13 % of basal) and a cell model which has a very high leak (INS1E, leak is 75 % of basal) demonstrates that HEK293 UCP1 cells are in this physiological range (leak is 60 % of basal). Although results from trypsinised cells suggest that due to basal UCP1 activity HEK293 UCP1 cells are more similar to INS1E cells this cannot be concluded from experiments with adherently growing HEK293 UCP1, where basal respiration was also at 55 % of  $FCCP_{max}$  but leak accounted only for 30 % of basal respiration (**Figure 21**). This is also in accordance with published values for hepatocytes, thymocytes and neuronal cells (Nobes et al., 1990; Buttgereit et al., 1992; Jekabsons and Nicholls, 2004).

In adherently growing BFC basal respiration was with about 50 % of  $FCCP_{max}$  comparable to the value in HEK293 UCP1 cells but the contribution of leak to basal respiration was clearly increased with 60-80 % (**Figure 30**). This might be caused by using oligomycin below saturating concentrations, which was not optimised for BFC, or by an activated uncoupling protein. Simulation of BFC with isoproterenol and retinoic acid before the measurement might have activated lipolysis and provide free fatty acids for the activation of UCP1. The fact that BFC kept in differentiation medium have the highest leak respiration cannot be explained by this hypothesis. Others determined the contribution of leak to basal respiration for immortalised brown adipocytes between 50 % and 70 %, depending on previous treatment of the cells (Uldry et al., 2006), arguing for a physiological phenomenon rather than non-optimised measurement conditions.

Overall it seems that HEK293 UCP1 cells do not change the proportions of basal and leak respiration due to the presence of the uncoupling protein, as long as free fatty acids are absent. The proportions between basal and leak respiration which were found are similar to many other cell types. BFC show a higher leak respiration, which is still in the physiologically found range and would need to be assigned to uncoupling protein 1 activity or other cellular processes by further experiments.



#### 4.1.5 Secondary effects of UCP1 expression in HEK293 and BFC

##### 4.1.5.1 *Cellular adaptations resulting from heterologous expression of UCP1 in HEK293 cells*

Although UCP1 expression did not affect the proportions of basal, leak and maximum respiration in HEK293 cells there were slight adaptive reactions observable. The heterologous overexpression of any protein signifies an increased energy demand for the cell, as protein synthesis consumes ATP. Overexpression of an uncoupling protein is much more challenging, as there is not only an increased ATP demand but also a reduced efficiency of ATP production. Titration of different respiration states for isolated HEK293 and HEK293 UCP1 mitochondria revealed that besides an elevated basal respiration in the absence or presence of GDP also an increased state 3 respiration could be observed (**Figure 16**). State 3 respiration, which is recorded in the presence of GDP, reflects the maximum capacity for ATP synthesis. An increase in this parameter for the HEK293 UCP1 cells might reflect cellular adaptation, which allows sufficient production of ATP despite UCP1 expression. In 4.1.4 it was discussed that UCP1 might not be constantly active in the cellular context and increased basal and leak respiration in isolated mitochondria and trypsinised cells might represent non-optimum measurement conditions with too high FFA. But the cellular adaptation in ATP synthesis capacity argues clearly for regular activation of UCP1 in the cell. Constantly elevated basal respiration reduces the spare respiratory capacity of the cell, which is the difference between basal respiration and maximum respiratory capacity (Brand and Nicholls, 2011). Given that maximum respiratory capacity is unchanged by UCP1 expression (**Figure 16, Figure 20, Figure 21**), higher basal respiration would reduce this parameter, which means that the cells have less buffer to react to changing ATP demands by increasing respiratory activity. Determination of FFA levels in cultured HEK293 UCP1 cells and the analysis of HEK293 and HEK293 UCP1 cells with Seahorse technology in the presence of defined amounts of FFA acids might help to resolve the question of constantly elevated basal respiration in HEK293 UCP1 cells.

Preliminary data from a 2D gel analysis of the mitoproteome of HEK293 and HEK293 UCP1 cells (data not shown), suggested that mitochondria from HEK293 UCP1 cells contained elevated levels of the  $\beta$ -subunit of ATP synthase and of the mitochondrial chaperone Hsp60. This would have been in accordance with increased capacity for ATP-synthesis and might be explained by the need of more chaperones for the expression and insertion of the heterologously expressed protein. But these results could not be validated by western blots with three independent samples of isolated HEK293 and HEK293 UCP1 mitochondria (data not shown). Furthermore the interscapular BAT of heterozygous Hsp60 knockout animals did not show a reduced amount of UCP1 expression. Interestingly, a mitoproteome study on yeast with heterologous expression of UCP1 also detected an upregulation of ATP synthase and Hsp60, therefore it might be worthwhile validating the initial finding (Douette et al., 2006). It is possible that the upregulation of the two proteins is a transient phenomenon occurring only at very low passage number after the initial transfection.

In general the study of cellular adaptations occurring after heterologous expression of UCP1 or other orthologs and paralogs might be a promising strategy to learn more about their physiological function. Besides a proteome approach, studies employing new generation transcriptomics could lead to further insight. Given that the ATP-synthase subunit  $\beta$ , a component of the respiratory chain machinery may be regulated it would also be of interest to control the abundance of other complexes of the respiratory chain and their activities. The number of mitochondria in the cell would be a further parameter to control, as it seems to be very tightly regulated to allow sufficient ATP production. And the necessary crosstalk between mitochondria and nucleus, which encodes most of the mitochondrial proteins, is still not understood.

#### 4.1.5.2 Side effects of BFC stimulation, necessary to induce endogenous UCP1 expression

A major concern according to the suitability of BFC cells as a test system for UCP1 function is that UCP1 expression does not spontaneously occur as a terminal marker of differentiation but must be stimulated with isoproterenol and retinoic acid. This may induce several other changes in the cell, which mimic the adaptive response of cold exposed brown adipocytes, but it can also provoke an unbalanced stimulation of the expression of a subset of genes. It should be noted that UCP1 expression can be induced in MEFs, a commonly used model for white adipocytes, by treatment with retinoic acid (Mercader et al., 2010), so it may be necessary to define further parameters in addition to the presence of UCP1 to define a cell culture model as *bona fide* brown adipocyte. As there is considerable research on the differentiation and recruitment of brown adipocytes, not only in BAT depots but also on cells appearing interspersed in white adipose tissue (brite cells), in the meantime several markers have been identified that can distinguish “true” brown adipocytes from other cell types with UCP1 expression (PRDM 16, Myf5, e.g. (Kajimura et al., 2010)). It could be of interest to control the expression of these factors in BFC cells.

The analysis of UCP1 function in isolated BFC mitochondria can be confounded by other mitochondrial proteins which influence proton leak. A potential upregulation of these proteins by agonist treatment was addressed by controlling the abundance of their transcripts. Other transcripts were tested as markers for a very global effect of agonist treatment. cDNA samples were generated from RNA isolated from differentiated and stimulated BFC (**Figure 26**). Among the possible contributors to proton leak ANT1 and UCP2 were 2 fold upregulated, UCP3 could not be detected and ANT2 was 3.5 fold upregulated (**Figure 26**). ANT has been suggested to be involved in fatty acid induced uncoupling (Wojtczak and Wieckowski, 1999; Shabalina et al., 2006). Therefore it will be important to include the ANT inhibitor CAT in the proton leak measurements with BFC mitochondria, in order to be sure that only the UCP1 dependent effects on proton leak are recorded in the different conditions. This is especially relevant as 1 mM GDP was not able to reduce proton leak to the basal level if palmitate was present at the same time. The problem of confounding effects during the

analysis of UCP1 function might be resolved by generating a cell line from the interscapular BAT of UCP1 knockout mice, or by performing proton leak measurements with mitochondria from differentiated but unstimulated BFC. Thereby the contribution of UCP1 to the effects on proton leak could be assigned.

CideA is regulated by PPAR $\alpha$  and PPAR $\gamma$  in liver (Viswakarma et al., 2007) and its expression is drastically reduced after RNAi mediated depletion of PPAR $\gamma$  in 3T3L1 adipocytes and brown adipocytes (Puri et al., 2008). This can explain the upregulation of CideA expression in rosiglitazone treated BFC which was observed for the single treatment and the combined treatment with isoproterenol and retinoic acid. Others have found a cold-induced downregulation of CideA, which was mediated via  $\beta$ 3 adrenergic receptors (Shimizu and Yokotani, 2009). A downregulation of CideA after isoproterenol treatment could not be observed in this thesis.

The agonist treatment of differentiated BFC in general had a much lower effect on the expression of a few candidate genes than it had on UCP1 transcript levels, although it would be important to validate these findings with further biological replicates. But the regulation of the ANT for example underlines the importance of this approach and suggests that the application of further inhibitors during proton leak measurements might be important to dissect UCP1 mediated effects on proton leak in BFC mitochondria.

#### 4.1.6 Catalytic activity of UCP1 in the different test systems

A first look at the direct comparison of UCP1 catalytic activity in the different test systems shows the large impact of fatty acid level (**Figure 37**). The curve describing UCP1 dependent uncoupling in HEK293 UCP1 mitochondria in the presence of palmitate is clearly separated from the others which only reflect catalytic rate as differential of active and inactive UCP1 in one test system. A closer look at these curves reveals that although they cluster, they do have different maxima at different membrane potential values. The catalytic rate of UCP1 in the two cell culture systems which were applied in this thesis is clearly different and much lower for the immortalised brown adipocytes.

It has been shown for brown fat mitochondria that they need to be resuspended in a hyposmotic buffer during functional analyses, as this allows expansion of the matrix, which shrinks during the isolation process. Only in low salt buffers full activation and inhibition of UCP1 can be detected (Nicholls and Lindberg, 1972). This is why mitochondria from BFC were also analysed in BAT-respiration buffer. Isolation protocol and calculation of membrane potential were also adopted from BAT. HEK293 cells on the other hand were treated like liver cells concerning isolation protocol and correction factor for TPMP-binding. Additionally palmitate was delivered differently and at higher concentration during the analyses of BAT and BFC. HEK293 mitochondria were analysed in the presence of 0.3 % BSA and palmitate was added dissolved in ethanol at a final concentration of 100

$\mu\text{M}$ . According to (Richieri et al., 1993) this results in a FFA concentration of 12.7 nM, being available for activation of UCP1. BFC mitochondria were assessed in the presence of 0.4 % BSA and palmitate was delivered in complex with BSA at a concentration of 300  $\mu\text{M}$ , as lower concentrations were not reliably effective in inducing proton leak. This concentration will lead to a FFA concentration of 97.9 nM and could already uncouple mitochondria non-specifically, as shown by Wojtczak and Wieckowski (Wojtczak and Wieckowski, 1999). All mentioned differences in protocol may in part be the explanation for the different proton leak kinetics or also catalytic activities/ $\mu\text{g}$  UCP1 observed in HEK293 UCP1 and BFC mitochondria. For precise comparisons different buffer concentrations should be tested to determine buffer conditions suitable for both, as it was reported for WT and UCP1-knockout BAT mitochondria. Shabalina and colleagues suggested that buffer conditions can selectively harm one subset of mitochondria and lead to differences between experimental groups that reflect a technical problem rather than a physiological phenotype (Shabalina et al., 2010). Furthermore the correction factor for matrix volume should be determined for the mitochondria from both cell lines as described by Brand, in order to have more accurate calculations (Brand, 1995).

When including the catalytic activities of UCP1 calculated for mitochondria isolated from RT- and thermoneutral-acclimated mice into the comparison, it can be noted that the curves describing them are more similar to the ones for HEK293 UCP1 cells than to the BFC curve. This is the case although BFC and BAT mitochondria were analysed using the same isolation and measurement conditions. The explanation for the differences in UCP1 catalytic activity seen in **Figure 37** could be the differential expression level of UCP1 in the respective system. As pointed out in 3.1.5.4 the lower the amount of UCP1 per mitochondrial protein, the higher the membrane potential at which leak respiration increases steeply. In hamster mitochondria it has been demonstrated, that UCP1 increases the sensitivity towards FFA. If this increase was not linear, this might explain the results illustrated in **Figure 37**, as a linear adjustment for UCP1 content could not correct for that (Rial et al., 1983; Shabalina et al., 2004).

Another reason, why UCP1 catalytic activity in BFC mitochondria is different from the other systems is its potential underestimation. It was calculated by subtraction of the GDP-palmitate regression from the regression for the palmitate condition. But as proton leak in the presence of GDP and palmitate did not reach basal leak in the presence of GDP alone, it is possible that the differential curve does not reflect all of the UCP1 mediated leak. More experiments with saturating amounts of GDP are required to define the UCP1-dependent component of palmitate induced leak in BFC. As already suggested when discussing uncoupling artefacts and basal leaks in the two test systems, it will be important to include the ANT inhibitor CAT in the measurements, especially as data on RNA expression suggested that the fatty acid sensitive subform ANT2 was upregulated by the BFC stimulation.

A problem for all comparisons between different test systems reported in the literatures certainly is that experimental conditions largely vary between studies and actual free fatty acid levels in control conditions or at an intermediate activation status are not known. Meaningful comparisons could probably only be made for saturating fatty acid concentrations which are difficult to titrate as the activation of other carriers may occur.

#### 4.1.7 Potential of the HEK293 cells and BFC for UCP research

There is considerable interest in the analysis of proton translocating activity of UCP1 orthologs from different species and in the functional description of UCP1 paralogs, like UCP2 and UCP3, of which the physiological function as well as details on their mechanistic function and regulation are largely unclear.

Liposomes and the model organism yeast have been applied for such studies, but both yielded contradictory results on transported substrates, necessary cofactors or the mechanism of interaction with fatty acids (Echtay et al., 2000; Esteves et al., 2004; Winkler and Klingenberg, 1994; Garlid et al., 1996). Furthermore liposomes are an artificial test system in which protein integrity is difficult to control, whereas an uncoupling artefact has been reported for the yeast system. Thus, new test systems are required as direct comparisons of UCP orthologs deliver inconclusive results as long as proteins are evaluated in different mitochondrial backgrounds. Expression of tagged versions with native function, as shown for tagUCP1 in HEK293 cells, will further facilitate determination of proton leak rates per mol UCP1. This is essential for direct comparisons, which could be very useful as changes in function might be assigned to differences in primary structure, similar to what has been done in mutational studies on UCP1 in yeast. These identified residues which are important for nucleotide binding or fatty acid sensitivity for example (Klingenberg and Huang, 1999). Performing such studies with naturally occurring protein variants has the advantage that effects of mutations on protein structure can be excluded. In mutational studies it can never be ruled out that the mutation of an amino acid affects uncoupling function only because it is important for maintenance of overall protein structure, and not because it is a functional residue. As the crystal structure of UCP1 has not been resolved yet, the structure of mutated variants cannot be controlled for.

The fact that HEK293 UCP1 cells allow the expression of uncoupling proteins at relevant expression levels without causing an uncoupling artefact and that this seems to be true also for a tagged protein version underlines the high potential of HEK293 cells to conduct such comparative studies. Furthermore the robust expression and native regulation make it a valuable tool for screening approaches which will be needed to identify new drugs for the activation of UCP1, possibly as a target for the treatment of obesity.

BFC cells on the other hand are a useful tool to study possible interaction partners of UCP1 by knockdown in a brown adipocyte environment. Such factors, like CideA, may not be present in the heterologous expression model or effects might depend on the specialised metabolism of a brown adipocyte.

**Table 3 Comparison of the two mammalian cell lines used for UCP1 analysis.**

	HEK293 UCP1	BFC
UCP1 amount /mg mitoprotein	4.8 µg	2.8 µg
expression	heterologous	endogenous
native regulation	+	+
influence on basal leak	-	-
main advantage	- stable and easy to handle - comparison of paralogs and orthologs	- close to native background - knockdown experiments possible

## 4.2 Interaction of UCP1 and CideA in different test systems

### 4.2.1 CideA, a mitochondrial protein?

The identification of CideA and CideB based on their sequence similarity to a subunit of DFF $\alpha$  suggested their involvement in caspase-independent apoptosis. They were supposed to mediate their effect after translocation to mitochondria and dimerisation (Inohara et al., 1998b; Chen et al., 2000). With the generation and characterisation of the CideA knockout mouse this view changed, and CideA was thought to be a mitochondrial protein, specifically expressed in mouse BAT. There it was proposed to reduce lipolysis and beta oxidation by inhibition of UCP1 (Zhou et al., 2003). Later on CideC was reported to be a lipid droplet protein, located on the droplet surface like perilipin and thereby inhibiting lipolysis or promoting lipid accumulation (Puri et al., 2007). The same was soon also found for CideA (Puri et al., 2008), with evidence collected in 3T3-L1 adipocytes, human white adipocytes and cultured brown adipocytes. The underlying co-localisation experiments of GFP-fusion proteins with Oil Red O or mitotracker staining are difficult to interpret. Two studies using cell fractionation detected CideA either in the heavy membrane fraction, interpreted as mitochondrial localisation, or in the ER fraction (Zhou et al., 2003; Qi et al., 2008).

In this study the subcellular localisation was not addressed in detail, but it was observed that immunological detection in isolated mitochondria resulted in weak signals, whereas total protein extracts gave better results. The tissue specific expression of CideA in mouse could be confirmed, and even the two protein variants of different molecular mass, which had been reported to be present by others, were detected on the respective membranes (Puri et al., 2008).

Observations from the heterologous expression of CideA in *E.coli* are in accordance with a membrane association of the protein, mediated by the C-terminal part, as full length CideA was located in inclusion bodies and part of the C-terminus were located to the membrane fraction of the bacterial cells. Furthermore a hydropathicity plot of the protein sequence predicted overall lipid solubility, especially for a sequence around AA70 and for the C-terminal part of the sequence. This was most likely the reason why the protein precipitated several times during the purification process and renaturation of the C-terminus was not possible.

### 4.2.2 No effect of CideA expression on UCP1 activity in the test systems

Considering the contradictory data on CideA function and its subcellular localisation in the literature, this thesis can contribute data from three different test systems for UCP1 function, which all argue against a direct or functional interaction of CideA and UCP1. Liposome experiments argue against a direct physical interaction. Co-expression in HEK293 UCP1 cells suggests lack of an interaction in the

cellular context, relying on intermediate reactions. An influence on UCP1 function via modulation of lipolysis could not be proven with experiments on immortalised brown adipocytes.

For the interpretation of the liposome experiments it may be considered that CideA was not completely refolded to its native form after purification from *E.coli* inclusion bodies. This concern does not apply to the separately expressed N-terminal half of the protein, which was recovered from the soluble fraction of bacterial cells (**Figure 42**). Here the buffer in which the proteins were added might have covered a possible inhibitory effect. The buffer effect was a dose dependent increase of lauric acid induced activation of UCP1 in liposomes and possibly depending on changes in pH (**Figure 44**). Fatty acid activation of UCP1 is dependent on pH, and more acidic values, increasing the probability of free carboxylic groups enforce the effect of fatty acids (Rial et al., 1983). Another possible explanation for the lack of an inhibitory effect is that the interaction surface is not located in the N-terminal half of the protein, although the solution structure of the CIDE-N domain of CideB suggested its suitability for interaction with other CIDE-N domains and had a regulatory effect on DFF40/45 (Lugovskoy et al., 1999). Functional experiments with the full sequence of CideB, however, argued for the importance of a region in the C-terminus for mitochondrial localisation and dimerisation, which both were prerequisites for fulfilling apoptotic function (Chen et al., 2000). And functional importance was also assigned to the C-terminal part of CideA in a study describing its interaction with AMPK in the endoplasmatic reticulum, leading to ubiquitin mediated degradation of AMPK (Qi et al., 2008).

The lack of an effect of CideA expression on UCP1 function in HEK293 cells cannot be explained by the lack of mediating cellular processes, if these were not brown fat specific processes. The analysis of adherently growing HEK293 cells should be repeated in the presence of fatty acids, as HEK293 UCP1 cells do not display basal activation of UCP1 in this experimental system and inhibitory action of CideA can probably not be detected with an inactive UCP1.

Assays in brown adipocytes, which might contain necessary cofactors which still were absent in the HEK293 test system, did not aim to characterise UCP1 function in cells overexpressing CideA so far. As an outlook, the analysis of fatty acid activation of UCP1 by Seahorse technology is desirable and should be compared between CideA expressing and control BFC. Furthermore large scale transductions of BFC with subsequent isolation of mitochondria for measurements of proton leak kinetics could help to clarify the interaction of CideA and UCP1. Respiration analyses should, but do not necessary have to reflect effects on leak, if two conditions differ only in the membrane potential which is maintained at the same leak respiration rate. The reported functional interaction between UCP1 and CideA after heterologous expression in yeast was defined by an effect on membrane potential (Zhou et al., 2003).



#### 4.2.3 CideA as a regulator of lipid metabolism?

Except of the very first publications on CideA function, which supposed an involvement in the regulation of apoptosis, all others include a possible regulation of lipid metabolism. The knockout mouse displays increased beta oxidation in BAT and has lower serum FFA levels. Cell culture models including HEK293T cells, COS 1 cells, 3T3 L1 cells, cultured brown adipocytes and cultured human white adipocytes have been shown to increase lipid storage and lipid droplet size upon increased endogenous or heterologous overexpression of CideA. Cell culture models do increase  $\beta$ -oxidation upon CideA knockdown and show increased ACC activity (Qi et al., 2008). Furthermore the transcription factor PPAR $\gamma$ , which is a regulator of lipid metabolism, also regulates CideA expression. Associations with overall human metabolism have been established by the discovery of a BMI (body mass index) -associated SNP (single nucleotide polymorphism) in the CideA sequence and correlations of CideA expression and insulin sensitivity (Dahlman et al., 2005; Puri et al., 2008).

Initial experiments in the adipocyte cell culture model BFC set out to reproduce these effects on lipid storage or breakdown and test if this might affect UCP1 function.

##### 4.2.3.1 *BFC lipid droplet size is not affected by overexpression of CideA*

Neither neutral lipid staining nor quantification of lipid droplet number and size revealed a significant difference between lipid accumulation in BFC overexpressing GFP or CideA. Both methods showed a trend towards higher lipid accumulation in BFC expressing CideA, but this was not significant due to high variation (**Figure 50**, **Figure 51**). Publications demonstrating increased lipid droplet size often depended on microscopic pictures of single cells. A reanalysis of data on lipid droplet size should be performed with regard to the distribution pattern of lipid droplet sizes rather than the mean size as it is possible that more single big droplets are present in CideA expressing cells. In some of the published cell culture models cells were additionally supplied with fatty acids as substrates after the transfection with CideA (Puri et al., 2008). This might be a way to enhance the phenotype and also lead to different results in BFC. Additionally effects on lipid accumulation might have to be evaluated at different timepoints of differentiation, as in other publications lipid droplet size is evaluated 24 h after transfection. Fully differentiated cells which were not stimulated could also be compared, as the agonist treatment seemed to reduce fatty acid content of the cells, especially the treatment with isoproterenol (**Figure 51**).

##### 4.2.3.2 *CideA expression does not change stimulated lipolysis of BFC*

Glycerol release was determined as a measure for lipolysis rate and compared in BFC overexpressing GFP or CideA. No difference in glycerol release was detected between the two groups, neither during

the 48 h stimulation period of the thermogenic phenotype nor during a 2 h acute stimulation with different isoproterenol concentrations (**Figure 52**). Glycerol release experiments with tissue samples from CideA knockout mice had shown higher lipolysis in the tissue of knockout animals. Interestingly free fatty acids were not released in the ratio which would be expected for simple lipid breakdown and release, but seemed to be metabolised more efficiently in knockout BAT (Zhou et al., 2003). Data on free fatty acid release are missing for BFC expressing CideA and should be determined to verify the findings from the glycerol release assay. Additionally, unstimulated cells or various differentiation states of BFC with heterologous overexpression of either GFP or CideA should be tested. Assessment of glycerol release after stimulation with isoproterenol and retinoic acid, which is supposed to induce the thermogenic phenotype and UCP1 expression of the adipocytes, may be problematic, on the one hand as it reduced lipid content in the cells (**Figure 51**), on the other hand because chronic  $\beta$ -adrenergic stimulation has been shown to desensitize a human BAT cell line for further adrenergic signals (Jockers et al., 1998). This is an explanation for the lacking responsiveness of isoproterenol pre-treated cells to the acute stimulation (**Figure 52**).

Even in the 48 h stimulation period no difference in glycerol release between control cells, GFP or CideA expressing cells could be detected, and only 2 to 1.5 fold elevated concentrations of glycerol in the medium, compared to the 2 h period were determined. As brown adipocytes have the enzymatic equipment to metabolise glycerol, it cannot be excluded that due to higher oxidation rates upon thermogenic stimulation some of the glycerol is withdrawn from the medium again. And with regard to the lipid metabolism phenotype of CideA knockout mice it has to be noted, that despite increased glycerol release from tissue in the *in vitro* assay, plasma levels of glycerol are not different between wildtype and knockout animals. They only differ upon a fasting challenge, which leads to a stronger reduction of triglycerides and NEFA in the plasma of knockout animals (Zhou et al., 2003). Cells might have to be supplied with fatty acids first or challenged with a starvation period to detect differences caused by CideA overexpression. Furthermore biochemical assays of enzyme activities for lipolytic enzymes could help to evaluate changes in lipid metabolism due to CideA overexpression.

#### 4.2.4 Interaction of CideA and UCP1 via fatty acid levels

The amount of data available on CideA function in lipid metabolism, ranging from heterologous cell culture models to human association studies, led to the assumption that CideA effects on UCP1 function might be indirect through modulation of free fatty acid levels. This would still be in accordance with most of the results from the publication characterising the knockout mouse, despite the direct functional interaction. The suggested model which is illustrated in **Figure 55** would explain high UCP1 activity in the UCP1 knockout mouse or in knockdown models by high levels of free fatty acids, which are available due to high rates of lipolysis, not influenced by CideA.

High expression levels of CideA on the other hand would shield lipid droplets from the action of lipases, which lowers free fatty acid levels and thereby reduces UCP1 activity. No significant effect on lipid storage or lipolysis was observed upon overexpression of CideA in BFC, but only a trend towards increased lipid accumulation. Data on lipolysis suggested no effect of CideA overexpression and the consequence for UCP1 function was not addressed in the experiments conducted up to now. But concerning literature data illustrating convincing effects on lipolysis and beta-oxidation it has to be noted that they were raised in tissue or cells from knockout animals or in cells with knockdown of CideA expression. It might be possible, that in BFC already other lipid droplet proteins exert the shielding function which CideA fulfils in other models, which could explain why overexpression does not lead to a clear phenotype. It might be interesting to go back to the immortalised adipocyte cell lines which were generated in this thesis and displayed endogenous CideA protein expression. They might be used for knockdown studies of CideA, and subsequent determination of lipolysis or UCP1 function. The most forward approach would of course be to isolate BAT mitochondria from CideA knockout mice and compare their proton leak kinetics to the one for BAT mitochondria from WT littermates.

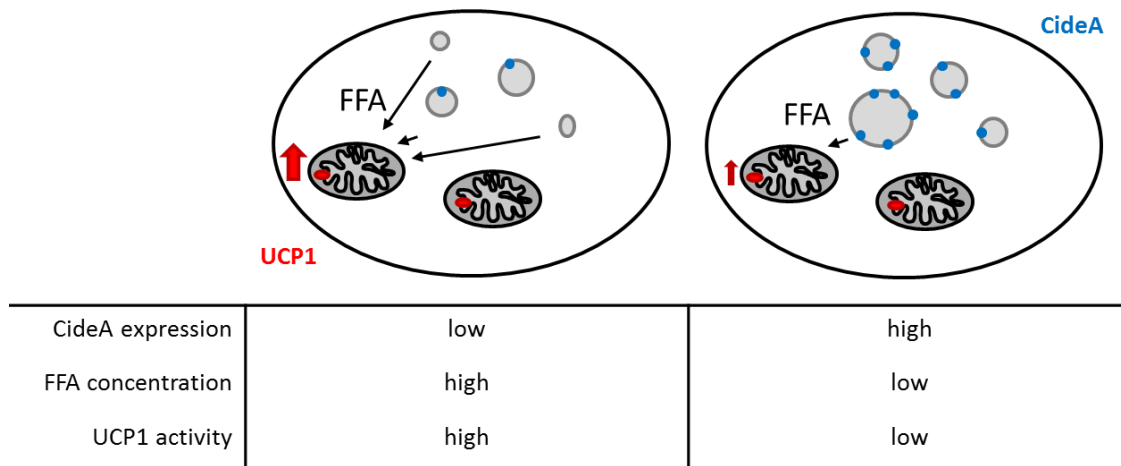


**Figure 55 Hypothesis on the indirect interaction of CideA and UCP1.**

CideA is lipid droplet protein which promotes lipid storage. At low expression level triglycerides are easily accessible for lipolysis and high levels of FFA are released, which can increase UCP1 activity and expression level. At high CideA expression level triglycerides are protected from breakdown to FFA and glycerol, which increases number and size of lipid droplets. Low levels of FFA lead to low UCP1 activity.

## 5 Summary and Conclusion

The aim of this PhD thesis was to characterise the function of uncoupling protein 1 (UCP1) and CideA in two mammalian cell lines, which were HEK293 cells with stable overexpression of UCP1 and immortalised brown preadipocytes (BFC), which could be differentiated into mature brown adipocytes. The suitability of both cell lines as test systems for UCP1 function was analysed by characterising first the expression of UCP1 and second the regulation of its activity by known activators and inhibitors in isolated mitochondria or intact cells.

The HEK293 UCP1 cell line, which was generated previous to this work in the laboratory, proved to be a valuable model for heterologous expression of UCP1, with expression levels in the physiological range and native regulation of activity, not displaying an uncoupling artefact. Therefore these cells could serve as powerful new test system for research on the function of uncoupling proteins allowing the direct comparison of orthologs and paralogs, which could help to elucidate the exact mechanistic function of UCP1. This test system furthermore allows high-throughput screening of pharmacological activators and inhibitors of UCP1 representing potential lead components to target brown adipose tissue for the treatment of obesity and its associated diseases.

The second cell line, BFC, represents an experimental model with agonist-inducible endogenous UCP1 expression. After stimulation the UCP1 expression level was comparable to HEK293 UCP1 cells. Due to variations in differentiation degree and responsiveness to agonist treatment the expression level was more variable than in HEK293 UCP1 cells. Side effects of the agonist treatment may bias the results of subsequent analyses. This cell line, however, more closely resembles the native situation and provides a cellular environment and metabolism which is better suited to fuel uncoupling function. The adipocyte line can also be used for knockdown studies on factors which are not present in heterologous models like the HEK293 UCP1 cells.

Both cell lines were used to investigate the interaction of CideA and UCP1, in order to learn more about the mechanistic function of UCP1 and to explore the suitability of the cell culture models in this context. Neither a direct nor a functional interaction of CideA could be detected in experiments which compared the activity of UCP1 in the absence and presence of CideA in HEK293 UCP1 cells. Furthermore the overexpression of CideA in BFC cells did not affect lipid accumulation or stimulated lipolysis, which could have been the basis for a functional interaction of the two proteins. Based on these results the previously suggested function of CideA as an inhibitor of UCP1 must be revised.

Test systems for UCP1 function have largely contributed to the current state of knowledge about the regulation of its expression and its function, as well as about its physiological role. Still, the detailed mechanistic function of UCP1 is not clarified and only very few activators and inhibitors have been described. As brown adipose tissue is present in adult humans the activation of UCP1 in the tissue

---

could be a target for the treatment of obesity, allowing the dissipation of excess energy in form of heat. The applicability of this approach should be tested in a mammalian cell system in order to rule out negative side effects of increased uncoupling and to find molecules which can modulate UCP1 activity to a desired extent in this cellular context. Based on the results of this thesis HEK293 UCP1 cells and BFC cells can be valuable models for this type of studies.

## 6 References

Adams,A.E., Kelly,O.M., and Porter,R.K. (2010). Absence of mitochondrial uncoupling protein 1 affects apoptosis in thymocytes, thymocyte/T-cell profile and peripheral T-cell number. *Biochim. Biophys. Acta* 1797, 807-816.

Affourtit,C. and Brand,M.D. (2008). Uncoupling protein-2 contributes significantly to high mitochondrial proton leak in INS-1E insulinoma cells and attenuates glucose-stimulated insulin secretion. *Biochem. J* 409, 199-204.

Aquila,H., Link,T.A., and Klingenberg,M. (1985). The uncoupling protein from brown fat mitochondria is related to the mitochondrial ADP/ATP carrier. Analysis of sequence homologies and of folding of the protein in the membrane. *EMBO J* 4, 2369-2376.

Arsenijevic,D., Onuma,H., Pecqueur,C., Raimbault,S., Manning,B.S., Miroux,B., Couplan,E., ves-Guerra,M.C., Gubern,M., Surwit,R., Bouillaud,F., Richard,D., Collins,S., and Ricquier,D. (2000). Disruption of the uncoupling protein-2 gene in mice reveals a role in immunity and reactive oxygen species production. *Nat. Genet.* 26, 435-439.

Barbera,M.J., Schluter,A., Pedraza,N., Iglesias,R., Villarroya,F., and Giralt,M. (2001). Peroxisome proliferator-activated receptor alpha activates transcription of the brown fat uncoupling protein-1 gene. A link between regulation of the thermogenic and lipid oxidation pathways in the brown fat cell. *J Biol. Chem.* 276, 1486-1493.

Bartelt,A., Bruns,O.T., Reimer,R., Hohenberg,H., Ittrich,H., Peldschus,K., Kaul,M.G., Tromsdorf,U.I., Weller,H., Waurisch,C., Eychmuller,A., Gordts,P.L., Rinninger,F., Bruegelmann,K., Freund,B., Nielsen,P., Merkel,M., and Heeren,J. (2011). Brown adipose tissue activity controls triglyceride clearance. *Nat. Med.* 17, 200-205.

Baur,J.A., Pearson,K.J., Price,N.L., Jamieson,H.A., Lerin,C., Kalra,A., Prabhu,V.V., Allard,J.S., Lopez-Lluch,G., Lewis,K., Pistell,P.J., Poosala,S., Becker,K.G., Boss,O., Gwinn,D., Wang,M., Ramaswamy,S., Fishbein,K.W., Spencer,R.G., Lakatta,E.G., Le,C.D., Shaw,R.J., Navas,P., Puigserver,P., Ingram,D.K., de,C.R., and Sinclair,D.A. (2006). Resveratrol improves health and survival of mice on a high-calorie diet. *Nature* 444, 337-342.

Bouillaud,F., Weissenbach,J., and Ricquier,D. (1986). Complete cDNA-derived amino acid sequence of rat brown fat uncoupling protein. *J Biol. Chem.* 261, 1487-1490.

Brand,M.D. (1995). Measurement of mitochondrial protonmotive force. In *Bioenergetics. A practical approach*, G.C.Brown and C.E.Cooper, eds. (Oxford: IRL Press), pp. 39-62.

Brand,M.D., Chien,L.F., Ainscow,E.K., Rolfe,D.F., and Porter,R.K. (1994). The causes and functions of mitochondrial proton leak. *Biochim. Biophys. Acta* 1187, 132-139.

- Brand, M.D. and Esteves, T.C. (2005). Physiological functions of the mitochondrial uncoupling proteins UCP2 and UCP3. *Cell Metab* 2, 85-93.
- Brand, M.D. and Nicholls, D.G. (2011). Assessing mitochondrial dysfunction in cells. *Biochem. J* 435, 297-312.
- Brand, M.D., Pakay, J.L., Ocloo, A., Kokoszka, J., Wallace, D.C., Brookes, P.S., and Cornwall, E.J. (2005). The basal proton conductance of mitochondria depends on adenine nucleotide translocase content. *Biochem. J.* 392, 353-362.
- Brookes, P.S., Rolfe, D.F., and Brand, M.D. (1997). The proton permeability of liposomes made from mitochondrial inner membrane phospholipids: comparison with isolated mitochondria. *J. Membr. Biol.* 155, 167-174.
- Buttgereit, F., Brand, M.D., and Muller, M. (1992). ConA induced changes in energy metabolism of rat thymocytes. *Biosci. Rep.* 12, 381-386.
- Cannon, B. and Nedergaard, J. (2004). Brown adipose tissue: function and physiological significance. *Physiol Rev.* 84, 277-359.
- Casteilla, L., Blondel, O., Klaus, S., Raimbault, S., Diolez, P., Moreau, F., Bouillaud, F., and Ricquier, D. (1990). Stable expression of functional mitochondrial uncoupling protein in Chinese hamster ovary cells. *Proc. Natl. Acad. Sci. U. S. A* 87, 5124-5128.
- Chen, C.A. and Okayama, H. (1988). Calcium phosphate-mediated gene transfer: a highly efficient transfection system for stably transforming cells with plasmid DNA. *Biotechniques* 6, 632-638.
- Chen, Z., Guo, K., Toh, S.Y., Zhou, Z., and Li, P. (2000). Mitochondria localization and dimerization are required for CIDE-B to induce apoptosis. *J Biol. Chem.* 275, 22619-22622.
- Clapham, J.C., Arch, J.R., Chapman, H., Haynes, A., Lister, C., Moore, G.B., Piercy, V., Carter, S.A., Lehner, I., Smith, S.A., Beeley, L.J., Godden, R.J., Herrity, N., Skehel, M., Changani, K.K., Hockings, P.D., Reid, D.G., Squires, S.M., Hatcher, J., Trail, B., Latcham, J., Rastan, S., Harper, A.J., Cadenas, S., Buckingham, J.A., Brand, M.D., and Abuin, A. (2000). Mice overexpressing human uncoupling protein-3 in skeletal muscle are hyperphagic and lean. *Nature* 406, 415-418.
- Cypess, A.M., Lehman, S., Williams, G., Tal, I., Rodman, D., Goldfine, A.B., Kuo, F.C., Palmer, E.L., Tseng, Y.H., Doria, A., Kolodny, G.M., and Kahn, C.R. (2009). Identification and importance of brown adipose tissue in adult humans. *N. Engl. J Med.* 360, 1509-1517.
- Dahlman, I., Kaaman, M., Jiao, H., Kere, J., Laakso, M., and Arner, P. (2005). The CIDEA gene V115F polymorphism is associated with obesity in Swedish subjects. *Diabetes* 54, 3032-3034.
- Digby, J.E., Montague, C.T., Sewter, C.P., Sanders, L., Wilkison, W.O., O'Rahilly, S., and Prins, J.B. (1998). Thiazolidinedione exposure increases the expression of uncoupling protein 1 in cultured human preadipocytes. *Diabetes* 47, 138-141.

- Douette,P., Gerkens,P., Navet,R., Leprince,P., De,P.E., and Sluse,F.E. (2006). Uncoupling protein 1 affects the yeast mitoproteome and oxygen free radical production. *Free Radic. Biol. Med.* **40**, 303-315.
- Echtay,K.S., Bienengraeber,M., Winkler,E., and Klingenberg,M. (1998). In the uncoupling protein (UCP-1) His-214 is involved in the regulation of purine nucleoside triphosphate but not diphosphate binding. *J Biol. Chem.* **273**, 24368-24374.
- Echtay,K.S., Esteves,T.C., Pakay,J.L., Jekabsons,M.B., Lambert,A.J., Portero-Otin,M., Pamplona,R., Vidal-Puig,A.J., Wang,S., Roebuck,S.J., and Brand,M.D. (2003). A signalling role for 4-hydroxy-2-nonenal in regulation of mitochondrial uncoupling. *EMBO J.* **22**, 4103-4110.
- Echtay,K.S., Roussel,D., St-Pierre,J., Jekabsons,M.B., Cadenas,S., Stuart,J.A., Harper,J.A., Roebuck,S.J., Morrison,A., Pickering,S., Clapham,J.C., and Brand,M.D. (2002). Superoxide activates mitochondrial uncoupling proteins. *Nature* **415**, 96-99.
- Echtay,K.S., Winkler,E., Bienengraeber,M., and Klingenberg,M. (2000). Site-directed mutagenesis identifies residues in uncoupling protein (UCP1) involved in three different functions. *Biochemistry* **39**, 3311-3317.
- Enerback,S., Jacobsson,A., Simpson,E.M., Guerra,C., Yamashita,H., Harper,M.E., and Kozak,L.P. (1997). Mice lacking mitochondrial uncoupling protein are cold-sensitive but not obese. *Nature* **387**, 90-94.
- Esteves,T.C., Echtay,K.S., Jonassen,T., Clarke,C.F., and Brand,M.D. (2004). Ubiquinone is not required for proton conductance by uncoupling protein 1 in yeast mitochondria. *Biochem. J* **379**, 309-315.
- Feldmann,H.M., Golozoubova,V., Cannon,B., and Nedergaard,J. (2009). UCP1 ablation induces obesity and abolishes diet-induced thermogenesis in mice exempt from thermal stress by living at thermoneutrality. *Cell Metab* **9**, 203-209.
- Garlid,K.D., Jaburek,M., and Jezek,P. (1998). The mechanism of proton transport mediated by mitochondrial uncoupling proteins. *FEBS Lett.* **438**, 10-14.
- Garlid,K.D., Orosz,D.E., Modriansky,M., Vassanelli,S., and Jezek,P. (1996). On the mechanism of fatty acid-induced proton transport by mitochondrial uncoupling protein. *J Biol. Chem.* **271**, 2615-2620.
- Golozoubova,V., Hohtola,E., Matthias,A., Jacobsson,A., Cannon,B., and Nedergaard,J. (2001). Only UCP1 can mediate adaptive nonshivering thermogenesis in the cold. *FASEB J.* **15**, 2048-2050.
- Gong,D.W., Monemdjou,S., Gavriloova,O., Leon,L.R., Marcus-Samuels,B., Chou,C.J., Everett,C., Kozak,L.P., Li,C., Deng,C., Harper,M.E., and Reitman,M.L. (2000). Lack of obesity and normal response to fasting and thyroid hormone in mice lacking uncoupling protein-3. *J. Biol. Chem.* **275**, 16251-16257.
- Gummesson,A., Jernas,M., Svensson,P.A., Larsson,I., Glad,C.A., Schele,E., Gripeteg,L., Sjöholm,K., Lystig,T.C., Sjöström,L., Carlsson,B., Fagerberg,B., and Carlsson,L.M. (2007). Relations of adipose



tissue CIDEA gene expression to basal metabolic rate, energy restriction, and obesity: population-based and dietary intervention studies. *J Clin. Endocrinol. Metab* *92*, 4759-4765.

Harper, M.E., Green, K., and Brand, M.D. (2008). The efficiency of cellular energy transduction and its implications for obesity. *Annu. Rev. Nutr.* *28*, 13-33.

Heaton, G.M., Wagenvoord, R.J., Kemp, A., Jr., and Nicholls, D.G. (1978). Brown-adipose-tissue mitochondria: photoaffinity labelling of the regulatory site of energy dissipation. *Eur. J. Biochem.* *82*, 515-521.

Hirschberg, V. (2006). Funktionelle Analyse von Entkopplerproteinen in human embryonalen Nierenzellen (HEK293). diploma thesis.

Hirschberg, V., Fromme, T., Klingenspor, M. (2011). Test systems to study the structure and function of uncoupling protein 1: a critical overview. *Frontiers in Cellular Endocrinology* *2*, 63.

Hofmann, W.E., Liu, X., Bearden, C.M., Harper, M.E., and Kozak, L.P. (2001). Effects of genetic background on thermoregulation and fatty acid-induced uncoupling of mitochondria in UCP1-deficient mice. *J Biol. Chem.* *276*, 12460-12465.

Inohara, N., Koseki, T., Chen, S., Wu, X., and Nunez, G. (1998a). CIDE, a novel family of cell death activators with homology to the 45 kDa subunit of the DNA fragmentation factor. *EMBO J* *17*, 2526-2533.

Inohara, N., Koseki, T., Chen, S., Wu, X., and Nunez, G. (1998b). CIDE, a novel family of cell death activators with homology to the 45 kDa subunit of the DNA fragmentation factor. *EMBO J* *17*, 2526-2533.

Ito, M., Nagasawa, M., Hara, T., Ide, T., and Murakami, K. (2010). Differential roles of CIDEA and CIDEC in insulin-induced anti-apoptosis and lipid droplet formation in human adipocytes. *J Lipid Res.* *51*, 1676-1684.

Ito, M., Nagasawa, M., Omae, N., Ide, T., Akasaka, Y., and Murakami, K. (2011). Differential regulation of CIDEA and CIDEC expression by insulin via Akt1/2- and JNK2-dependent pathways in human adipocytes. *J Lipid Res.* *52*, 1450-1460.

Jastroch, M., Hirschberg, V., Klingenspor, M. (2012). Functional characterization of UCP1 in mammalian HEK293 cells excludes mitochondrial uncoupling artefacts and reveals no contribution to basal proton leak. *Biochim. Biophys. Acta* *1817*, 1660-1670.

Jekabsons, M.B. and Nicholls, D.G. (2004). In situ respiration and bioenergetic status of mitochondria in primary cerebellar granule neuronal cultures exposed continuously to glutamate. *J Biol. Chem.* *279*, 32989-33000.

- Jezek,P., Orosz,D.E., Modriansky,M., and Garlid,K.D. (1994). Transport of anions and protons by the mitochondrial uncoupling protein and its regulation by nucleotides and fatty acids. A new look at old hypotheses. *J Biol. Chem.* *269*, 26184-26190.
- Jockers,R., Issad,T., Zilberfarb,V., de,C.P., Marullo,S., and Strosberg,A.D. (1998). Desensitization of the beta-adrenergic response in human brown adipocytes. *Endocrinology* *139*, 2676-2684.
- Kajimura,S., Seale,P., and Spiegelman,B.M. (2010). Transcriptional control of brown fat development. *Cell Metab* *11*, 257-262.
- Klaus,S., Cassard-Doulcier,A.M., and Ricquier,D. (1991). Development of Phodopus sungorus brown preadipocytes in primary cell culture: effect of an atypical beta-adrenergic agonist, insulin, and triiodothyronine on differentiation, mitochondrial development, and expression of the uncoupling protein UCP. *J Cell Biol.* *115*, 1783-1790.
- Klaus,S., Choy,L., Champigny,O., Cassard-Doulcier,A.M., Ross,S., Spiegelman,B., and Ricquier,D. (1994). Characterization of the novel brown adipocyte cell line HIB 1B. Adrenergic pathways involved in regulation of uncoupling protein gene expression. *J Cell Sci.* *107 ( Pt 1)*, 313-319.
- Klein,J., Fasshauer,M., Ito,M., Lowell,B.B., Benito,M., and Kahn,C.R. (1999). beta(3)-adrenergic stimulation differentially inhibits insulin signaling and decreases insulin-induced glucose uptake in brown adipocytes. *J Biol. Chem.* *274*, 34795-34802.
- Klein,J., Fasshauer,M., Klein,H.H., Benito,M., and Kahn,C.R. (2002). Novel adipocyte lines from brown fat: a model system for the study of differentiation, energy metabolism, and insulin action. *Bioessays* *24*, 382-388.
- Klingenberg,M. and Huang,S.G. (1999). Structure and function of the uncoupling protein from brown adipose tissue. *Biochim. Biophys. Acta* *1415*, 271-296.
- Kopecky,J., Clarke,G., Enerback,S., Spiegelman,B., and Kozak,L.P. (1995). Expression of the mitochondrial uncoupling protein gene from the aP2 gene promoter prevents genetic obesity. *J Clin. Invest* *96*, 2914-2923.
- Krauss,S., Zhang,C.Y., and Lowell,B.B. (2005). The mitochondrial uncoupling-protein homologues. *Nat. Rev. Mol. Cell Biol.* *6*, 248-261.
- Liebig,M. (2004). Funktionsanalyse der mitochondrialen Transportproteine UCP2, UCP3, UCPx und SOUP. PhD thesis.
- Lin,C.S. and Klingenberg,M. (1980). Isolation of the uncoupling protein from brown adipose tissue mitochondria. *FEBS Lett.* *113*, 299-303.
- Lin,C.S. and Klingenberg,M. (1982). Characteristics of the isolated purine nucleotide binding protein from brown fat mitochondria. *Biochemistry* *21*, 2950-2956.

- Liu,X., Rossmeisl,M., McClaine,J., Riachi,M., Harper,M.E., and Kozak,L.P. (2003). Paradoxical resistance to diet-induced obesity in UCP1-deficient mice. *J Clin. Invest* *111*, 399-407.
- Lugovskoy,A.A., Zhou,P., Chou,J.J., McCarty,J.S., Li,P., and Wagner,G. (1999). Solution structure of the CIDE-N domain of CIDE-B and a model for CIDE-N/CIDE-N interactions in the DNA fragmentation pathway of apoptosis. *Cell* *99*, 747-755.
- Mercader,J., Palou,A., and Bonet,M.L. (2010). Induction of uncoupling protein-1 in mouse embryonic fibroblast-derived adipocytes by retinoic acid. *Obesity (Silver. Spring)* *18*, 655-662.
- Meyer,C.W., Willershauser,M., Jastroch,M., Rourke,B.C., Fromme,T., Oelkrug,R., Heldmaier,G., and Klingenspor,M. (2010). Adaptive thermogenesis and thermal conductance in wild-type and UCP1-KO mice. *Am. J Physiol Regul. Integr. Comp Physiol* *299*, R1396-R1406.
- Miroux,B. and Walker,J.E. (1996). Over-production of proteins in Escherichia coli: mutant hosts that allow synthesis of some membrane proteins and globular proteins at high levels. *J Mol. Biol.* *260*, 289-298.
- Modriansky,M., Murdza-Inglis,D.L., Patel,H.V., Freeman,K.B., and Garlid,K.D. (1997). Identification by site-directed mutagenesis of three arginines in uncoupling protein that are essential for nucleotide binding and inhibition. *J Biol. Chem.* *272*, 24759-24762.
- Monemdjou,S., Kozak,L.P., and Harper,M.E. (1999). Mitochondrial proton leak in brown adipose tissue mitochondria of Ucp1-deficient mice is GDP insensitive. *Am. J Physiol* *276*, E1073-E1082.
- Mozo,J., Ferry,G., Masscheleyn,S., Miroux,B., Boutin,J.A., and Bouillaud,F. (2006a). Assessment of a high-throughput screening methodology for the measurement of purified UCP1 uncoupling activity. *Anal. Biochem.* *351*, 201-206.
- Mozo,J., Ferry,G., Studeny,A., Pecqueur,C., Rodriguez,M., Boutin,J.A., and Bouillaud,F. (2006b). Expression of UCP3 in CHO cells does not cause uncoupling, but controls mitochondrial activity in the presence of glucose. *Biochem. J.* *393*, 431-439.
- Neschen,S., Katterle,Y., Richter,J., Augustin,R., Scherneck,S., Mirhashemi,F., Schurmann,A., Joost,H.G., and Klaus,S. (2008). Uncoupling protein 1 expression in murine skeletal muscle increases AMPK activation, glucose turnover, and insulin sensitivity in vivo. *Physiol Genomics* *33*, 333-340.
- Neupert,W. and Herrmann,J.M. (2007). Translocation of proteins into mitochondria. *Annu. Rev. Biochem.* *76*, 723-749.
- Nicholls,D.G. (1976). Hamster brown-adipose-tissue mitochondria. Purine nucleotide control of the ion conductance of the inner membrane, the nature of the nucleotide binding site. *Eur. J Biochem.* *62*, 223-228.
- Nicholls,D.G. (2006). The physiological regulation of uncoupling proteins. *Biochim. Biophys. Acta* *1757*, 459-466.

- Nicholls,D.G. and Lindberg,O. (1972). Inhibited respiration and ATPase activity of rat liver mitochondria under conditions of matrix condensation. *FEBS Lett.* *25*, 61-64.
- Nicholls,D.G. and Rial,E. (1999). A history of the first uncoupling protein, UCP1. *J Bioenerg. Biomembr.* *31*, 399-406.
- Nobes,C.D., Brown,G.C., Olive,P.N., and Brand,M.D. (1990). Non-ohmic proton conductance of the mitochondrial inner membrane in hepatocytes. *J Biol. Chem.* *265*, 12903-12909.
- Nordstrom,E.A., Ryden,M., Backlund,E.C., Dahlman,I., Kaaman,M., Blomqvist,L., Cannon,B., Nedergaard,J., and Arner,P. (2005). A human-specific role of cell death-inducing DFFA (DNA fragmentation factor-alpha)-like effector A (CIDEA) in adipocyte lipolysis and obesity. *Diabetes* *54*, 1726-1734.
- Oelkrug,R., Kutschke,M., Meyer,C.W., Heldmaier,G., and Jastroch,M. (2010). Uncoupling protein 1 decreases superoxide production in brown adipose tissue mitochondria. *J Biol. Chem.* *285*, 21961-21968.
- Parker,N., Crichton,P.G., Vidal-Puig,A.J., and Brand,M.D. (2009). Uncoupling protein-1 (UCP1) contributes to the basal proton conductance of brown adipose tissue mitochondria. *J Bioenerg. Biomembr.* *41*, 335-342.
- Puri,V., Konda,S., Ranjit,S., Aouadi,M., Chawla,A., Chouinard,M., Chakladar,A., and Czech,M.P. (2007). Fat-specific protein 27, a novel lipid droplet protein that enhances triglyceride storage. *J Biol. Chem.* *282*, 34213-34218.
- Puri,V., Ranjit,S., Konda,S., Nicoloso,S.M., Straubhaar,J., Chawla,A., Chouinard,M., Lin,C., Burkart,A., Corvera,S., Perugini,R.A., and Czech,M.P. (2008). Cidea is associated with lipid droplets and insulin sensitivity in humans. *Proc. Natl. Acad. Sci. U. S. A* *105*, 7833-7838.
- Qi,J., Gong,J., Zhao,T., Zhao,J., Lam,P., Ye,J., Li,J.Z., Wu,J., Zhou,H.M., and Li,P. (2008). Downregulation of AMP-activated protein kinase by Cidea-mediated ubiquitination and degradation in brown adipose tissue. *EMBO J* *27*, 1537-1548.
- Rafael,J., Ludolph,H.J., and Hohorst,H.J. (1969). [Mitochondria from brown adipose tissue: uncoupling of respiratory chain phosphorylation by long fatty acids and recoupling by guanosine triphosphate]. *Hoppe Seylers. Z. Physiol Chem.* *350*, 1121-1131.
- Rehmark,S., Nechad,M., Herron,D., Cannon,B., and Nedergaard,J. (1990). Alpha- and beta-adrenergic induction of the expression of the uncoupling protein thermogenin in brown adipocytes differentiated in culture. *J Biol. Chem.* *265*, 16464-16471.
- Reynafarje,B., Costa,L.E., and Lehninger,A.L. (1985). O<sub>2</sub> solubility in aqueous media determined by a kinetic method. *Anal. Biochem.* *145*, 406-418.
- Rial,E., Poustie,A., and Nicholls,D.G. (1983). Brown-adipose-tissue mitochondria: the regulation of the 32000-Mr uncoupling protein by fatty acids and purine nucleotides. *Eur. J Biochem.* *137*, 197-203.

- Richieri,G.V., Anel,A., and Kleinfeld,A.M. (1993). Interactions of long-chain fatty acids and albumin: determination of free fatty acid levels using the fluorescent probe ADIFAB. *Biochemistry* 32, 7574-7580.
- Rolfe,D.F. and Brand,M.D. (1996). Contribution of mitochondrial proton leak to skeletal muscle respiration and to standard metabolic rate. *Am. J Physiol Cell Physiol* 271, C1380-C1389.
- Rolfe,D.F., Hulbert,A.J., and Brand,M.D. (1994). Characteristics of mitochondrial proton leak and control of oxidative phosphorylation in the major oxygen-consuming tissues of the rat. *Biochim. Biophys. Acta* 1188, 405-416.
- Schleiff,E. and McBride,H. (2000). The central matrix loop drives import of uncoupling protein 1 into mitochondria. *J Cell Sci.* 113 ( Pt 12), 2267-2272.
- Shabalina,I.G., Jacobsson,A., Cannon,B., and Nedergaard,J. (2004). Native UCP1 displays simple competitive kinetics between the regulators purine nucleotides and fatty acids. *J Biol. Chem.* 279, 38236-38248.
- Shabalina,I.G., Kramarova,T.V., Nedergaard,J., and Cannon,B. (2006). Carboxyatractyloside effects on brown-fat mitochondria imply that the adenine nucleotide translocator isoforms ANT1 and ANT2 may be responsible for basal and fatty-acid-induced uncoupling respectively. *Biochem. J* 399, 405-414.
- Shabalina,I.G., Ost,M., Petrovic,N., Vrbacky,M., Nedergaard,J., and Cannon,B. (2010). Uncoupling protein-1 is not leaky. *Biochim. Biophys. Acta* 1797, 773-784.
- Shimizu,T. and Yokotani,K. (2009). Acute cold exposure-induced down-regulation of CIDEA, cell death-inducing DNA fragmentation factor-alpha-like effector A, in rat interscapular brown adipose tissue by sympathetically activated beta3-adrenoreceptors. *Biochem. Biophys. Res. Commun.* 387, 294-299.
- Skulachev,V.P. (1991). Fatty acid circuit as a physiological mechanism of uncoupling of oxidative phosphorylation. *FEBS Lett.* 294, 158-162.
- Skulachev,V.P. (1996). Role of uncoupled and non-coupled oxidations in maintenance of safely low levels of oxygen and its one-electron reductants. *Q. Rev. Biophys.* 29, 169-202.
- Speakman,J.R., Talbot,D.A., Selman,C., Snart,S., McLaren,J.S., Redman,P., Krol,E., Jackson,D.M., Johnson,M.S., and Brand,M.D. (2004). Uncoupled and surviving: individual mice with high metabolism have greater mitochondrial uncoupling and live longer. *Aging Cell* 3, 87-95.
- Stuart,J.A., Cadenas,S., Jekabsons,M.B., Roussel,D., and Brand,M.D. (2001a). Mitochondrial proton leak and the uncoupling protein 1 homologues. *Biochim. Biophys. Acta* 1504, 144-158.
- Stuart,J.A., Harper,J.A., Brindle,K.M., Jekabsons,M.B., and Brand,M.D. (2001b). A mitochondrial uncoupling artifact can be caused by expression of uncoupling protein 1 in yeast. *Biochem. J.* 356, 779-789.

- Ukropec,J., Anunciado,R.P., Ravussin,Y., Hulver,M.W., and Kozak,L.P. (2006). UCP1-independent thermogenesis in white adipose tissue of cold-acclimated Ucp1<sup>-/-</sup> mice. *J Biol. Chem.* *281*, 31894-31908.
- Uldry,M., Yang,W., St-Pierre,J., Lin,J., Seale,P., and Spiegelman,B.M. (2006). Complementary action of the PGC-1 coactivators in mitochondrial biogenesis and brown fat differentiation. *Cell Metab* *3*, 333-341.
- van Marken Lichtenbelt,W.D., Vanhommerig,J.W., Smulders,N.M., Drossaerts,J.M., Kemerink,G.J., Bouvy,N.D., Schrauwen,P., and Teule,G.J. (2009). Cold-activated brown adipose tissue in healthy men. *N. Engl. J Med.* *360*, 1500-1508.
- Vidal-Puig,A.J., Grujic,D., Zhang,C.Y., Hagen,T., Boss,O., Ido,Y., Szczepanik,A., Wade,J., Mootha,V., Cortright,R., Muoio,D.M., and Lowell,B.B. (2000). Energy metabolism in uncoupling protein 3 gene knockout mice. *J. Biol. Chem.* *275*, 16258-16266.
- Virtanen,K.A., Lidell,M.E., Orava,J., Heglind,M., Westergren,R., Niemi,T., Taittonen,M., Laine,J., Savisto,N.J., Enerback,S., and Nuutila,P. (2009). Functional brown adipose tissue in healthy adults. *N. Engl. J Med.* *360*, 1518-1525.
- Viswakarma,N., Yu,S., Naik,S., Kashireddy,P., Matsumoto,K., Sarkar,J., Surapureddi,S., Jia,Y., Rao,M.S., and Reddy,J.K. (2007). Transcriptional regulation of Cidea, mitochondrial cell death-inducing DNA fragmentation factor alpha-like effector A, in mouse liver by peroxisome proliferator-activated receptor alpha and gamma. *J Biol. Chem.* *282*, 18613-18624.
- Whittle,A.J., Lopez,M., and Vidal-Puig,A. (2011). Using brown adipose tissue to treat obesity - the central issue. *Trends Mol. Med.* *17*, 405-411.
- Winkler,E. and Klingenberg,M. (1994). Effect of fatty acids on H<sup>+</sup> transport activity of the reconstituted uncoupling protein. *J Biol. Chem.* *269*, 2508-2515.
- Winkler,E., Wachter,E., and Klingenberg,M. (1997). Identification of the pH sensor for nucleotide binding in the uncoupling protein from brown adipose tissue. *Biochemistry* *36*, 148-155.
- Wojtczak,L. and Wieckowski,M.R. (1999). The mechanisms of fatty acid-induced proton permeability of the inner mitochondrial membrane. *J Bioenerg. Biomembr.* *31*, 447-455.
- Zhang,C.Y., Parton,L.E., Ye,C.P., Krauss,S., Shen,R., Lin,C.T., Porco,J.A., Jr., and Lowell,B.B. (2006). Genipin inhibits UCP2-mediated proton leak and acutely reverses obesity- and high glucose-induced beta cell dysfunction in isolated pancreatic islets. *Cell Metab* *3*, 417-427.
- Zhou,Z., Yon,T.S., Chen,Z., Guo,K., Ng,C.P., Ponniah,S., Lin,S.C., Hong,W., and Li,P. (2003). Cidea-deficient mice have lean phenotype and are resistant to obesity. *Nat. Genet.* *35*, 49-56.

## 7 Appendix

### 7.1 Material

*SV Total RNA Isolation System (Promega Z3100)*

*Quantitect Reverse Transcription Kit (QIAGEN 205313)*

*Modified Lowry Protein Assay Kit. (Thermoscientific Pierce 23240)*

*BCA Protein Assay Kit (Thermoscientific Pierce 23228)*

*Amersham ECL Western Blotting System (GE Healthcare RPN2108)*

*Glycerol Detection Kit (R-Biopharm 10 148 270 035)*

*Goat anti rabbit Alexa 488 (A11008)*

*Goat anti rabbit HRP conjugated (Dako P0448)*

*Mitotracker Deep Red (Invitrogen M22426)*

*Normal Goat Serum (Dako X0907)*

*DMEM (Gibco 41965)*

*FBS (Biochrom S0615)*

*PBS solution (Sigma P4417)*

*Trypsin solution (Biochrom L2163)*

*Gentamicin (Biochrom A2712)*

*Penicillin/ Streptomycin (A2213)*

*Geneticin (Gibco 10131-027)*

*Puromycin (InvivoGen 58-58-2)*

*Poly-D-Lysin (Sigma P7280)*

*Collagen (Biochrom L7220)*

*Insulin (Sigma I9278)*

*T3 (Sigma T2877)*

*Indomethacin (Sigma I7378)*

*Dexamethasone (Sigma D4902)*

*IBMX (Sigma I5879)*

*Retinoic acid (Sigma R2625)*

*Isoproterenol (Sigma I2760)*

*Rosiglitazone (Biozol 71740)*

*Polybreen (Santa Cruz sc-134220)*

*Nigericin (Sigma N7143)*

*Rotenone (Sigma R8875)*

*Antimycin A (Sigma A8674)*

*Oligomycin (Sigma O4876)*

*Succinic acid (Sigma S3674)*

*Malonic acid (Sigma M129-6)*

*FCCP (Sigma C2920)*

*Pyruvic acid (Sigma P2256)*

*Malic acid (Sigma M9138)*

*ADP (Sigma A2754)*

*GDP (Sigma G7127)*

*Palmitic acid (Sigma P0500)*

*Retinoic acid (Sigma R2625)*

*BSA<sub>FAF</sub> (Sigma A3803)*

*TPMP (Sigma 130079)*

*Diethylphthalate (Sigma D201154)*



*Tetrahydrofuran (Roth 4745.1)*

*Polyvinylchlorid (Sigma 81388)*

*Tetraphenylborat (Sigma 72018)*

*XF96 FluxPaks (Seahorse 101107-001)*

*Seahorse Calibrant Solution (Seahorse 100840-000)*

*Seahorse DMEM (Seahorse 101022-100)*

## 7.2 qRT PCR

*Primer*

Transcript	Forward Primer	Reverse Primer
UCP1	TCTCTGCCAGGACAGTACCC	AGAAGCCCAATGATGTTTCAG
UCP2	TGAGGTGGGAAGTAAATCGG	ACTGTGCCCTTACCATGCTC
UCP3	AAGATGGTGGCTCAGGAGG	GGACGAAACACGGAGGACTA
ANT1	AAAAATATGTGTAATACCCAAGCTCACA	TGTTTTCTTTCCTCAAGAATAGTCTGTAAAC
ANT2	AGGGCGCATGGTCCAA	ATCTCATCATACAAGACAAGCACAAAC
CideA	TGCTCTTCTGTATCGCCCAGT	GCCGTGTTAAGGAATCTGCTG
HSL	gcttggttcaactggagagc	gcctagtccttctggtctg
PGC alpha	GGACGGAAGCAATTTTCAA	GAGTCTTGGGAAAGGACACG
HSP60	GGAAAAAGGAATCATTGACCC	TTGGTGAGGAACACTGCCTT
Hsp90	AGGAGGGTCAAGGAAGTGGT	TTTTTCTTGTCTTTGCCGCT
Beta actin	AGAGGGAAATCGTGCGTGAC	CAATAGTGATGACCTGGCCGT

*PCR program*

1. 7 min 95°C

2. 40x: 10 s 95°C

15 s 52°C

20 s 72°C

3. Melting Curve (5 s 95°C; 15 s 60°C; in in 20 min heat to 95°C, 15 s 95°C)

4. 4 °C ∞

## 7.3 Vectors

*pcDNA 3 (Invitrogen V79020)*

*pEGFPN1 (CLontech 6085-1)*

*pHis17 (supplied by Bruno Miroux)*

*pcDNA 4(Invitrogen V86220)*

*pMXS IRES puro (Cell Biolabs RTV-014)*

## 7.4 Seahorse protocol

1. Calibrate
2. Equilibration
3. 3 min Mix
4. 3 min Measure
5. go back to 3 for 3 more times
6. Injection A
7. 3 min Mix
8. 3 min Measure
9. go back to 7 for 2 more times
10. Injection B
11. 3 min Mix
12. 3 min Measure
13. go back to 7 for 2 more times

## 8 Kurzfassung (Abstract)

In der Dissertation „Analysis of uncoupling protein 1 and CideA function in two mammalian cell lines“ wurde die Eignung zweier Zellkultursysteme zur Untersuchung der Funktion des Entkopplerproteins 1 (UCP1) charakterisiert. Ein genaues Verständnis dieses mitochondrialen Transporters ist von Interesse, da es sich um ein mögliches Ziel für die pharmakologische Behandlung von Adipositas und deren Folgeerkrankungen handelt. Das aktivierte UCP1 katalysiert die direkte Umwandlung der Nahrungsenergie in Wärme. Die verwendeten Zellkultursysteme wurden hinsichtlich der Stärke der Expression, der Regulation der Proteinaktivität sowie einer möglichen Fehlfunktion des Proteins charakterisiert. Eine besondere Eignung des heterologen Expressionssystems wurde festgestellt. In anschließenden Funktionsstudien mit diesen Zelllinien wurde die Interaktion von UCP1 und CideA untersucht.

The thesis “Analysis of uncoupling protein 1 and CideA function in two mammalian cell lines“, investigated the suitability of two cell culture models for functional studies on uncoupling protein 1 (UCP1). A more detailed understanding of this mitochondrial carrier is of interest as it could be a target for pharmacological treatment of obesity. UCP1 in brown adipose tissue dissipates food energy as heat. Heterologous and homologous cell culture systems were characterised with respect to the expression level and the regulation of UCP1 activity, excluding an artificial function of misfolded protein in the test systems. The heterologous system proved to be particularly suited for functional analysis of UCP1. Both cell lines were furthermore used to investigate the functional interaction of UCP1 and CideA.

## 9 Erklärung

Ich erkläre an Eides statt, dass ich die dem  
Wissenschaftszentrum Weihenstephan  
der Technischen Universität München zur Promotionsprüfung vorgelegte Arbeit mit dem Titel:

Analysis of uncoupling protein 1 and CideA function in two mammalian cell lines

in der Molekularen Ernährungsmedizin  
unter der Anleitung und Betreuung durch  
Prof. Dr. Martin Klingenspor.....

ohne sonstige Hilfe erstellt und bei der Abfassung nur die gemäß § 6 Abs. 5  
angegebenen Hilfsmittel benutzt habe.

- (x) Ich habe die Dissertation in keinem anderen  
Prüfungsverfahren als Prüfungsleistung vorgelegt.
- ( ) Die vollständige Dissertation wurde in .....  
..... veröffentlicht. Die Fakultät für  
..... hat der  
Vorveröffentlichung zugestimmt.
- (x) Ich habe den angestrebten Doktorgrad noch nicht erworben  
und bin nicht in einem früheren Promotionsverfahren für  
den angestrebten Doktorgrad endgültig gescheitert.
- ( ) Ich habe bereits am ..... bei der  
Fakultät für .....  
der Hochschule .....  
unter Vorlage einer Dissertation mit dem Thema .....  
.....  
die Zulassung zur Promotion beantragt mit dem Ergebnis:  
.....

Die Promotionsordnung der Technischen Universität München ist mir bekannt.

München, den .....

Unterschrift

**10****Curriculum Vitae**

Verena Hirschberg

**KONTAKTDATEN**

20 Regent Street, Flat 21

Hauptstraße 107b

PL4 8AS Plymouth

41352 Korschenbroich

United Kingdom

(alternativ in Deutschland)

Telefon: +44-7570-818077

Email: verena.hirschberg@plymouth.ac.uk

(aktuell)

**PERSÖNLICHE INFORMATIONEN**

Geburtsdatum / Geburtsort

12.06.1981 / Neuss

Nationalität

deutsch

Familienstand

ledig

**AUSBILDUNG**Promotion

05/2006 – 01/2012

*“Analysis of uncoupling protein 1 and CideA function in two mammalian cell lines.”* (Abschluss 07/2012)

05/2011

Seahorse XF Trainingskurs in Kopenhagen

09/2008 – 12/2008

Forschungsaufenthalt an der Université Paris V, Institut Necker, bei Dr. Bruno Miroux

Diplom

03/2006	Biologie-Diplom (Note: 1,3 (sehr gut))
05/2005 - 03/2006	„Funktionelle Analyse von Entkopplerprotein 1 in humanen embryonalen Nierenzellen (HEK293).“
10/2000 – 03/2006	Diplomstudium der Biologie am Lehrstuhl Tierphysiologie, Fachbereich Biologie, Philipps-Universität Marburg  Hauptfächer: Tierphysiologie, Genetik, Psychologie
1991-2000	Abitur, Gymnasium Korschenbroich

**BERUFLICHER WERDEGANG**

05/2009 – 01/2012	Wissenschaftliche Mitarbeiterin am Lehrstuhl für Molekulare Ernährungsmedizin, Wissenschaftszentrum Weiherstephan, Technische Universität München, bei Prof. Dr. Martin Klingenspor
-------------------	---

**STIPENDIEN**

05/2006 – 04/2009	DFG Graduiertenkolleg 1216: „Intra- and Intercellular transport and communication“, Projekt: „Novel modulators of uncoupling proteins“
-------------------	--

**PUBLIKATIONEN**

2012	<b>Hirschberg V.*</b> , Jastroch M.*, and Klingenspor M. Functional characterisation of uncoupling protein 1 in mammalian HEK293 cells excludes mitochondrial uncoupling artefacts and reveals no contribution to basal proton leak. * these authors contributed equally to the study. <i>BBA Bioenergetics</i> , 2012, 1817:1660-70.
------	---

2011 **Hirschberg V.**, Fromme T. and Klingenspor M. Test systems to study the structure and function of uncoupling protein 1: a critical overview. Invited Review, *Frontiers in Cellular Endocrinology*, 2011, 2.

2008 Jastroch M., Withers K. W., Taudien S., Frappell P. B., Helwig M., Fromme T., **Hirschberg V.**, Heldmaier G., McAllan B. M., Firth B. T., Burmester T., Platzer M. and Klingenspor M. Marsupial uncoupling protein 1 sheds light on the evolution of mammalian nonshivering thermogenesis. *Physiol Genomics*, 2008, 32(2):161-9.

2008 Klingenspor M., Fromme T., Hughes D. A. Jr, Manzke L., Polymeropoulos E., Riemann T., Trzcionka M., **Hirschberg V.** and Jastroch M. An ancient look at UCP1. Review, *BBA*, 2008, 1777(7-8):637-41.

#### KONFERENZEN

08/2006 Jastroch M., **Hirschberg V.**, Brand M. D., Liebig M., Weber K., Bolze F. and Klingenspor M. Introducing a mammalian cell system to study the function of evolutionary distant uncoupling proteins. *EBEC 2006*, Moscow, 2006. Poster

## 11 Danksagung

Zunächst möchte ich mich bei Prof. Dr. Martin Klingenspor dafür bedanken, dass er es mir ermöglicht hat diese Arbeit anzufertigen und mich in dieser langen Zeit, einschließlich des stressigen Endes, immer unterstützt hat.

Dr. Bruno Miroux danke ich dafür, dass ich einen Teil meiner Arbeit in seinem Labor anfertigen durfte, merci Paris!

Bei Dr. Martin Jastroch möchte ich dafür bedanken, dass er mir die Messungen von Membranpotential und Sauerstoffverbrauch beigebracht hat, die für die Anfertigungen dieser Arbeit essentiell waren. Außerdem für sehr viele gemeinsame Büro- und Freizeitstunden und Gespräche über Wissenschaft und was es sonst noch so gibt.

Vielen Dank allen Mitgliedern der Arbeitsgruppen in Freising und Marburg, wegen derer immer eine hilfsbereite und angenehme Arbeitsatmosphäre herrschte, ohne die all diese Arbeiten nicht möglich gewesen wären.

Ein herzlicher Dank für Gesprächs-, Kaffee-, Lauf-, Sushi- und sonstige Treffen an Julia, Kerstin, Melina und Trixi.

Ein riesiger Dank geht auch an all die lieben Münchner, vor allem Sonja, Patti und den Rest der Sardinien-Crew, die mich so nett aufgenommen haben und wegen derer ich mich in der Stadt so schnell zu Hause gefühlt habe.

Danke an Jeppe für die seelisch-moralische Unterstützung am Ende der Arbeit ohne die mir manches wohl viel schwerer gefallen wäre, mange tak!

Abschließend möchte ich einen ganz besonderen Dank an meine Eltern und meine Familie richten, die mich bis hierher immer unterstützt haben und ohne die ich all dies nicht geschafft hätte.